INL/EXT-14-32970
Revision 2

AGR-1, AGR-2 and AGR-3/4 Release-to-Birth Ratio Data Analysis

Binh T. Pham
Jeffrey J. Einerson
Dawn M. Scates
John T. Maki
David A. Petti

June 2019

The INL is a
U.S. Department of Energy
National Laboratory
operated by
Battelle Energy Alliance

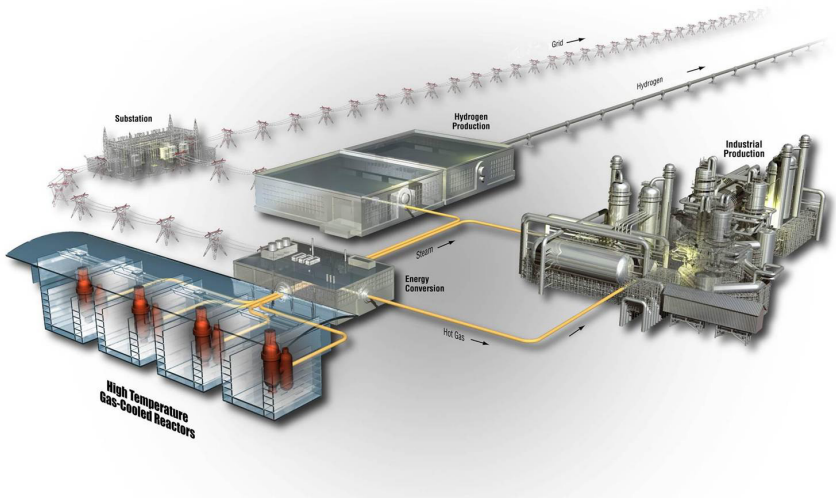

Idaho National Laboratory

INL/EXT-14-32970
Revision 2

AGR-1, AGR-2 and AGR-3/4 Release-to-Birth Ratio Data Analysis

Binh T. Pham
Jeffrey J. Einerson
Dawn M. Scates
John T. Maki
David A. Petti

June 2019

Idaho National Laboratory
INL ART Program
Idaho Falls, Idaho 83415

http://www.inl.gov

Prepared for the
U.S. Department of Energy
Office of Nuclear Energy
Under DOE Idaho Operations Office
Contract DE-AC07-05ID14517

INL ART Program

AGR-1, AGR-2 and AGR-3/4 Release-to-Birth Ratio Data Analysis

INL/EXT-14-32970
Revision 2

June 2019

Author:

Binh T. Pham — 06/06/2019 (Date)

Technical Reviewer: (Confirmation of mathematical accuracy, and correctness of data, and appropriateness of assumptions.)

Mitchell A. Plummer
NDMAS Technical Lead — 6/06/2019 (Date)

Approved by:

Paul Demkowicz
TRISO Fuel Director — 6/10/19 (Date)

Michelle T. Sharp
INL ART Quality Assurance — 6/10/19 (Date)

ACKNOWLEDGEMENT

This work is supported by the Advanced Reactor Technologies Technology Development Office Research and Development Program at Idaho National Laboratory under the U.S. Department of Energy Contract DE-AC07-05ID14517.

SUMMARY

A series of Advanced Gas Reactor (AGR) irradiation tests is being conducted in the Advanced Test Reactor at Idaho National Laboratory in support of development and qualification of tristructural isotropic (TRISO) low-enriched fuel used in the high-temperature gas-cooled reactor (HTGR). Each AGR test consists of multiple independently controlled and monitored capsules containing fuel compacts placed in a graphite cylinder shrouded by a steel shell. These capsules are instrumented with thermocouples (TC) that are embedded in the graphite, thus enabling temperature control. AGR configuration and irradiation conditions are based on prismatic HTGR technology that is distinguished primarily through use of helium coolant, a low-power-density ceramic core capable of withstanding very high temperatures, and TRISO-coated particle fuel. The AGR tests provide valuable irradiation-performance data to support fuel process development, qualify fuel for normal operation and accident conditions, and support development and validation of fuel performance and fission-product transport models and codes.

The release-to-birth ratios (R/B) for fission-gas isotopes (i.e., krypton and xenon) are calculated from release rates into the sweep-gas flow, measured by the high-purity germanium detectors used in the AGR Fission Product Monitoring System (FPMS) installed downstream from each irradiated capsule. Birth rates are calculated based on the fission power in the experiment and models of fission-product generation. Thus, R/B is a measure of the ability of fuel kernel, particle coating layers, and compact matrix to retain fission-gas atoms, preventing their release into the sweep-gas flow, especially in the presence of initially defective particle and/or the event of particle-coating failures that occurred during the irradiation. For fission-gas isotopes, particle failure occurred when all coating layers are fractured that allow gaseous fission atoms to escape from a particle. In this case, the R/B per exposed kernel is used to compare fuel performance across experiments.

The major factors that govern the transport of fission gases are the effective diffusion coefficient, temperature, and radioactive-decay constant. For each of the AGR capsules, ABAQUS-based, three-dimensional, finite-element thermal models are created to predict daily averages of fuel-compact temperature for the entire irradiation period. The post-irradiation examination dimensional measurements are used to estimate the time-varying gas gap models for use in thermal models. These time-variable gas gap models led to better fit between measured and calculated TC temperatures in most capsules. The average temperatures experienced by failed particles are used to establish the R/B per exposed kernel correlation with temperature and decay constant for each fission gas. In-pile particle failures in a capsule were detected using the independent capsule-specific FPMS. R/B data for 12 krypton and xenon isotopes were received into the Nuclear Data Management and Analysis System database for the AGR-1, AGR-2, and AGR-3/4 experiments.

For AGR-3/4 capsules, particle failures were expected because of the inclusion of 20 designed-to-fail fuel particles in each compact, the kernels of which are identical to the driver-fuel kernels and whose coatings are designed to fail during irradiation. Therefore, R/B data obtained from the AGR-3/4 experiment can be used to establish correlation of R/B per exposed kernel. To

reduce measurement uncertainty of the release rate, the krypton and xenon isotopes selected for regression analysis have a half-life that is short enough to achieve equilibrium in the capsule, but long enough to provide a measureable signal in the FPM detector. Therefore, only a total of 18,479 values of AGR-3/4 daily average R/Bs for three krypton isotopes (Kr-85m, Kr-87, and Kr-88) and three xenon isotopes (Xe-135, Xe-137, and Xe-138) were used for the regression analysis to establish the R/B per exposed kernel relationship as a function of the isotope-decay constant and fuel temperature. The uncertainty of the estimated number of failed particles in AGR-3/4 capsules is found to have minor impact on the established R/B correlation. This correlation can be used to estimate fission-gas release from postulated failed fuel particles in HTGR cores, which is a key safety factor for a fuel-performance assessment. This parameter can be used in fission-product behavior models.

To validate the R/B per exposed kernel correlation based on data from the AGR-3/4 capsules, the R/B per exposed kernel data from historic experiments were used. These historical irradiations of low-enriched uranium carbide/oxide TRISO fuel had either designed-to-fail particles or had in-pile failures, so they can provide additional data for comparison to fuel-performance data obtained from the AGR-3/4 irradiation. The four key irradiations are (1) HRB-17/18, (2) COMEDIE-BD1, (3) HFR-B1, and (4) HRB-21.This study demonstrates that R/B values for AGR test fuel are comparable to R/B obtained in historic tests. The R/B correlation with isotopic-decay constant is very stable with irradiation time, indicating no strong influence of burnup on release.

In Revision 1 of this report, one exposed kernel was assumed in each of the AGR-2 UCO capsules based on the exposed-kernel fraction at 95% confidence, and AGR-2 R/B data were included in establishing the R/B per exposed kernel correlation. However, this assumption was not statistically supported by the average exposed-kernel fractions for AGR-2 compacts. Therefore, in this revision, AGR-2 release data are not included in R/B per exposed kernel model. On the other hand, neither the exposed-kernel fraction of the as-fabricated fuel nor the incomplete post-irradiation examination (PIE) results support the conclusion that no exposed kernels existed in the capsules. As well, higher measured R/B values in AGR-2 capsules, compared to AGR-1 capsules, also indicate possible exposed kernels. Subsequently, AGR-2 release data were not used for estimation of release from dispersed uranium (DU) contamination.

In contrast, no in-pile particle failures were identified during irradiation of AGR-1 experiment, based on monitoring of the gross gamma counts and low level of R/Bs. This was confirmed by PIE of as-irradiated compacts. Then, fission-product releases from AGR-1 capsules originated mainly from DU in fuel compacts. Therefore, the AGR-1 release data are used to study the DU release factor defined as a ratio between release from DU and release from an exposed kernel with the same uranium mass. A total of 18,349 values of AGR-1 daily average R/Bs for three krypton isotopes (Kr-85m, Kr-87, and Kr-88) and three xenon isotopes (Xe-135, Xe-137, and Xe-138) were used to calculate DU release factor for each fission-gas isotope. The DU release factor can be used to provide a rough estimate of releases from the heavy-metal contamination; thus, it can help to differentiate releases from exposed kernels, which could be useful in accessing fuel performance. The large amount of R/B data from AGR-1 irradiation reveals the following trends of DU release factor: (1) the effect of

isotopic decay constant is insignificant, (2) fuel temperature has contradicting trends—the factor increases with temperature for krypton isotopes but decreases for xenon isotopes—and (3) higher fast fluence and burnup lead to a higher DU release factor. In general, the DU release factor is 5.1 ±3.1 for all isotopes: 6.1 ±3.5 for krypton and 4.0 ±2.4 for xenon.

CONTENTS

FIGURES

TABLES

ACRONYMS

AGR	Advanced Gas Reactor
ART	Advanced Reactor Technologies
ATR	Advanced Test Reactor
cps	counts per second
DLBL	deconsolidation and leach burn leach
DTF	designed to fail
DU	dispersed uranium contamination
DUF	dispersed uranium fraction
EFPD	effective full-power day
FPMS	Fission Production Monitoring System
HTGR	high temperature gas-cooled reactor
IMGA	irradiated microsphere gamma analyzer
IPyC	inner pyrolytic carbon
LEUCO	low-enriched uranium carbide/oxide
OPyC	outer pyrolytic carbon
ORNL	Oak Ridge National Laboratory
PIE	post-irradiation examination
R/B	release-to-birth ratio
SiC	silicon carbide
TC	thermocouple
TRISO	tristructural isotropic
UCO	uranium carbide/oxide
UO_2	uranium dioxide
VHTR	very high temperature reactor

AGR-1, AGR-2 and AGR-3/4 Release-to-Birth Ratio Data Analysis

1. INTRODUCTION

The fission-product behavior of tristructural isotropic (TRISO)-coated particle fuel is a key factor for performance assessment of very high temperature reactors (VHTRs). The activity of gaseous fission products (such as krypton and xenon isotopes) in the coolant is a direct indicator of fuel performance. The technical basis for VHTR fuel performance and quality requirements rely on quantitative assessment of the fission-product release (General Atomics 2009). The main sources of release are from heavy-metal contamination in the fuel coatings and graphite matrix material and from defective or failed particles (IAEA 1997). A few historical irradiation studies in the 1980s were designed to study fission-gas releases from low-enriched uranium carbide/oxide (UCO) TRISO fuels. Those studies included either designed-to-fail (DTF) particles or identified in-pile failures (General Atomics 1987, Richards 1994, ORNL 1994, and DOE 1995). Since 2006, three Advanced Gas Reactor (AGR) irradiation tests have been conducted in the Advanced Test Reactor (ATR) at Idaho National Laboratory (INL). These tests support development and qualification of U.S. TRISO fuel for use in a high temperature gas-cooled reactor (HTGR). Each AGR test included multiple independent capsules, each containing cylindrical fuel compacts housed within a graphite cylinder shrouded by a steel shell. Thermocouples (TCs) were embedded in the graphite, to monitor temperature and enable its control. AGR configuration and irradiation conditions are based on prismatic HTGR technology, a technology involving use of helium coolant, a low-power-density ceramic core capable of withstanding very high temperatures, and coated particle fuel (PLN-3636 2018). These tests provide valuable irradiation performance data to support fuel process development, qualify fuel for normal operating conditions, and support development and validation of fuel performance and fission-product transport models and codes.

Under normal operating conditions, the kernel retains more than 95% of the radiologically important, short-lived fission gases (IAEA 1997). Some of the noble-gases produced by fission in a failed particle may escape via various transport mechanisms into the surrounding materials. It is modelled as diffusion with a rate dependent on the effective diffusivity encompassing all mechanisms. This effective diffusivity is determined by material properties of the kernel, particle coatings, and compact matrix. In the AGR experiments, the escaping gases are carried by the capsule gas-collection system to the Fission Product Monitoring System (FPMS). The activity of radioactive species reaching that monitoring system depends on both the diffusive transport rate and the decay constant of the species. Species with very short decay constants might not reach the detector if the transport time is sufficiently long that most of the gas decays in transit.

The two governing processes (diffusion and radioactive decay) form the basis for a physics-based fission-product release model. The ratio of release rate to the generation, or 'birth,' rate of the fission products (calculated from neutronics simulations) is a measure of the ability of fuel kernels, particle coating layers, and compact matrix material to retain fission-gas species, thus preventing their release into the sweep gas. In the absence of particle failure, this release-to-birth ratio (R/B) is expected to be very low, because intact particles without fabrication defects are not expected to contribute to the release of fission products under normal operating conditions. In the case of particle failure, the R/B per exposed kernel is used to compare release behavior between different irradiation experiments. This parameter could be used in the fission-product behavior models within the HTGR research and development program.

Because radioisotope transport rates are temperature dependent, the R/B depends on temperature. In the absence of direct measurements, fuel-compact temperatures are calculated using thermal simulations. For each of the AGR capsules, ABAQUS-based, three-dimensional, finite-element heat transport models are created to predict daily averages of fuel compact temperatures for the entire irradiation period. To

reduce uncertainty of fuel-temperature prediction, post-irradiation-examination (PIE) dimensional measurements are used to estimate the time-dependent gas gap models. An average temperature of failed particles is estimated for use in the R/B per exposed kernel model.

In this study, R/B data from three completed AGR fuel irradiation experiments were used to examine fission-gas releases from compacts containing TRISO fuel particles. For the AGR-1 experiment, the data indicate that there were no in-pile particle failures. This is based on both the R/B ratios during irradiation (which were significantly below values that would indicate any particles with complete TRISO failure) and PIE data (which failed to identify particles with TRISO failure in systematic examination of a number of irradiated compacts). The low fission-gas releases in the AGR-1 capsules are believed to have originated from dispersed uranium contamination (DU) in the fuel compacts. Thus the R/B data obtained from the AGR-1 experiment provide data for assessing fission gas releases from DU.

Currently, preliminary data from the incomplete PIE of AGR-2 as-irradiated compacts suggest the possibility of one or more exposed kernels in some capsules (either due to as-fabricated exposed kernel defects or from TRISO coating failure that occurred in-pile). This result is consistent with the exposed-kernel fraction measured at fabrication, which could not exclude possible existence of particle failure in AGR-2 capsules. In addition, AGR-2 R/B data were much higher than AGR-1, where no particle failure occurred. However, the number of failed particles in each capsule has not been conclusively determined. As a result, AGR-2 R/B data cannot be used to study either R/B per exposed kernel or the DU release factor.

For the combined AGR-3/4 experiment, particle failures in all capsules were expected because they each included particles with kernels identical to the driver fuel kernels, but the coatings of which were designed to fail (DTF) under irradiation. Eighty of DTF fuel particles (20 per compact) were included in each AGR-3/4 capsule, distributed along the central axis of the fuel compacts. The in-pile particle failures in each capsule were counted by looking at the temporal profile of the gross gamma counts, monitored continuously for each capsule. A fuel particle failure causes the gross gamma activity to peak for a short time at a count higher than normal and raises the subsequent background activity. Interpretation of changes in that activity becomes more complicated due to (a) simultaneous failures, (b) release spikes from already-failed particles (i.e., sudden release from exposed kernels due to kernel restructuring cause by irradiation), and (c) high background noise once a significant number of failures have occurred. These complications increased uncertainty in the number of failures for some capsules. Because of DTF particles, AGR-3/4 experiment can provide data for establishing correlation of R/B per exposed kernel as function of decay constant and temperature for the U.S. TRISO fuel.

1.1 Purpose and Scope

Fission-product release behavior under normal operating conditions is of significant interest in reactor design. The release correlation with decay constant and temperature can be useful for reactor designers to estimate fission-gas release from postulated exposed fuel kernels in HTGR cores, which is essential for fuel-performance assessments. It is also important to know the fission-gas releases from DU in fuel compacts. AGR-2 fission-gas release data are not included here because of the uncertainty on the number of exposed kernels in each capsule. The fuel irradiation data used for analyses are from the AGR-1 and AGR-3/4 capsules, which include R/B data for selected krypton and xenon isotopes, number of particle failures, and calculated fuel temperature.

The R/B data analysis in this report describes the following:

- Technical aspects of fission-gas release behaviors, including model form for R/B per exposed kernel
- Data preparation:
  - Selection of isotopes and R/B data used for this analysis
  - Estimation of in-pile failed particles among DTF particles for AGR-3/4 capsules

- Estimation of the number of equivalent DU kernels from uranium contamination fraction measured at fabrication for compact lots used in AGR-1 capsules

- The effect of isotopic-decay constant on fission-gas releases
- Regression analysis to establish the relationship of R/B per exposed kernel as a function of decay constant and fuel temperature for krypton and xenon isotopes, using R/B data from AGR-3/4 irradiations
- Comparison between the AGR-3/4 correlation of R/B per failed article and data from historical irradiations for Kr-85m isotope for validation.
- Estimation of DU release factor based on AGR-1 R/B data as the ratio between releases from an equivalent DU kernel and a failed particle.

2. TECHNICAL APPROACH

2.1 Fission-gas Release from Exposed Kernel

2.1.1 Tristructural Isotropic Coated Fuel Particle

Figure 1 shows layers of the TRISO coated fuel, fuel particles, and fuel compacts. Each fuel particle consists of the fissile fuel kernel, buffer layer, and three coating layers (the inner pyrolytic carbon [IPyC], silicon carbide [SiC], and outer pyrolytic carbon [OPyC] shown in the image on the left in Figure 1). The coating system sets up a miniature pressure vessel that has been engineered to provide containment of the radionuclides and gases generated by fission of the nuclear material in the kernel. Thousands of these TRISO-coated particles (see image in the middle) are bonded in a carbonaceous material into a cylindrical fuel compact for the prismatic HTGR (see image on the right). These fuel particles can withstand extremely high temperatures without losing their ability to retain radionuclides, even under accident conditions. The particles can endure fuel temperatures up to 1,800°C for several hundred hours without loss of particle-coating integrity (INL 2010). This high-temperature radionuclide retention capability is the key element in the design and licensing of modular HTGRs. The technical basis for VHTR fuel performance and quality requirements relies on quantitative assessment of the fission-product release (General Atomics 2009).

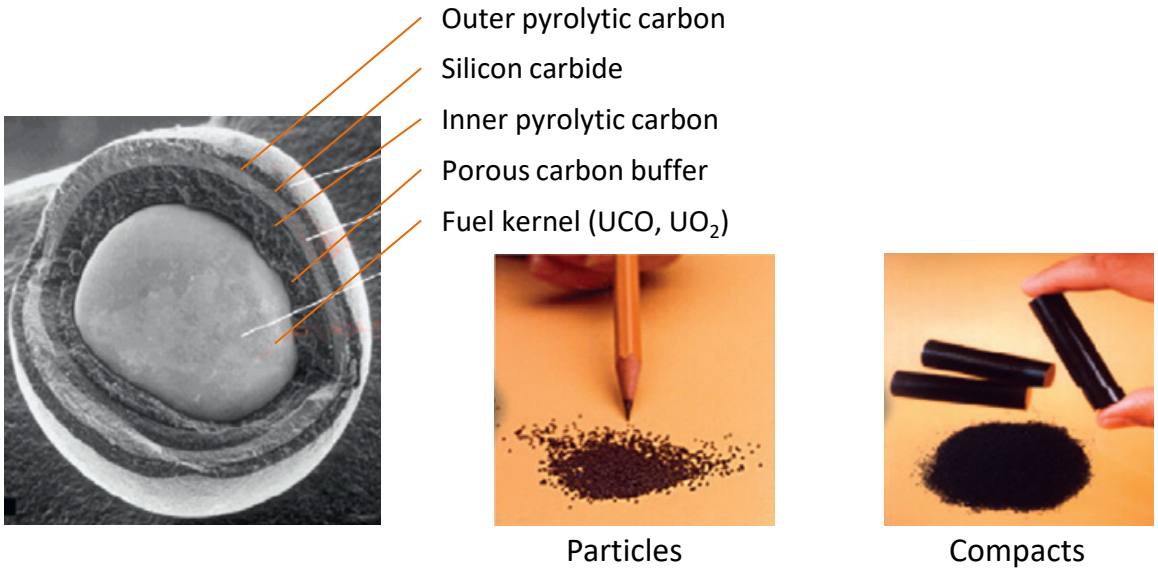

Figure 1. TRISO-coated particle fuel and compacts used in AGR experiments.

Lessons learned from the comparison of process attributes and irradiation conditions (burnup, fast neutron fluence, temperature, degree of acceleration) between the superior German and the historic U.S TRISO-coated particle fuel were used as a basis for improvement of the manufacturing process of the modern U.S. TRISO-coated fuel (Petti et al. 2003). Performance of the TRISO coated-particle fuel, based on an extensive review of irradiation tests conducted globally since the seventies, was also assessed (Petti et al. 2012). This assessment resulted in a list of conditions to ensure the successful manufacturing of high-quality, low-defect TRISO fuel, which is the heart of the HTGR. Since 2006, three AGR irradiation tests have been conducted in the ATR at INL in support of the development and qualification of the modern U.S. TRISO fuel for use in an HTGR. Multiple compacts of the TRISO-coated fuel particles were irradiated under high neutron flux and high temperature in the ATR core for an extended period of time (several years). These tests provide crucial data for understanding the behavior of fission product releases from the TRISO coated-fuel particles, which is a key factor for performance assessment of the VHTRs.

2.1.2 Fission-gas Release and Transport

The activity of gaseous fission products in the HTGR coolant is dependent on fuel performance in term of particle failure. Heavy-metal contamination in the fuel graphite and defective/failed particles (typically referred to as an "exposed kernel") are the main sources of fission-gas releases. Analysis of fission-gas release focuses on the short-lived isotopes of krypton and xenon because these elements are the greatest contributors to activity in the primary coolant. Standard particles (intact particles without fabrication defects in coating layers) within the specification limits are not expected to contribute to the release of fission products under normal operating conditions (IAEA 1997). This is because, under normal operating conditions, the kernel retains more than 95% of the radiologically important short-lived fission gases, such as Kr-88, and the SiC layer is considered to be impermeable to most fission products, except for some metallic species at high temperatures (General Atomics 2009, Martin 1993). Fission-produced atoms of the noble gases released from the kernels of failed particles, however, can diffuse through cracks in the coatings of failed particle and into the surrounding materials to reach the sweep gas.

Several processes are involved in the transport of gaseous fission products within an AGR capsule. Gas atoms diffuse to the grain surfaces where they accumulate in pores, form bubbles, and are finally released by bubble migration and interconnection of the pores (Martin 1993). The diffusion rate depends on fuel kernel and graphite properties and temperatures. Radioactive decay reduces the activity of fission products in the sweep-gas flow. The radioactive gaseous depletion rate (or decay constant) is characterized by isotope half-life, defined as the time required for one-half of the isotope atoms to disintegrate. The two governing processes, diffusion and decay, form a basis to formulate a physics-based mathematical model that describes R/B per exposed kernel as a function of fuel temperature and decay constant. Details of these physical processes and fission-product gas-release models are discussed in following subsections.

2.1.2.1 Diffusion of fission gas

Fission-produced atoms of noble gases born in the kernel of fuel particles diffuse through the surrounding materials—the fuel kernel, coating layers, and compact matrix. Figure 2 shows the principal release barriers in an HTGR radionuclide-containment system. For the TRISO coated-fuel particle, the fuel kernel itself is the main barrier to fission-product release because diffusion in the solid structure takes place only by lattice diffusion. The particle coatings, particularly the SiC layer, form the second barrier to fission-product release. The fuel-compact matrix and fuel-element structural graphite are relatively porous, so diffusion in those materials occurs via a combination of molecular diffusion and Knudsen flow and is relatively fast compared to transport processes in the fuel kernel.

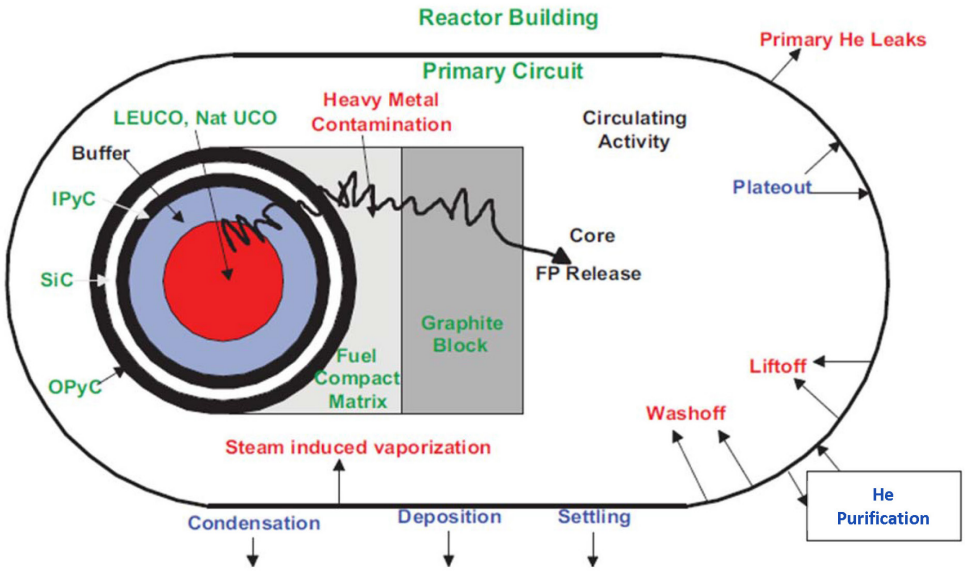

Figure 2. HTGR fission product containment system (General Atomics 2009).

For an intact, coated fuel particle, fission-product species are mostly contained within its coatings, and releases are insignificant. By contrast, for a fuel particle with a complete TRISO coating failure (e.g., exposed kernel due to loss of integrity of all three dense coating layers), a fraction of the fission gas released from the kernel penetrates through the cracks (or opening) in coating layers via gas-phase diffusion. These fission gases then diffuse through the graphite matrix with much less obstruction and are released into the sweep-gas flow. The diffusion coefficient depends mainly on fuel-kernel properties and temperatures. The temperature dependence of the diffusion coefficient is usually expressed by the Arrhenius equation:

$$D = D_0 e^{-\frac{E_a}{RT}} \tag{1}$$

where D_0 is the pre-exponential factor [m^2/J], E_a is the diffusion process activation energy [J/mol], R is the universal gas constant [8.3143 J/(mol K)], and T is the absolute temperature [K].

To characterize release resulting from diffusion within a solid spherical material, such as a bare fuel kernel, the reduced diffusion coefficient D' (s^{-1}) is used. It is defined as the diffusion coefficient D (m^2/s) divided by the squared "equivalent sphere" diffusion radius, a (m):

$$D' = \frac{D}{a^2}. \tag{2}$$

2.1.2.2 Radioactive decay of fission gas

Radioactive decay is the process by which a nucleus of an unstable atom loses energy by emitting ionizing radiation. Right after birth in a fuel kernel, fission-product isotopes begin depleting over time due to radioactive decay. The decay rate for the collection is characterized by the decay constants (λ) of the nuclides or the isotope half-life ($\tau_{1/2}$). The decay constant is related to the half-life as follows:

$$\lambda = \frac{ln2}{\tau_{1/2}}. \tag{3}$$

2.1.2.3 Release-to-birth ratio model

The R/B for a radioactive gas released from a bare kernel is a function of the kernel's effective diffusion coefficient, the decay constant of the fission product, and the surface-area-to-volume ratio, ($3/a$) of a sphere with radius (a) equivalent to a representative fuel kernel. Under equilibrium conditions when

isotope production, radioactive decay, and diffusion through the kernel reach a steady-state activity at the kernel surface, the R/B per exposed kernel (R_p) can be expressed as (IAEA 1997; ANS, 2011):

$$R_p = \frac{3}{x}\left(\coth x - \frac{1}{x}\right) \tag{4}$$

where $x = \left(\frac{\lambda}{D'}\right)^{0.5}$, λ is the decay constant (s^{-1}), and *D'* is the reduced diffusion coefficient (s^{-1}).

For short-lived isotopes, where $x \gg 1$,

$$R_p \approx \frac{3}{x} = 3\sqrt{\frac{D}{\lambda a^2}}. \tag{5}$$

Given experiment-specific reduced diffusion coefficient *D',* and radius *a* of the fuel kernel, *Equation* (5) shows the characteristic feature of the $1/\sqrt{\lambda}$ dependence of release for short-lived isotopes. However, when the kernel is surrounded by fuel-particle coatings (which compose the second barrier to fission-gas release); some of the releases from the kernel actually terminate in the remaining coatings. This is known as the recoil effect, which will lower the power of D/λ to less than 0.5. In previous experiments, these values ranged from 0.1 to 0.5.

Substituting the diffusion coefficient of *Equation* (1) into *Equation* (5), the R/B for a TRISO-coated failed particle can be expressed as a function of fuel temperature and decay constants as:

$$R_p \approx \frac{3}{x} = 3\left[\frac{D_0 e^{-\frac{E_a}{RT}}}{\lambda a^2}\right]^n \tag{6}$$

where, instead of using the theoretical value of 0.5, a variable *n* is introduced in the power of D/λ to account for the dependence of release on particle coatings.

2.1.3 Regression Fitting Function for Release-to-Birth Ratio per Failed Particle

We use *Equation* (6) as a basis for a linear regression analysis to establish the functional relationships of R/B per exposed kernel for krypton and xenon isotopes with decay constants and temperature for the TRISO coated fuel. The fission-gas release model can be derived for R/B per exposed kernel by taking the natural logarithm of *Equation* (6) and simplifying with regression coefficients as:

$$\ln R_p = n \ln\frac{1}{\lambda} + \frac{B}{T} + C \tag{7}$$

where *B* is a fuel-particle-specific constant representing diffusion coefficient dependence on temperature, and *C* is an irradiation-specific constant. This revision helps transform the non-linear *Equation* (6) into the linear form in *Equation* (7). The regression analysis is performed to best fit this equation to R/B data obtained from AGR-3/4 irradiation to estimate Parameters *n*, *B*, and *C*.

2.2 Fission-gas Release from Dispersed Uranium

Fission-gas released from DU in fuel compacts also contributes to the measured release from a capsule, so this release portion must be determined to differentiate from release of exposed kernels. Prior measurements at General Atomics (Martin 1993) have indicated that the release from DU is many times that from an exposed dense kernel with the same mass of uranium. The DU release factor, defined as a ratio between release from DU and release from a failed particle, can be useful in differentiating release sources. Thus, DU release factor and release from a DU kernel can be expressed as

$$F_{DU} = R_{DU}/R_p \quad \text{or} \quad R_{DU} = F_{DU} * R_p \tag{8}$$

where:

F_{DU} = DU release factor

R_{DU} = R/B for release from DU with amount of uranium equivalent to one kernel (can be called DU kernel)

R_p = R/B for one exposed kernel (or R/B per exposed kernel).

For AGR experiments, the measured release rate from a capsule is a sum of releases from exposed kernels and from DU. When there are no exposed-kernel defects and no in-pile particle failures, then the fission-gas release comes solely from DU contamination, and R/B per equivalent DU kernel is estimated as:

$$R_{DU} = R/\left(N_{DU} * B_1\right) \tag{9}$$

where:

R = Release rate measured in a capsule

N_{DU} = Number of DU equivalent kernels in a capsule, can be determined as $N_{DU} = N * f_{DU}$, where N is number of particle in capsule and f_{DU} is the dispersed-uranium fraction (DUF) (g leached U/g U in compact) measured from compacts without exposed kernels

B_1 = Birth rate from a single fuel kernel

The R/B values from each capsule are reported in ECAR-907, "Release-to-Birth Ratios for AGR-1 Operating Cycles 138B through 145A," ECAR-2420, "Release-to-Birth Ratios for AGR-2 Operating 147A through 1548," and ECAR-2457, "Release-To-Birth Ratios for AGR-3/4 Operating Cycles 151A-155B." These R/Bs were the ratio between the capsule measured release rate (R) and the total birth rate from all particles in a capsule ($B = B_1 \times N$) as:

$$R/B = R/[B_1 \times N] \tag{10}$$

Then, the release rate per capsule can be calculated as:

$$R = [R/B] * [B_1 \times N] \tag{11}$$

Substituting release rate (R) in *Equation* (11) to *Equation* (9), the term birthrate per single particle (B_1) was cancelled and *Equation* (9) becomes:

$$R_{DU} = \frac{[\mathrm{R/B}*\mathrm{N}]}{N_{DU}} \tag{12}$$

And it can be further simplified to:

$$R_{DU} = \frac{\mathrm{R/B}}{f_{DU}} \tag{13}$$

The release-to-birth ratio from a failed particle, R_p, can be predicted using *Equation* (7) established based on AGR-3/4 R/B data. By substituting *Equation* (12), the DU release factor in *Equation* (8) can be calculated from the reported R/B from capsules without exposed kernels and the number of DU equivalent kernels as

$$F_{DU} = \frac{\mathrm{R/B}}{R_p * f_{DU}} \tag{14}$$

2.3 Irradiation Data Used for Analysis of Fission-gas Release

The AGR irradiation tests each include an array of capsules stacked on top of each other to form the test train. A leadout tube holds the experiment in position and contains and protects the gas lines and TC wiring extending from the test train to the reactor penetration. Temperature within each capsule is

independently controlled by varying the neon/helium gas mixture to maintain a predefined set point. Gases exiting each capsule were independently monitored for fission-gas release of 12 isotopes—Kr-85m, Kr-87, Kr-88, Kr-89, Kr-90, Xe-131m, Xe-133, Xe-135, Xe-135m, Xe-137, Xe-138, and Xe-139—using the FPMS. In addition to experimental measurements, several physical parameters of the experiment conditions were calculated using numerical simulation methods. Those parameters include fast-neutron fluence from ATR fuel elements, test-fuel burnup, and fuel-compact temperature.

Deconsolidation and leach burn leach (DLBL) analyses of the as-fabricated fuel compacts in the AGR-1, AGR-2, and AGR-3/4 capsules were conducted at Oak Ridge National Laboratory (ORNL). DLBL analysis effectively measures the total inventory of uranium located in the compact outside of the SiC layer (i.e., it includes the contributions from both the OPyC and surrounding matrix). Thus, it measures the mass of uranium in leached particles with exposed kernels due to defective coating layers and in DU in the compact matrix or OPyC. For each measurement sample of several compacts, an exposed kernel is counted when the measured uranium inventory is more than half of a kernel; otherwise, the uranium inventory is considered to have originated from DU. Consequently, the DLBL analysis provides an estimate of the exposed-kernel contamination fraction—that is, the ratio of the total number of exposed kernels to the total number of particles. For samples without apparent exposed kernels, the DUF is calculated as the ratio between the measured mass of uranium and total mass of uranium in samples without exposed kernels. Results from DLBL analysis in Table 1 are crucial to support an assumption that no initial exposed kernel existed in AGR-1 capsules.

Table 1. Selected irradiation and configuration data for AGR-1, AGR-2, and AGR-3/4 capsules.

Property	AGR-1[d]	AGR-2	AGR-3/4
Irradiation Data			
Number of compacts per capsule/capsules	12/6	12/3	4/12
Effective full power days of irradiation[a]	620.2	559.3	369.1
Range of fuel temperature[b] (°C)	600–1,400	700–1,410	820–1,500
Compact burnup at end of irradiation (min-max compact, % fissions per initial metal atom)	11.30–19.56	7.26–13.15	4.85–15.27
Compact fast fluence at end of irradiation (min-max compact, 10^{25} n/m^2, E > 0.18 MeV)	2.17–4.30	1.94–3.53	1.19–5.32
Configuration Data			
Compact mass (g)	5.337 – 5.593	6.294	2.998
Mean uranium loading (g U/compact)	0.904–0.917	1.257	0.450
Number of driver particles per capsule[c]	49,140–49,848	38,112 / 18,516	7,488
Number of DTF particles per capsule	0	0	80
Particle volume packing fraction (%)	36–37	37	37
Exposed kernel fraction (exposed kernels / particles in compact)	0[e]	9.4×10^{-6}[f] / 8.1×10^{-6}[f]	$< 3.5 \times 10^{-5}$[g]
DUF (g leached U / g U in compact [without exposed kernel])	1.62×10^{-7}–3.85×10^{-7}	3.94×10^{-6}[h] / 9.66×10^{-7}[h]	—

a. Only R/B data during equilibrium of fission gas release were used in this analysis
b. Fuel temperature ranges are daily volume-average for AGR-1 and AGR-2; and centerline-average for AGR-3/4
c. Calculated value derived from other characterized properties
d. For AGR-1, values are for Baseline, Variant 1, Variant 2, and Variant 3, respectively or a min-max data range
e. Actual failure fraction: 0 failure was found among 372,311 particles from examined as-fabricated compacts (Collin, 2015)

Property	AGR-1[d]	AGR-2	AGR-3/4
f. Actual failure fraction: 9.4×10^{-6} is ratio of 3 failures in 317,625 particles as reported in ORNL/TM 2010/017 for 3 UCO capsules and 8.1×10^{-6} is ratio of 2 failures in 246,840 particles as reported in ORNL/TM-2010/055 for UO_2 Capsule 3			
g. 80% confidence of defect fraction			
h. 3.94×10^{-6} for AGR-2 UCO capsules and 9.66×10^{-7} for UO_2 capsule 3			

Details of experimental and simulation data for the three completed irradiations are reported in the final AGR irradiation test as-run reports (Collin 2015, 2014, and 2016, respectively). The fission-product R/B of gaseous isotopes measured independently for each of the AGR capsules can be used to investigate releases from both a failed particle and DU.

In addition to R/B data from the AGR irradiations, this analysis includes data from a few historical irradiations of LEUCO TRISO fuel conducted in the 1980s for comparison. These historical tests had either DTF particles or in-pile failures from which R/B data on fission-gas releases from UCO kernels could be obtained. The four key irradiations are: (1) HRB-17/18 (General Atomics 1987), (2) COMEDIE-BD1 (Richards 1994), (3) HFR-B1 (ORNL 1994), and (4) HRB-21 (DOE 1995). The R/B per exposed kernel for Kr-85m, from historical irradiations, is used to validate the *Equation* (7) model established using AGR-3/4 data.

2.3.1 Fission-gas Release

Each capsule has an independent gas line to route its helium/neon gas mixture to transport any fission gas released from the capsules to the corresponding FPMS detector (Figure 3). The FPMS detector is capable of detecting individual fuel-particle failures and providing release rates for the 12 gaseous radionuclides, as specified in SPC-1345, "AGR-3/4 Irradiation Test Specification." The summary of FPMS and release-data determination for the AGR-1 experiment is given in Scates (2010). This procedure is also used for all AGR irradiations. Each AGR capsule is continuously and independently monitored by a gross radiation detector and a spectrometer detector in the FPMS installed downstream from the capsule sweep-gas line (as shown in the bottom left of Figure 3).

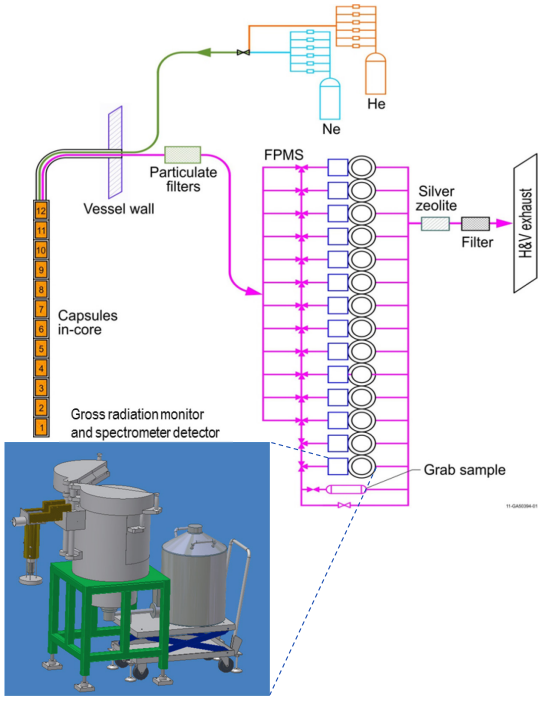

Figure 3. Simplified flow path for AGR-3/4 sweep gas (top) and a gross radiation monitor and spectrometer detector for each capsule (bottom).

Sweep gas carries released fission gases from the capsules to the detector system under normal conditions, with a transit time of about 150 seconds. Gas flow passes through a high-purity-germanium detector, gamma-ray spectrometer system. The continuous gamma-ray spectrum measurements from the high-purity-germanium detectors were used to compute the release activities of several isotopes of krypton and xenon. These measured activities were converted to capsule fission release rates by appropriate correction to account for decay that occurred during transport from the capsules to the detectors. Actual transport times were calculated from outlet-gas flow rates and the capsule-specific volumes through which samples flow to reach the respective monitoring detector. This conversion formula was derived under the assumption that the equilibrium release conditions were established (Scates 2010). This system provides the fission-gas release rate in individual capsules at 8-hour intervals. It also helps detect particle failure under irradiation.

2.3.2 Release-to-Birth Ratio per Failed Particle

The R/B per exposed kernel is calculated as the ratio between measured R/B and number of failed particles in a capsule for each of the krypton and xenon isotopes.

2.3.2.1 Fuel particle failures

For AGR capsules, fission gas release comes from three sources: (1) defective exposed kernels, (2) heavy-metal contamination, and (3) particle-coating failures under irradiation (in-pile failures). The number of initially exposed kernels and amount of heavy-metal contamination can be estimated based on characterization of as-manufactured compacts performed as part of fuel quality-control activities. Coated-particle in-pile failure is defined by the failure of both PyC layers and the SiC layer resulting in an exposed kernel (particle failure), such that the three coating layers cannot retain fission gases. In-pile failures are primarily due to manufacturing defects, such as a thin or missing buffer layer. In the AGR-1 experiment, R/B data confirmed the absence of in-pile particle failures. The PIE data also indicated that no through-particle failure was found (ORNL 2013; Demkowicz et al. 2015). This supports the claim that the in-pile failure among driver fuel particles is not likely.

During irradiation the in-pile particle failures in a capsule are detected using the capsule-specific gross-radiation monitor in the FPMS. The sweep gas carrying fission-gaseous species passes in front of the sodium iodide [NaI(Tl)] scintillation-detector-based gross-radiation monitor. This gross-radiation detector has the capacity to detect every fuel-particle failure, up to and including the first 250 failures from each capsule. These fuel particle failures are indicated by a rapid rise and drop (or spike) in the temporal profile of the measured gross gamma-count rate (as shown in Figure 4). Such spikes are the result of a sudden release of stored fission-product inventory inside a just-failed particle. The gross gamma data were used to count the number and record the time of particle failures.

Figure 4 depicts a classic example of a single particle failure that occurred in AGR-3/4 Capsule 10 on January 19, 2012. Before the failure occurs, the baseline count rate (B_{bf}) is equal to 3,239 counts per second (cps). At the time of failure, the rapid rise (peaking at 13,374 cps) and fall in activity were clearly observed for the event. After the failure, the new baseline count rate (B_{af}) increases to 3,788 cps (549 cps increase relative to before failure), which represents additional release from this failed particle. The release stabilizes after a particle failure in about 4 minutes, which is consistent with what was observed during the NPR-1A experiment (McIsaac et al. 1992). However, detection of in-pile particle failure is not always that simple, especially when there is uncharacteristically low fission-gas release following particle failure or multiple simultaneous failures. This occurred during AGR-3/4 irradiation and is described in Subsection 3.1.2.

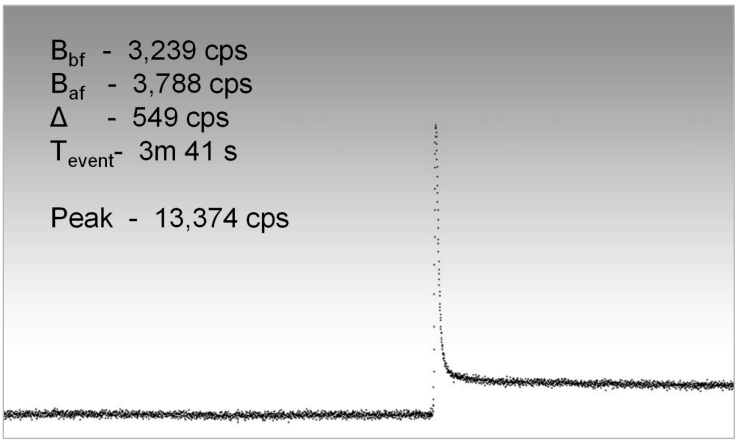

Figure 4. Classic particle failure.

2.3.2.2 Birth rate

By definition, the birth rate of an isotope is the rate of entire production for a specific isotopic atom, even if it is immediately lost to transmutation or decay. The isotope generation and depletion code ORIGEN is generally accepted as the standard for calculating the amount of fission-product species across the fuel zone (IAEA 1997). The isotope birth rates in each capsule are calculated from inventory data supplied using the MOCUP (MCNP-ORIGEN2 Coupled Utility Program) code that links neutronic data computed in Monte Carlo N-Particle (MCNP) to inventory data computed in ORIGEN2.2. For AGR irradiation, the JMOCUP (or Jim Sterbentz's MOCUP) was created functionally similar to the MOCUP for use in the birth-rate calculation (ECAR-2066). The birth-rate calculation used an ORIGEN2.2 depletion model, assuming no transmutation and decay for krypton and xenon isotopes. The JMOCUP simulation code uses daily averaged values of the ATR operating parameter inputs (such as lobe powers and control shim cylinder positions) to compute daily birth rates for many fission-gas isotopes, including krypton and xenon.

2.3.2.3 Release-to-birth ratio per exposed kernel

The R/B per exposed kernel is used for this analysis to compare the release behavior among the AGR capsules and historical experiments. This ratio can be expressed as:

$$R_p = \frac{\mathrm{R}_1}{B_1} \tag{15}$$

where R_p is R/B per exposed kernel, R_1 is release rate from one failed particle.

For an AGR capsule, assuming isotope release rate originated only from exposed kernels (neglecting release from DU), then this isotope release rate can be estimated as the product of R/B per exposed kernel and number of exposed kernel (or particle failures) as follows:

$$R = [R_p * B_1] * N_f \tag{16}$$

Here, $R_p * B_1$ represents release rate from a single exposed kernel according to *Equation* (15). Thus, R/B per exposed kernel can be calculated from the release rate, birth rate per particle, and number of failed particles as follows:

$$R_p = \frac{\mathrm{R}}{B_1 * N_f} \tag{17}$$

Substituting release rate from the entire capsule (R) in *Equation* (11) to *Equation* (17), the birth rate per single particle in both numerator and denominator is cancelled, and so, R/B per particle can be estimated from the reported R/B as follows:

$$R_p = \frac{[R/B]\times N}{N_f} \quad (18)$$

In the case when only one failure occurred in a capsule, then the product $[R/B] \times N$, indeed, represents R/B per a failed particle.

2.3.2.4 Data selection for fission gas release analysis

To reduce measurement uncertainty of the release rate used in this analysis, the krypton and xenon isotopes selected for regression analysis have a sufficiently short half-life to reach equilibrium in the capsule, but also a half-life long enough to provide a measureable signal in the FPMS detector. It is also important that only R/B data captured during capsule-equilibrium condition are used for regression analysis. This satisfies the condition of *Equation* (4) and ensures that the measured release rates at the downstream detector reflect the true release rate in the capsule. During reactor outages, test fuel temperature drops to around 30°C. Subsequently, the diffusion coefficients of the fuel kernel and surrounding material also decrease substantially. Thus, fission-product species resulted from beta decay during this time will accumulate within fuel particles. After reactor startup, fuel temperature rapidly increases to more than 1,000°C, allowing accumulated fission products to diffuse out of failed particles into the sweep-gas flow. Therefore, during this time, the release rate of isotopes of interest is higher than at a steady-state condition. Longer outages lead to larger fission-product accumulation, which leads to a longer time for the capsule to reach release equilibrium. As a result, data from the first 10 days after long outages between reactor cycles and data from the first 3 days after short outages within a reactor cycle are excluded.

All AGR R/B records are accompanied by measurement uncertainty estimated by the FPMS data generators. These records also provide the requirements for storage and display of FPMS data within the Nuclear Data Management and Analysis System database. These requirements prevent the use of data with high-measurement uncertainty in the analysis of fission-gas release data. As a result, the negative values and values where uncertainties are greater than 50% are omitted. These data filters remove data from the "short" leadout flow runs or measurements that were incomplete, while leaving other runs that have enough counting statistics unaffected.

After data cleaning, the isotopes Kr-85m, Kr-87, Kr-88, Xe-135, Xe-137, and Xe-138 were selected because the data acquired for them was adequate for use in this analysis.

2.3.3 Calculated Fuel Temperature

ABAQUS-based (Version 6.8-2), three-dimensional, finite-element thermal models are created for each capsule of the AGR experiments to predict daily averages of fuel compact and TC temperatures for the entire irradiation period when the ATR core is at power. The detailed model description was reported in ECAR-968, "AGR-1 Daily As-run Thermal Analyses," ECAR-2476, "AGR-2 Daily As-run Thermal Analyses," and ECAR-2807, "AGR-3/4 Daily As Run Thermal Analyses." The ABAQUS-based thermal model uses an approximate 350,000 eight-node hexahedral-brick finite-element mesh to estimate capsule temperature profiles for each day during the entire irradiation period.

The capsule temperature profiles are shown in the typical cutaway view of three fuel stacks presented in Figure 5 for one AGR-1 capsule (Hawkes et al. 2015). Fuel temperatures in one capsule can vary spatially by more than 200°C for each time step (e.g., 750 to 1013°C range, as shown in Figure 5). Because location of heavy metal contamination is spread throughout the fuel compacts, the temperature was assumed to be equal to volume-averaged fuel temperature for AGR-1 capsules. For AGR-3/4 capsules, each AGR-3/4 capsule has only one fuel stack that consists of four compacts. The majority of the compact temperatures are between 820 and 870°C (green to dark orange), as shown in Figure 6, for Capsule 12 compacts (ECAR-2807, Revision 1). The DTF fuel particles were inserted along the centerline of each compact, where temperatures are the hottest (Figure 6). Therefore, the failed-particle temperature for AGR-3/4 was considered to be the average temperature of compact centerlines.

Revision 0 of this report used fuel temperatures taken from the ECAR-2087, Revision 0, in which the variable gas gap models used in the thermal model were based on graphite shrinkage from the AGR-1 experiment. Then, the PIE dimensional measurements of AGR-3/4 capsules are used to estimate the end of irradiation gap sizes for the four gaps, and thermal analysis was revised in ECAR-2807, Revision 1, which predicted fuel temperatures approximately 20ºC higher than Revision 0. Both Revisions 1 and 2 of the R/B analysis report use fuel temperatures reported in the ECAR-2807, Revision 1.

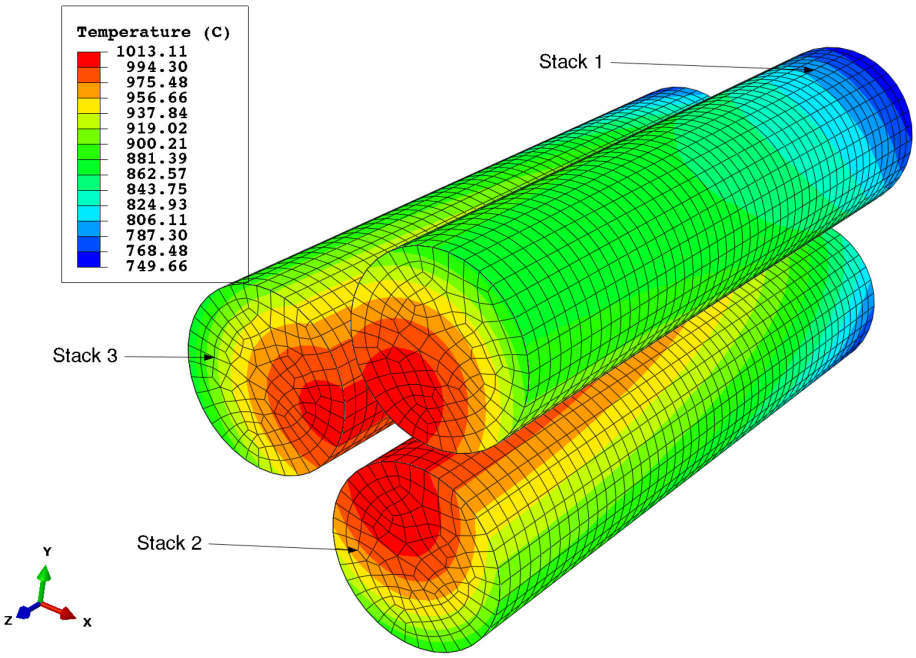

Figure 5. Temperature distribution in cutaway view of three fuel stacks of one AGR-1 capsule.

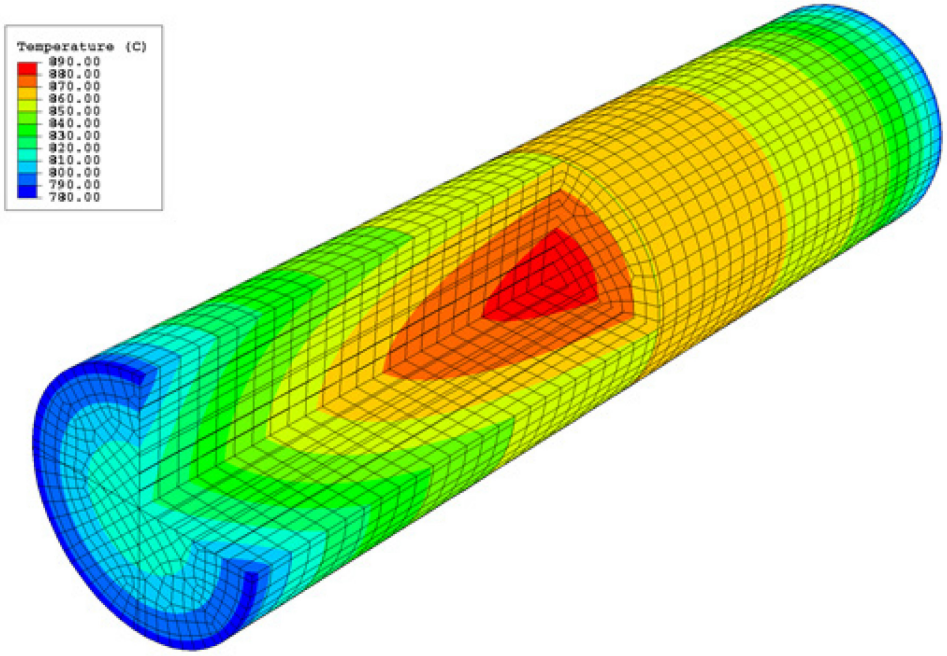

Figure 6. Temperature distribution in cutaway view of a fuel stack of AGR-3/4 Capsule 12.

3. ADVANCED GAS REACTOR-3/4 IRRADIATION USED FOR RELEASE TO BIRTH RATIO MODEL

3.1 Advanced Gas Reactor-3/4 Irradiation

AGR-3/4 is the combination of the third and fourth planned experiments to test TRISO-coated low-enriched uranium fuel. A detailed description of the experiment and results are provided in (Collin et al, 2018). Figure 7 depicts a schematic view of AGR-3/4 capsules.

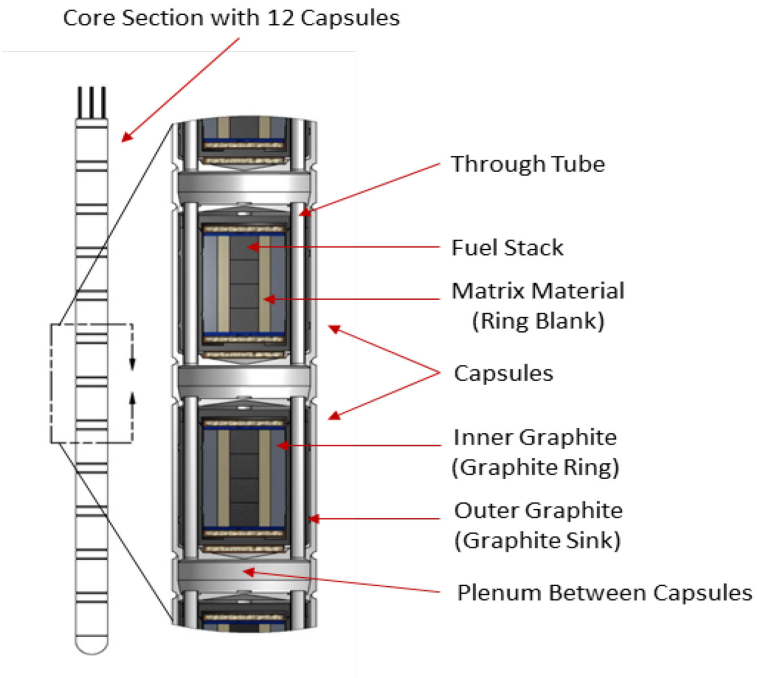

Figure 7. Drawing of AGR-3/4 capsules.

AGR-3/4 was composed of 12 independently controlled and monitored capsules, stacked on top of each other. Each capsule contained four 3.81-cm long compacts (Figure 7). Each fuel compact contained about 1,872 conventional UCO driver-fuel coated particles and 20 DTF UCO fuel particles. A leadout tube held the experiment in position and contained and protected the gas lines and TC wiring extending from the test train to the reactor penetration. Three TCs were located in Capsules 5, 10, and 12, and two TCs were in the remaining capsules. To control fuel temperature in each capsule, a variable mixture of helium/neon flow from a capsule specific mass-flow controller was delivered in response to variation of fuel fission power during the entire irradiation period.

3.1.1 Condition of Irradiated Fuel Particles

The ongoing AGR-3/4 PIE process has not yet determined the actual particle failure counts for the 12 capsules and will not be able to differentiate whether failures were from DTF or driver particles. However, the expected numbers of exposed kernels among the driver fuel particles and equivalent exposed kernels due to heavy-metal contamination were negligible based on the quality-control data presented in Table 1. Also, based on the AGR-1 PIE results (Demkowicz et al. 2015), it is reasonable to assume that there were no in-pile particle failures among the qualified driver fuel particles. Thus, it is reasonable to assume that all particle failures are DTF; subsequently, the total of failures in each capsule are capped at a maximum of 80 failures.

3.1.2 Number of Failed Particles

The in-pile failures of DTF particles in a capsule are detected using the independent capsule-specific NaI(Tl) total radiation detector. A particle failure is considered when a fuel kernel is exposed, allowing for gaseous fission-products release from the particle coatings. Even though the detector is sensitive to each fuel-particle failure, visually counting the exact number of failed particles during the AGR-3/4 irradiation was a challenging task due to multiple failures of DTF fuel particles occurring simultaneously, partial failures, and high background activity of releases from already failed particles. Figure 8 shows two examples of multiple-failure gross-gamma spectra. The top plot shows an example of a clean multiple-failure gross-gamma spectra. This spectra data set was collected from Capsule 7 on December 29, 2011; DTF particles began to fail only 16 days after the start of AGR-3/4 irradiation. Each failure event is clearly defined by a rapid rise and fall in activity, with a distinct increase in baseline count rate after each event. The area in the oval and its detail plot on the top left represent one such instance where two consecutive failures occurred. This double failure is further confirmed by the large-step increase in baseline count rate after the event. During this 8-hour period, five particle failures clearly occurred.

The bottom plot in Figure 8 shows an example of unclean multiple-failure gross-gamma spectra. This spectra output was collected from Capsule 9 on December 10, 2013, near the end of the AGR-3/4 irradiation, when all DTF particles in Capsule 9 were believed to have already failed. Multiple peaks are present in this output profile. However, as the baseline increases over time, and more fuel has failed, it becomes difficult to distinguish a failure from a burp (a small instantaneous release from a bubble of fission gases). By closely reviewing the baseline of the 8-hour period here, it can be argued that there are between one and three failure events. Also, the failed particles do not always provide a uniform, steady release of fission gas; they sometimes give little bursts. This makes true particle failure difficult to distinguish.

The challenges in the failure-detection process lead to high uncertainty in the total number of particle failures in some capsules. Therefore, each inspection period provides three estimates of failure counts: (1) best-estimate, (2) maximum, and (3) minimum. For Capsule 1 (Figure 9), the three failure estimates are quite different from each other, indicating high counting uncertainty. By contrast, for Capsule 9 (Figure 10), the three failure estimates are very similar (especially during the first 300 effective full-power days [EFPDs]), indicating low counting uncertainty or high confidence about the number of particle failures. Toward the end of irradiation, when failure counts in this capsule were high, the maximum counts increased more, indicating higher counting uncertainty in this capsule due to high background activity. Table 2 shows the final failure counts at the end of irradiation in each of 12 capsules. The number of failure counts capped at 80 because that's the number of DTF particles in a capsule (red numbers) for the purposes of this analysis. Here, Capsule 1 showed the largest difference between minimum and maximum failure counts and Capsule 9 had the highest number of failures; all three counts were capped at 80.

Table 2. Capsule best-estimate, minimum, and maximum failure counts at the end of irradiation.

Capsule	1	2	3	4	5	6	7	8	9	10	11	12
Best-estimate	41	80	80	76	54	47	52	78	80	47	69	40
Minimum	21	51	53	57	36	42	38	54	80	36	48	39
Maximum	80	80	80	80	80	53	75	80	80	75	80	49

Table 3 presents actual accumulative best-estimate failure counts calculated from weekly counts, and Figure 11 plots the daily interpolated best-estimate failure counts as a function of EFPDs for 12 AGR-3/4 capsules. For most capsules, fuel failures occurred soon after the start of irradiation in the first cycle (i.e., the first 55 EFPDs). For a few other capsules (e.g., Capsules 2 and 3), fuel failures occurred throughout irradiation. Capsules 2, 3, and 9 had actual best-estimate failure counts greater than 80.

Table 3. Weekly cumulative estimated number of failed particles in AGR-3/4 capsules.

Date	14-Dec-11	21-Dec-11	28-Dec-11	4-Jan-12	11-Jan-12	18-Jan-12	25-Jan-12	2-Feb-12	8-Feb-12	3-May-12	15-Jan-13	7-Jul-13	10-Oct-13	11-Jan-14	9-Apr-14
Capsule	151A									151B	152B	154A	154B	155A	155B
12	0	1	1	1	1	6	23	35	40	40	40	40	40	40	40
11	0	0	0	2	10	18	25	44	57	66	66	67	69	69	69
10	0	0	5	9	19	44	47	47	47	47	47	47	47	47	47
9	0	1	19	33	56	78	79	79	79	79	83	83	85	90	90
8	0	0	25	35	52	66	66	66	66	66	67	67	68	73	78
7	0	0	31	34	37	39	39	42	42	43	50	52	52	52	52
6	0	2	13	30	43	44	44	44	44	45	45	45	45	46	47
5	0	0	8	16	33	40	40	40	40	40	40	40	45	47	54
4	0	1	11	27	45	58	58	58	58	62	71	71	71	71	76
3	0	0	7	13	13	21	27	29	29	54	71	72	94	96	96
2	0	0	0	7	17	24	32	45	50	51	60	66	82	86	91
1	0	0	0	1	2	8	20	25	30	39	39	39	39	39	41

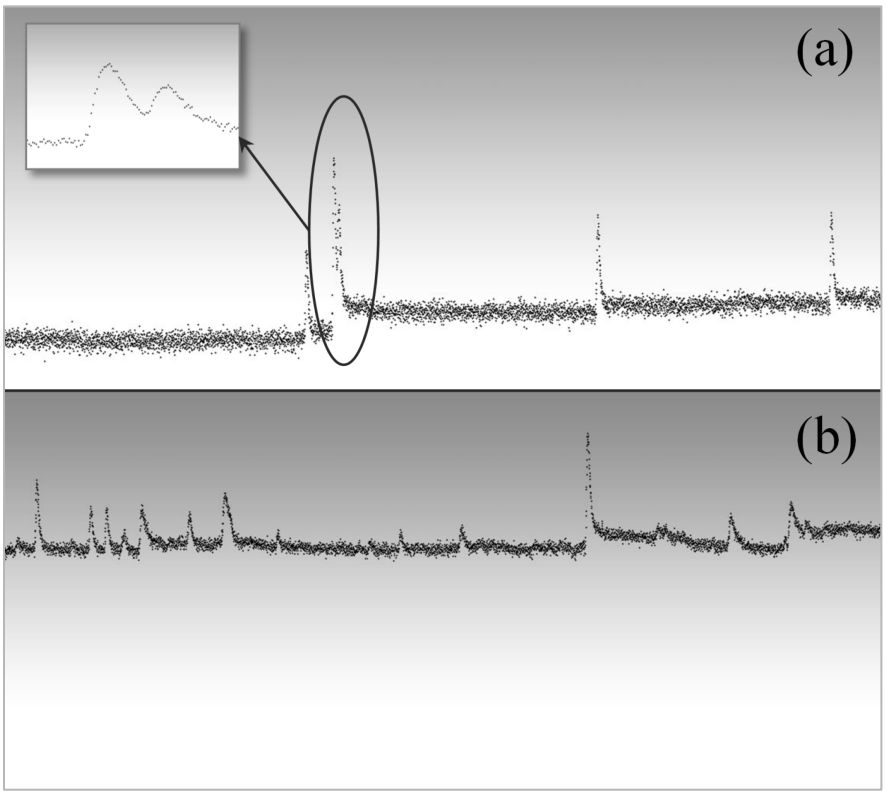

Figure 8. Examples of multiple failure gross gamma spectra: (a) “clean” multiple failure and (b) “unclean” multiple failure.

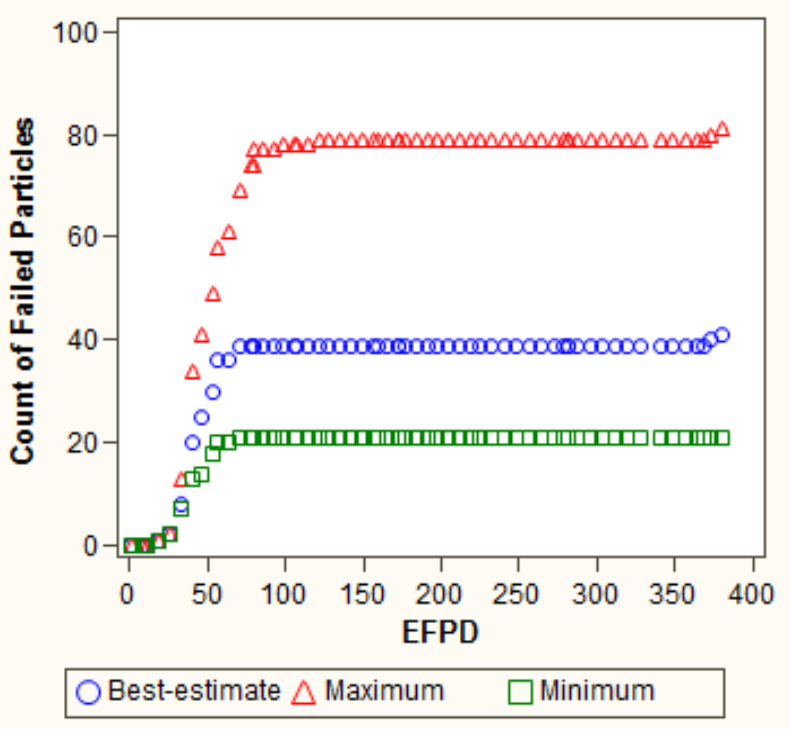

Figure 9. High uncertainty of particle failure count in Capsule 1.

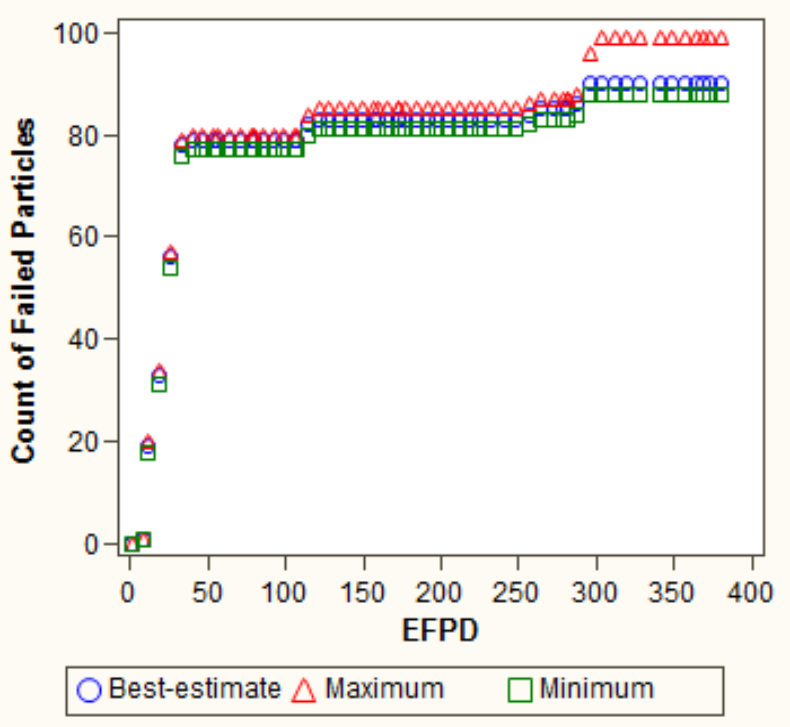

Figure 10. Low uncertainty of particle failure count in Capsule 9.

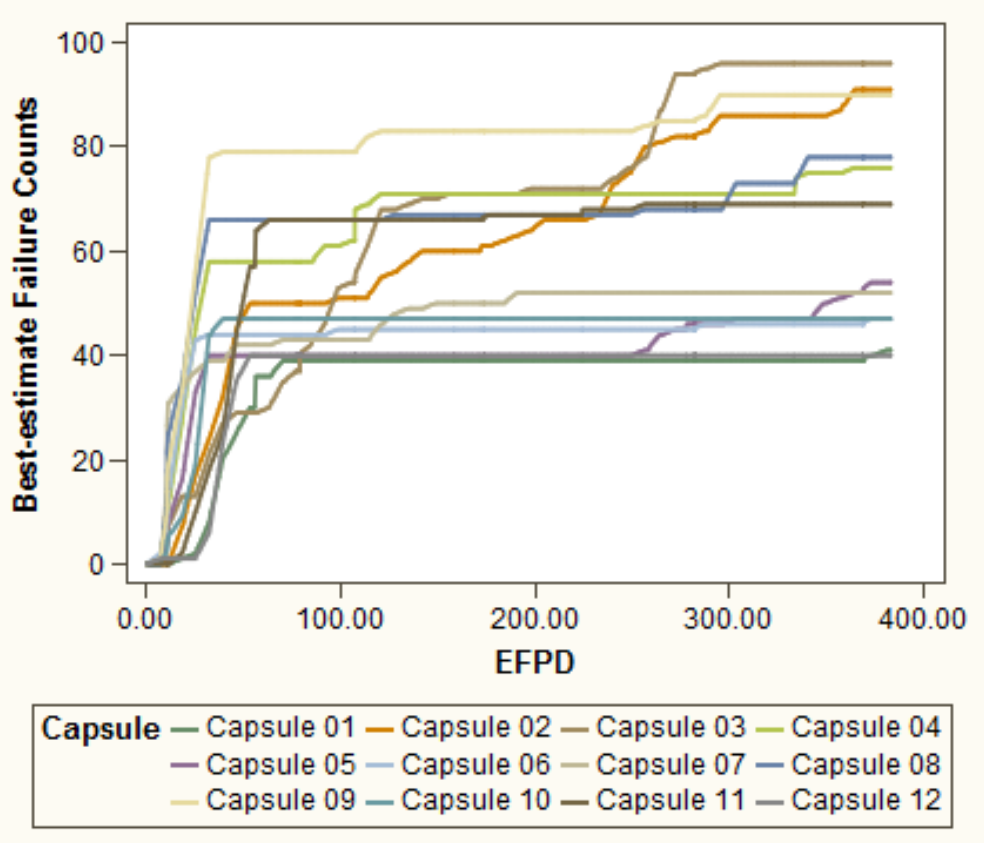

Figure 11. AGR-3/4 best-estimate failure counts.

3.1.3 Calculated Fuel Temperatures

A daily as-run thermal analysis was performed for AGR-3/4 capsules using the commercial finite-element heat-transfer code ABAQUS (ECAR-2807, Revision 1). In the previous version of this report (Revision 1) peak fuel-compact temperatures calculated for each capsule were used in the regression analysis. Figure 12 shows a profile of calculated centerline temperature of four compacts in Capsule 5 for one day during irradiation, with the red portions showing approximated locations of 80 DTF particles in this capsule (Collin 2017). The profile demonstrates that the DTF particles would have been exposed to a range of temperatures that is lower than the peak value. In this revision, calculated temperature averaged from temperatures along the whole centerline of four compacts in each AGR-3/4 capsule is used for R/B data analysis. This is because orientations of compacts in a capsule are not preserved, so the vertical locations of DTF particles are not exactly known.

Generally, variation of centerline temperatures (Figure 12) in the four compacts from Capsule 5 was among the highest variation representing capsules in the middle of the test train. The centerline temperature variation was lower in the top and bottom capsules. The differences between the capsule-average centerline and peak fuel temperatures presented in Figure 13 ranged from 20 to 60˚C, with lowest differences in the top (Capsule 12, yellow symbols) and highest differences in the middle (Capsule 5, purple symbols). The impact of slightly lower compact-average centerline temperatures relative to peak fuel temperature (less than 5%) on R/B correlation will be demonstrated in Section 3.3 by showing Revisions 1 and 2 parameter estimates side-by-side.

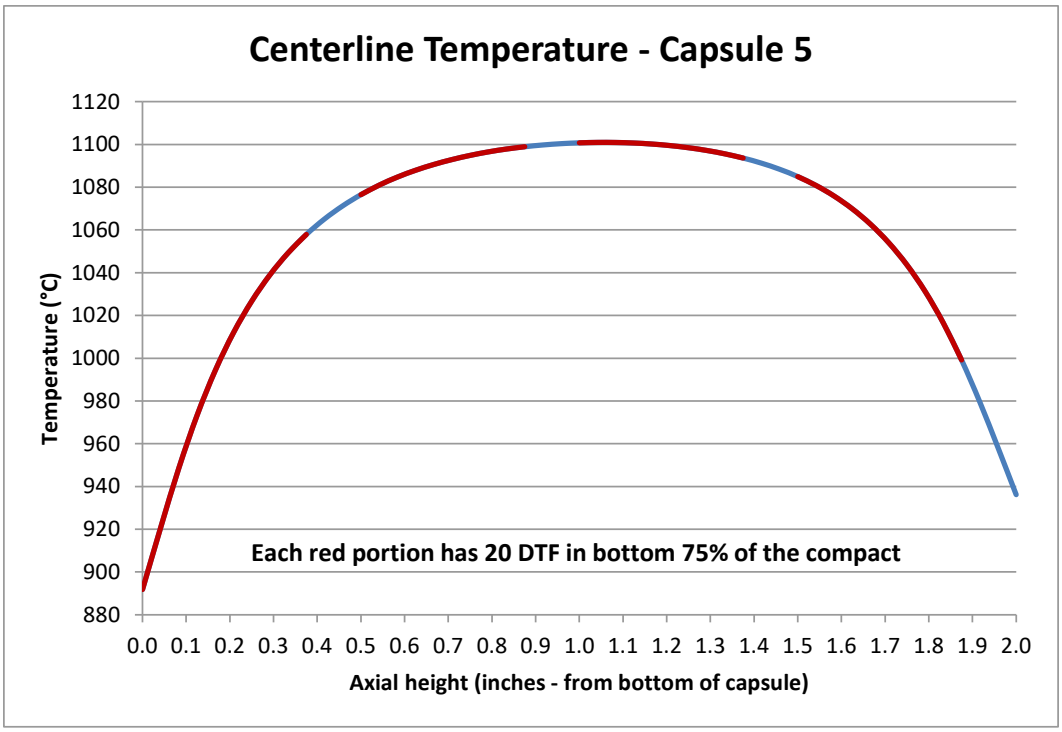

Figure 12. Profile of centerline temperature of four compacts in Capsule 5 with the red portions showing locations of 80 DTF particles (Collin 2017).

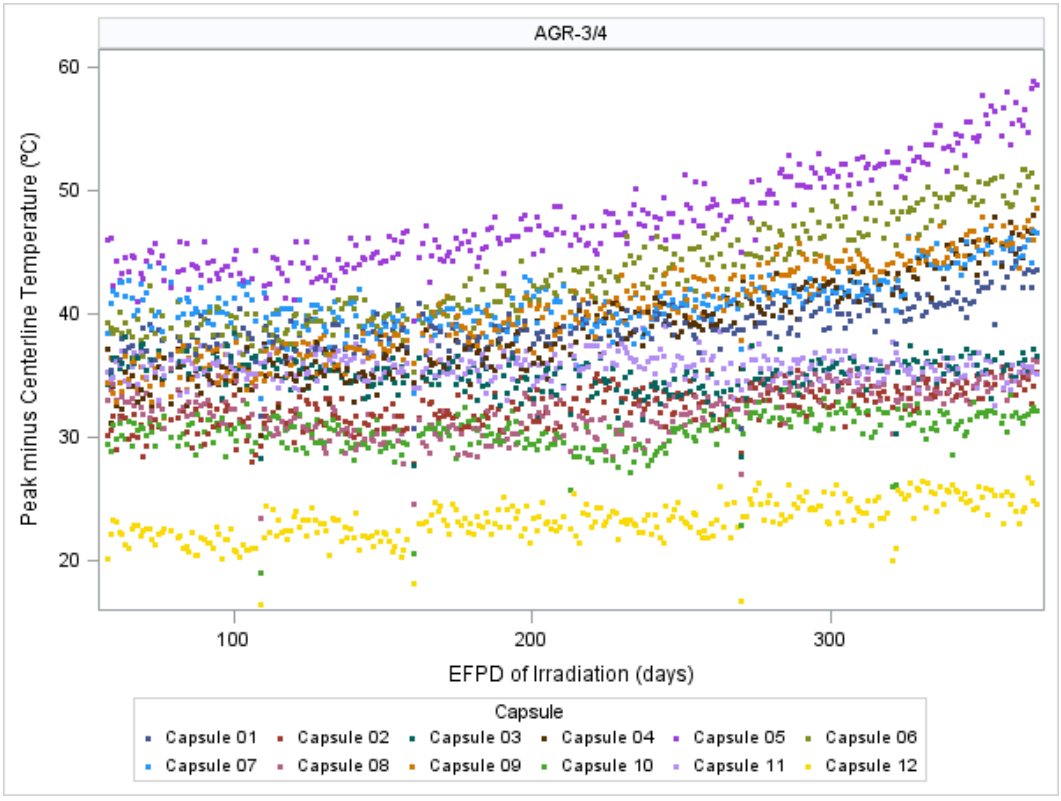

Figure 13. Differences between the capsule-average centerline and peak fuel temperatures.

There are three distinct groups of fuel temperatures among the 12 AGR-3/4 capsules. Figure 14 shows daily calculated capsule-averaged centerline temperatures in 12 capsules as a function of EFPDs for the entire irradiation (data not used in the analysis are excluded from all plots). The calculated centerline temperatures range broadly from 844°C (lowest temperature in Capsule 12 as shown by blue dots in the top frame of Figure 14) to 1,545°C (highest temperature in Capsule 7 as shown by red dots in the bottom frame of Figure 14). This wide fuel-temperature range provides adequate data to establish the relationship between R/B per exposed kernel and temperature. However, the goal of this experiment is to keep the fuel temperature in each capsule as uniform as possible, both spatially and temporally, in order to maintain equilibrium conditions for fission-gas releases.

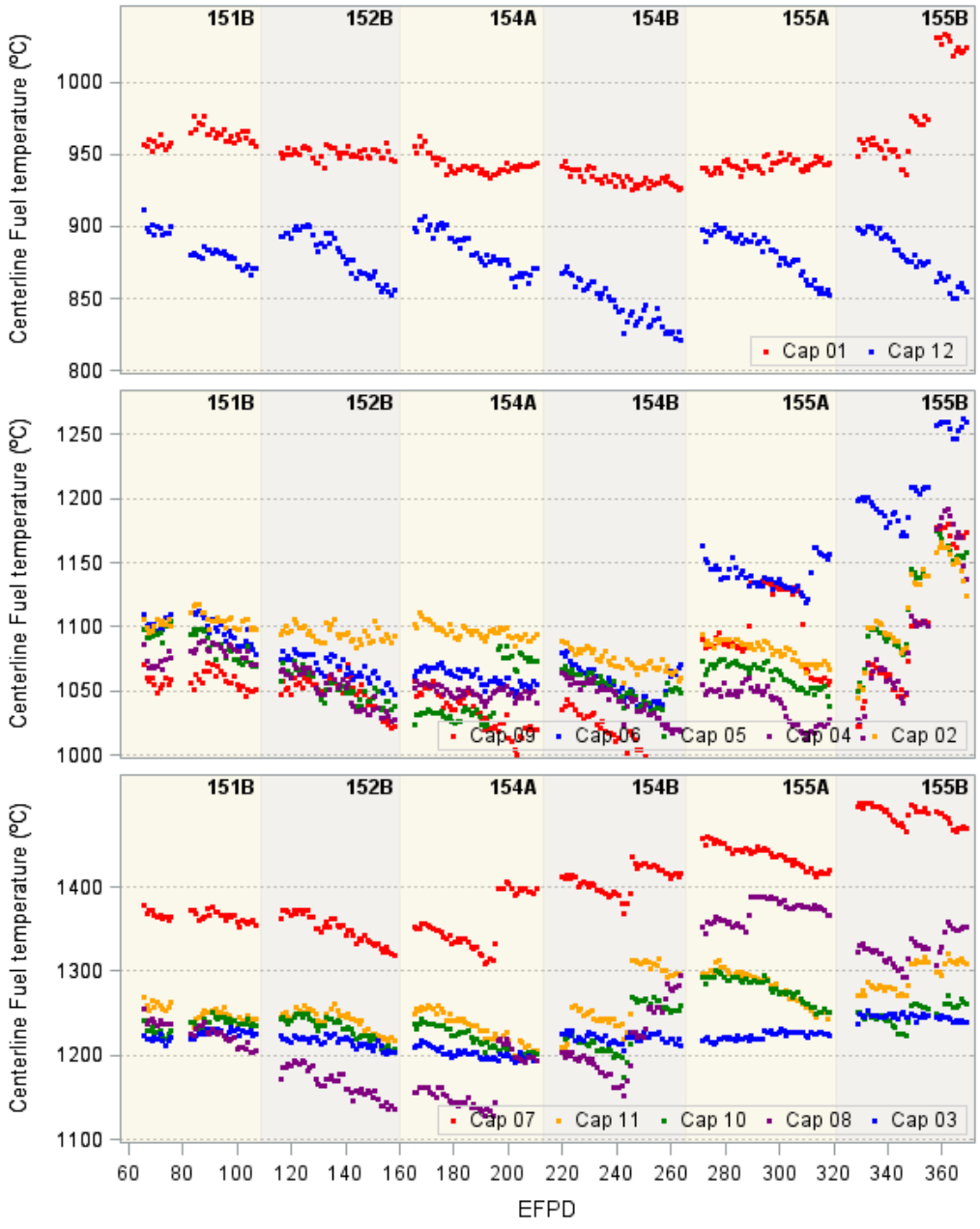

Figure 14. Daily capsule-average centerline temperatures for AGR-3/4 capsules.

3.1.4 Release-to-Birth Ratio per Exposed Kernel

The qualification status of AGR-3/4 R/B data was reported in ECAR-2457. As stated in the previous subsection, it is essential that equilibrium is achieved for the measured release rates at the downstream detector to reflect the true release rate in the capsule. Thus, only R/B data during fission-product release equilibrium are used for this analysis. The R/B data excluded from regression analysis are:

1. The first cycle (151A): about 60% of all DTF fuel particles failed by the cycle's end, which led to high uncertainty of daily failed-particle counts. This is because failure counts were made on a weekly basis, and the daily failure count had to be estimated by interpolation from weekly values. In addition, equilibrium may not have been achieved due to multiple particle failures throughout the cycle and rapid changes of material thermal properties due to fast-fluence exposure. This causes large variation of R/B per exposed kernel during the first cycle.
2. The first 10 days after each reactor startup following a long cycle outage and the first 3 days after a short, unplanned outage to avoid higher-than-normal fission-product releases after each reactor outage due to their accumulation at much lower temperature.

In addition, R/B data with uncertainty greater than 50% are also excluded. This exclusion largely eliminated R/B data acquired for intervals that are too short (a 20-minute instead of an 8-hour interval). After these exclusions, the uncertainties of suitable R/B data for selected krypton and xenon isotopes are around 6% (as presented in Table 4), except for the shortest isotope, Xe-137, with uncertainty greater than 10%.

Figure 15 and Figure 16 show daily averaged R/B per exposed kernel data for three krypton isotopes (Kr-85m, Kr-87, and Kr-88) obtained in Capsules 1 through 12 as a function of EFPDs during the six ATR cycles included in this analysis. Figure 17 and Figure 18 show daily averaged R/B per exposed kernel for three xenon isotopes (Xe-135, Xe-137, and Xe-138). Table 5 shows the statistics including average, minimum, and maximum values of R/B per exposed kernel of six selected isotopes. The R/B per exposed kernel data in the plots and summary table were calculated using the best-estimate failure counts. The R/B per exposed kernel for krypton isotopes varies widely in the range of 0.13 to 7.24%; the xenon R/B per exposed kernel is lower, in the range of 0.02 to 3.64%. The R/B data for AGR-3/4 irradiation showed that the fission products of isotopes with lower decay constants (e.g., Kr-85m among krypton isotopes or Xe-135 among xenon isotopes) are consistently released at a higher rate for the entire time relative to isotopes with a higher decay constant. This indicates the impact of decay constants on fission-product releases. Also, the temporal R/B plots for all isotopes are parallel with each other, indicating that R/B differences across isotopes are fairly constant despite changes in fuel temperatures. This fact demonstrates good consistency in the measurements of the FPMS for the AGR-3/4 capsules.

The R/B per exposed kernel correlation with fuel temperature is observable when comparing R/B temporal plots in Figure 15 through Figure 18 and fuel temperature plots in Figure 14. Especially during the last cycle, Cycle 155B, the R/B per exposed kernel increased in response to a notable increase in peak fuel temperatures in most capsules.

Table 4. AGR-3/4 R/B uncertainty statistics, decay constants, and half-lives for selected krypton and xenon isotopes.

Isotope	Uncertainty [a] (%)			Decay Constant λ (s^{-1})	Half-life (s)
	Mean	Minimum	Maximum		
Kr-85m	6.1	5.8	38	4.30E-05	16,127 (4.5h)
Kr-87	6.0	5.9	9.5	1.52E-04	4,560 (76mn)
Kr-88	5.9	5.8	6.6	6.78E-05	10,223 (2.8h)
Xe-135	6.1	5.8	26.3	2.12E-05	32,767 (9.1h)
Xe-137	14.1	10.2	17.8	3.01E-03	230 (3.8mn)
Xe-138	6.8	6.3	8.2	8.19E-04	846 (14.1mn)

a. Only R/Bs with uncertainty less than 50% and a standard 8-hour interval are used.

Table 5. Summary of AGR-3/4 R/B data used in analysis for selected krypton and xenon isotopes.

Isotope	N# of Daily R/B Values	R/B per exposed kernel		
		Average	Minimum	Maximum
Kr-85m	3,078	1.96E-02	2.12E-03	7.24E-02
Kr-87	3,078	1.33E-02	1.32E-03	5.99E-02
Kr-88	3,078	1.58E-02	1.67E-03	6.52E-02
Xe-135	3,078	8.52E-03	6.59E-04	3.64E-02
Xe-137	3,078	1.86E-03	1.51E-04	1.16E-02
Xe-138	3,078	4.11E-03	2.80E-04	2.35E-02

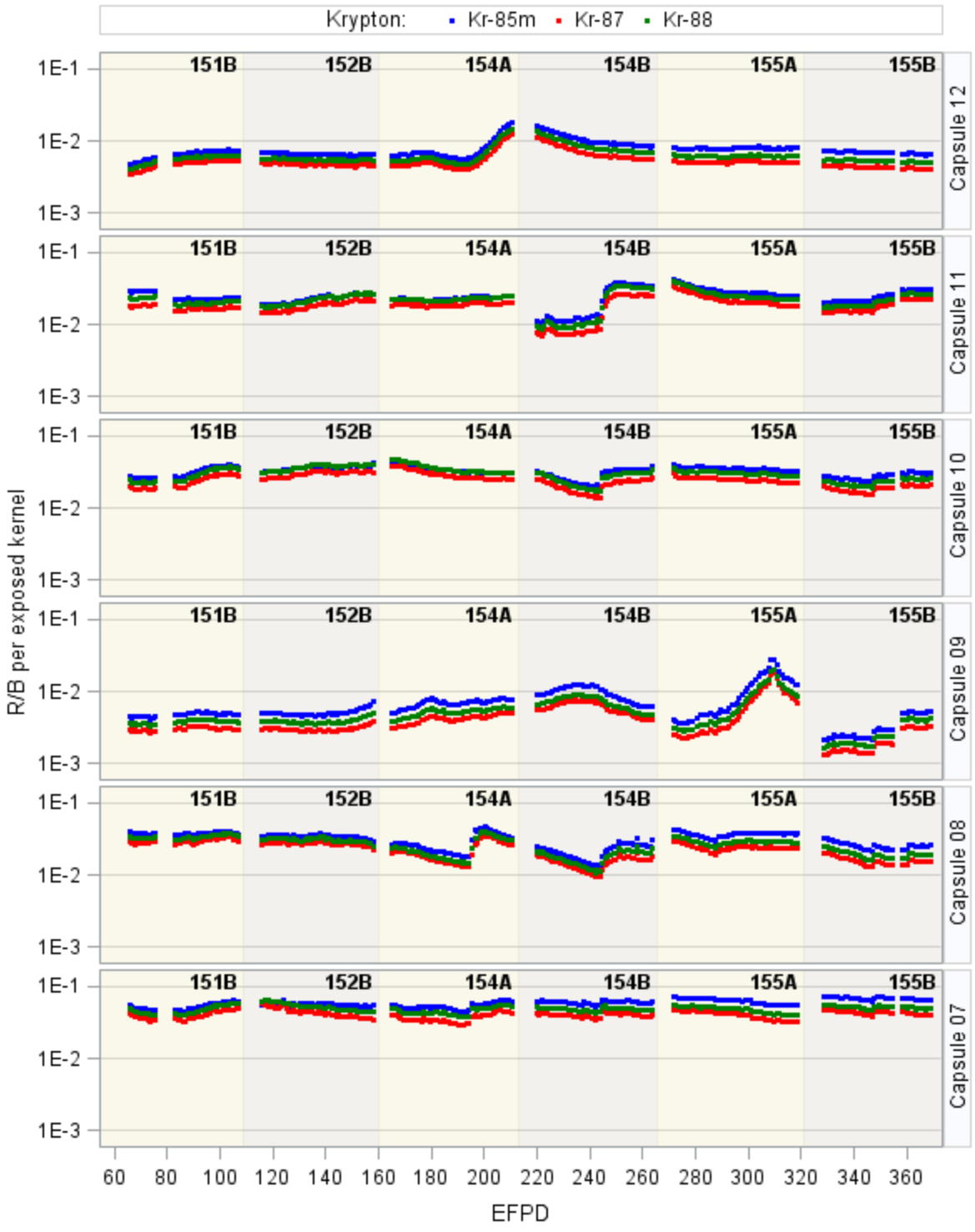

Figure 15. R/B per exposed kernel for krypton isotopes in AGR-3/4 Capsules 7 through 12.

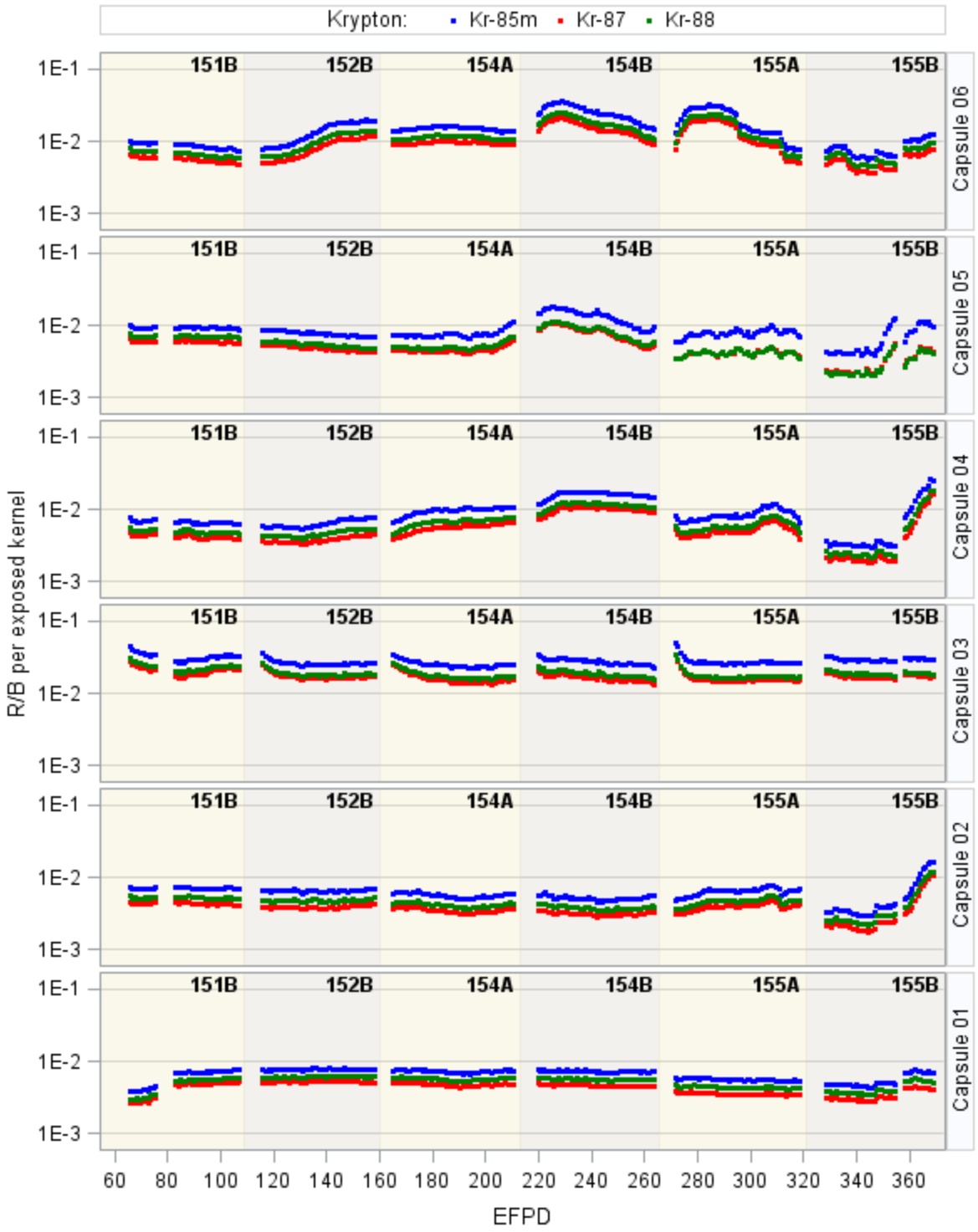

Figure 16. R/B per exposed kernel for krypton isotopes in AGR-3/4 Capsules 1 through 6.

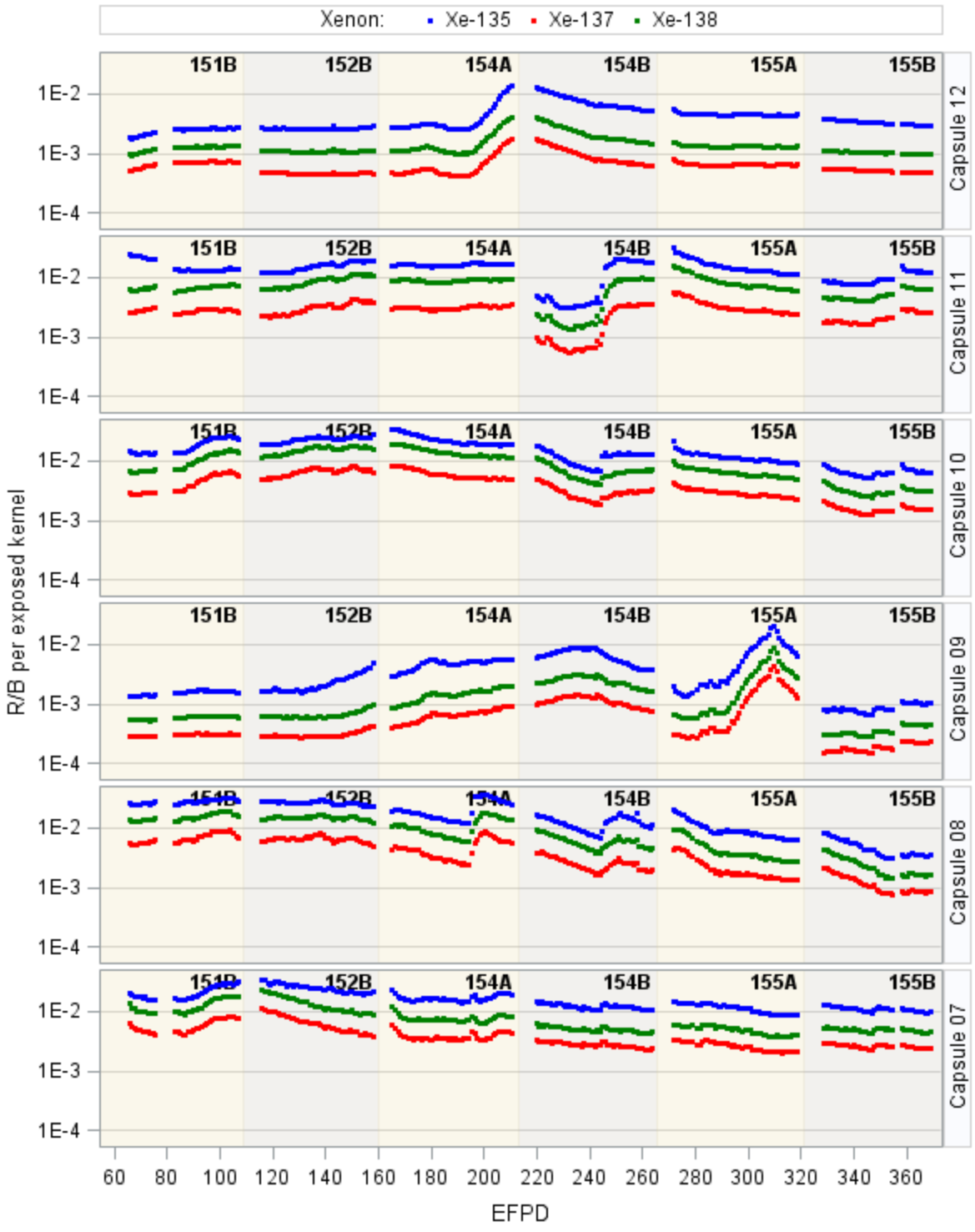

Figure 17. R/B per exposed kernel for xenon isotopes in AGR-3/4 Capsules 7 through 12.

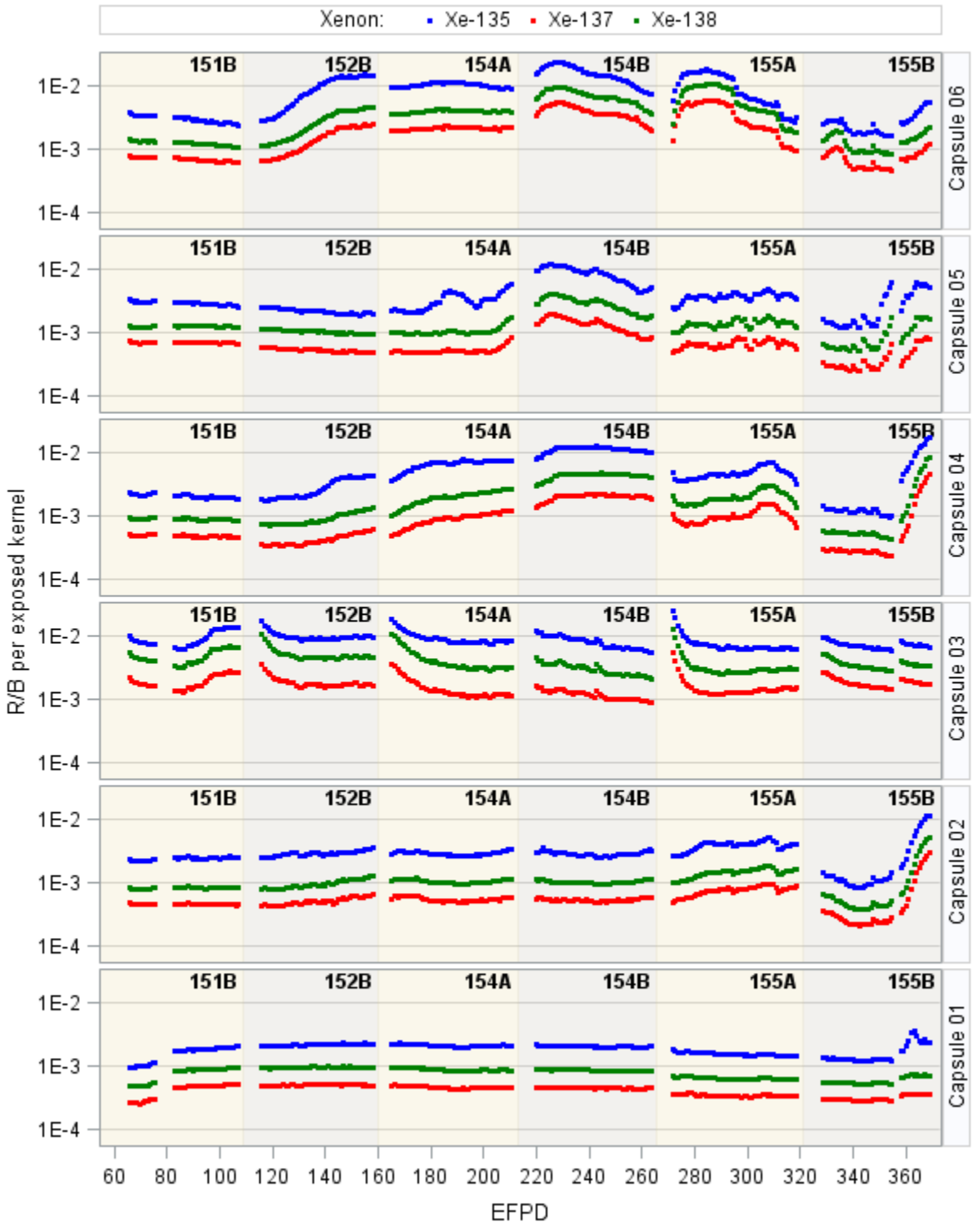

Figure 18. R/B per exposed kernel for xenon isotopes in AGR-3/4 Capsules 1 through 6.

3.2 Release-to-Birth Ratio Correlation with Decay Constants

As specified in Subsection 2.1.2.3, the n values for TRISO-coated fuel particles can range between 0.1 and 0.5, depending on the recoil effect of the particle coatings. For a constant fuel temperature, *Equation* (7) can be rewritten as:

$$\ln R_p = n \ln \frac{1}{\lambda} + C' \tag{19}$$

where C' is a new constant, including the reciprocal fuel-temperature term. In order to study the correlation between fission-product releases and decay constants, a few sets of R/B per exposed kernel data for selected krypton and xenon isotopes were taken for 2 days: one representing low burnup for a day near the start of irradiation (second cycle, Cycle 151B) and one representing high burnup (up to 15%) for a day near the end of irradiation (last cycle, Cycle 155B). For each capsule, assuming the fuel temperature is constant during a day, the n value can be estimated as the slope between $\ln R_p$ and $\ln \frac{1}{\lambda}$ for isotopes of each gas element (i.e., krypton or xenon). Because centerline fuel temperatures are quite different across AGR-3/4 capsules, these sets of R/B can help reveal the impact of fuel temperature and burnup on n values. Figure 19 illustrates the slopes for three fuel temperatures (see legend) and two burnup levels (Cycles 151B and 155B) for krypton and xenon elements. This figure also includes a data set in the COMEDIE test presented in Table 10 (purple stars).

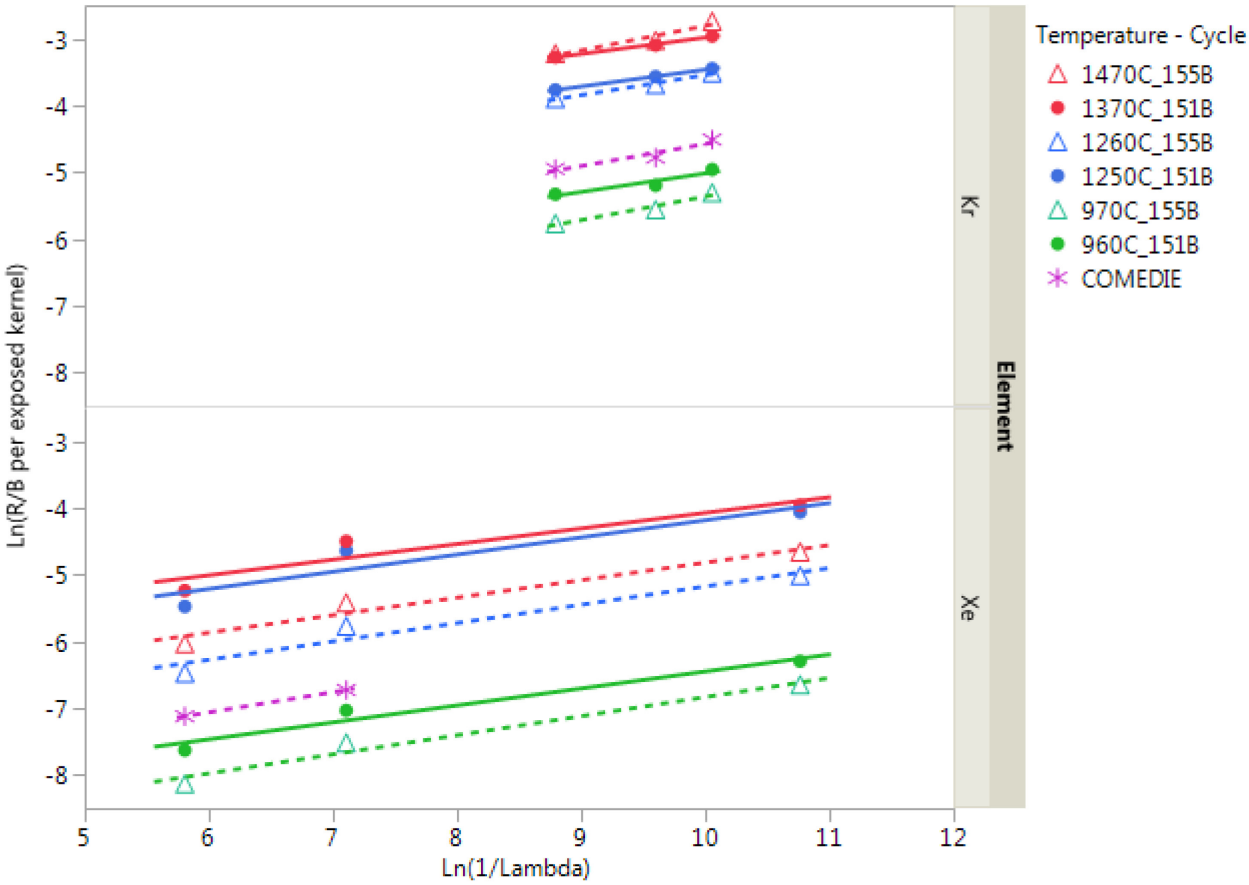

Figure 19. Slopes between ln R/B per exposed kernel and ln 1/λ for different temperatures and burnup.

All fitted lines in Figure 19 are quite parallel for both krypton and xenon isotopes, indicating that temperature and burnup have no significant influence on n values. Also, the slopes of AGR-3/4 R/B data

are similar to the slope of the COMEDIE R/B data (purple dashed lines). Figure 20 and Figure 21 show daily *n* values for krypton and xenon isotopes for the 12 AGR-3/4 capsules as a function of EFPDs. In general, *n* values for krypton isotopes (blue dots) and for xenon isotopes (red dots) are comparable and, on average, equal to about 0.3. For AGR-3/4, the *n* values are fairly constant over the entire irradiation (excluding the first cycle), indicating no significant burnup influence on fission product release, when the peak burnup reached as high as 15.3% fissions per initial metal atom.

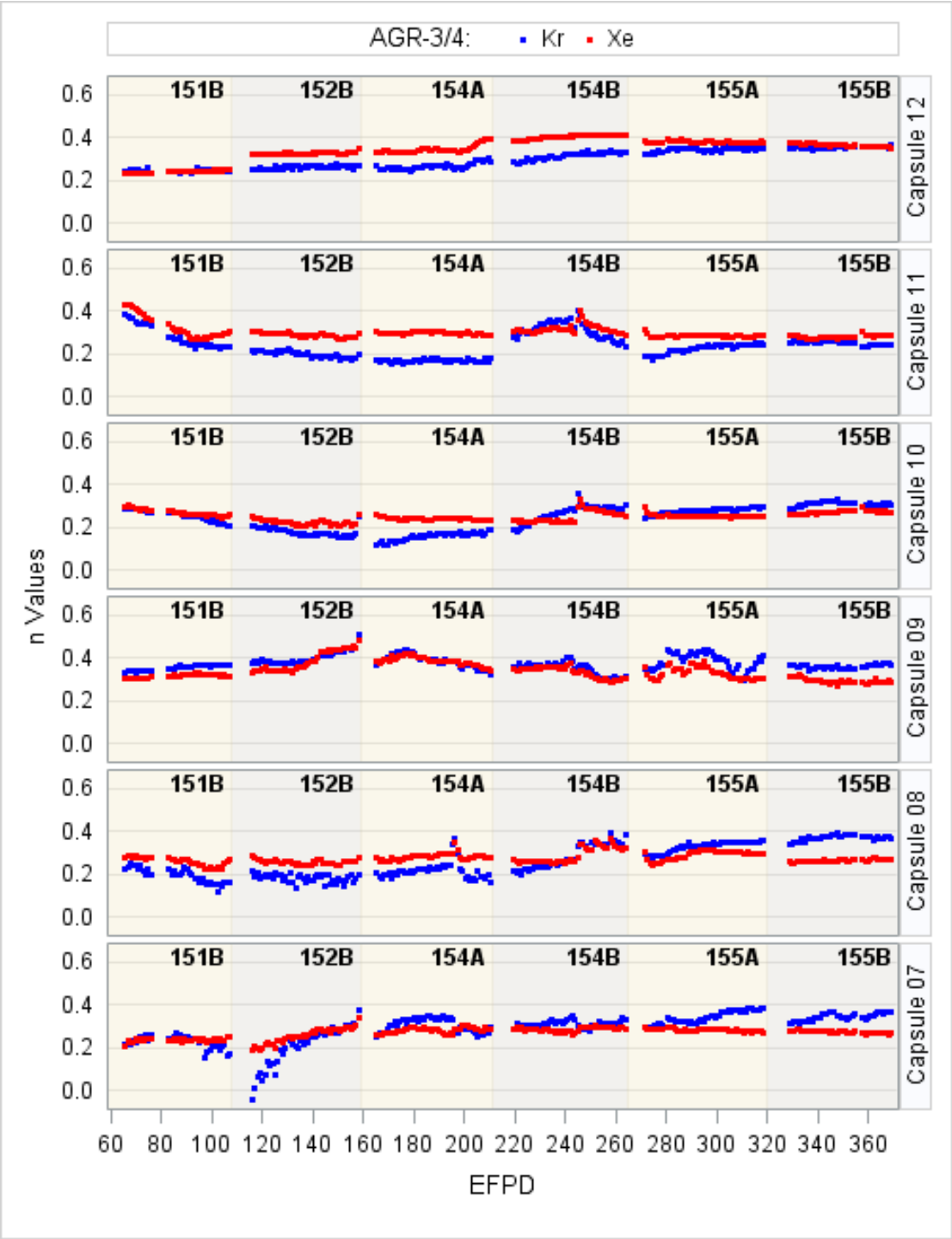

Figure 20. Krypton and xenon *n* values as function of EFPDs for AGR-3/4 Capsules 7 through 12.

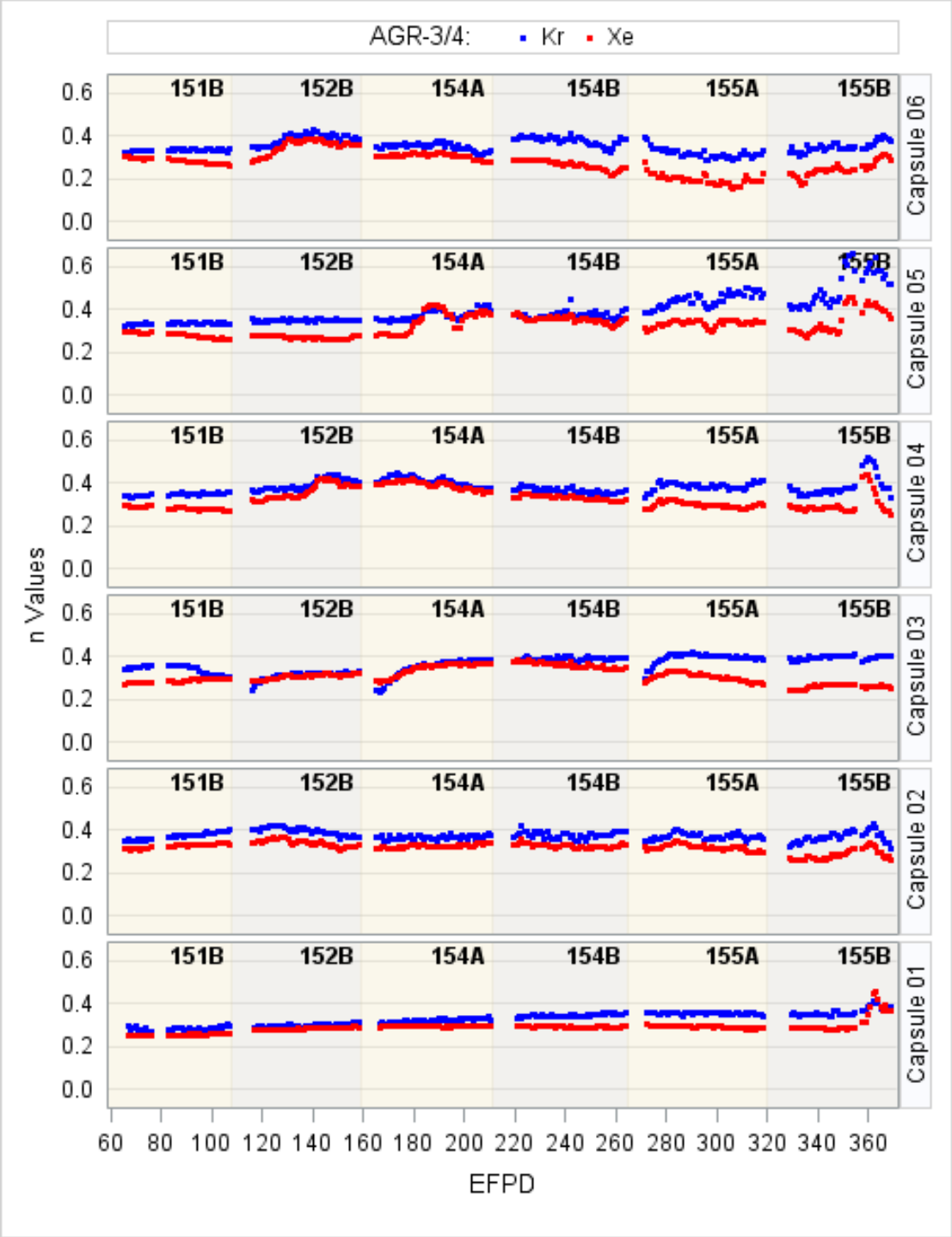

Figure 21. Krypton and xenon *n* values as function of EFPDs for AGR-3/4 Capsules 1 through 6.

3.3 Release to Birth Ratio Regression Model

Regression is performed to relate R/B per exposed kernel to fuel-particle temperature and decay constant. *Equation* (7) is used to fit to daily averaged R/B per exposed kernel data obtained from the 12 AGR-3/4 capsules. The regression results discussed in the following subsections are obtained using reciprocal fuel temperature in degrees Kelvin and decay constants in s^{-1}. The regression fitting was

performed separately for three sets of R/B per exposed kernel calculated using the best-estimate, maximum, and minimum failure counts to study the impact of failure-counting uncertainty on R/B correlation. In addition, to show impact of compact-average centerline temperature (a more accurate representation of DTF particles' temperature), used instead of peak fuel temperature (used in Revision 1 of this report), the parameter estimates for both Revisions 1 and 2 are presented side-by-side for comparison.

3.3.1 Impact of Failure Count Uncertainty

To study the impact of the uncertainty of particle-failure estimations on the release relationship as a function of fuel temperature and decay constants, regressions were performed separately for R/B per exposed-kernel data, calculated using the best-estimate, maximum, and minimum failure counts. Table 6 presents the three corresponding sets of parameter estimates (*n, B*, and *C*) of *Equation* (7) distinctly for krypton and xenon isotopes. As expected, the *n* value for AGR-3/4 fuel particles is equal to approximately 0.3 for both the krypton and xenon isotopes, which is consistent with the calculated daily *n* values plotted in Figure 20 and Figure 21. Also, *n* value is the same for the best estimate, maximum, and minimum number of failures. In addition, despite a large variation in the release data, there is a clear trend of temperature influence on R/B per exposed kernel, indicated by the statistically significant parameter B.

Table 6. Parameter estimates for AGR-3/4 R/B per exposed kernel.

	Best-estimated failures			Maximum failures			Minimum failures		
Isotopes	*n*	*B*	*C*	*n*	*B*	*C*	*n*	*B*	*C*
Kr-85m Kr-87 Kr-88	0.325	−8,572	−1.41	0.325	−8,858	−1.45	0.325	−9,094	−0.76
Xe-135 Xe-137 Xe-138	0.302	−7,793	−2.73	0.302	−8,080	−2.77	0.302	−8,316	−2.09

Figure 22 shows AGR-3/4 R/B per exposed kernel and their fitted function of reciprocal centerline fuel temperature for Kr-85m using best-estimated (blue), maximum (red), and minimum (green) failure counts. The large variation of R/B for reciprocal temperature around 7.5E−4 (R/B in Capsules 2, 4, 5, 6, and 9, with capsule-average centerline fuel temperature around 1,100°C) and unexpectedly higher R/B in Capsule 12, with the lowest centerline fuel temperature, led to the wide 95% bounds (light blue area) around the fitted line. The regression-analysis results presented in Figure 22 indicate a minor impact of failure-count uncertainty on the regression fitting parameters because of the following observations:

1. The *n* value estimates (Table 6) are the same for all three data sets of R/B per exposed kernel for both krypton and xenon isotopes, reflecting the consistency of decay constant influence on release.
2. Three fitted lines (blue, red, and green in Figure 22) are fairly parallel to each other, with a small shift indicating a small variation of Parameter *B* estimates that reflect the consistency of temperature influence on release.
3. The shaded area representing 95% confidence bounds on the fitted line using best-estimate failure counts covers most of the three sets of R/B per exposed kernel, indicating that variation due to failure-count uncertainty is well within the variation of the large quantity of R/B data used in the fitting process.

In conclusion, the uncertainty of the failure counts does not affect *n*, because *n* is defined mainly by fuel-particle material properties. Additionally, estimates for the *B* parameter are fairly similar for krypton and xenon isotopes, indicating the uncertainty of the failure counts does not affect the release correlation with temperature.

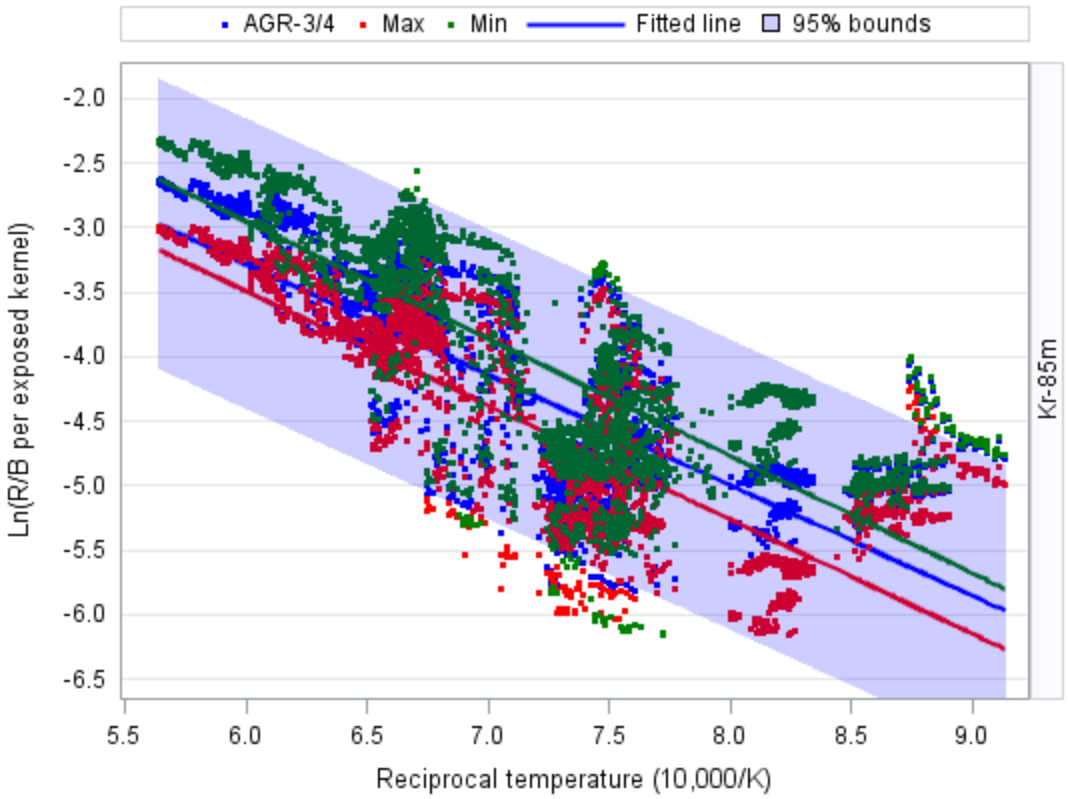

Figure 22. AGR-3/4 R/B per exposed kernel and their fitted function of reciprocal peak fuel temperature for Kr-85m using best-estimated, maximum, and minimum failure counts.

3.3.2 Average Centerline Temperature versus Peak Temperature

Table 7 presents the two sets of parameter estimates (*n, B*, and *C*) of *Equation* (7) distinctly for krypton and xenon isotopes using the best-estimate number of failed particles. The set of parameters on the right is for the Revision 1 model (previous version) using peak fuel temperatures, and the set on the left is for the Revision 2 model (current version) using average centerline temperatures.

As expected, the *n* values are identical for these two models. Lower average centerline temperatures used to fit Revision 2 model relative to the peak fuel temperature used in Revision 1 model led to (1) a slight decrease in the magnitude of Slope *B* (i.e., from −8,710 reduced to −8,572 for krypton), indicating a slightly smaller impact of the fuel temperature on the R/B per exposed kernel, and (2) a slight decrease in absolute value of the constant term *C* (i.e., from −1.47 reduced to –1.41 for krypton) that partially compensates for the smaller slope B. For visual illustration of these differences, fitted lines of these two models are presented in Figure 23. Generally, at a given fuel temperature, Revision 2 model predicts higher R/Bs than Revision 1 predictions as the Revision 2 model (blue line) lies above the Revision 1 model (red line). However, the fact that the Revision 1 model stays well within the 95% confident limits of the Revision 2 predictions (blue-shaded area) indicates influence of temperature variation on R/B per exposed kernel is insignificant comparing to variation in measured R/B per-exposed-kernel data.

Table 7. Parameter estimates for AGR-3/4 R/B per exposed kernel using capsule-average centerline (shaded columns) and peak fuel temperatures.

Isotopes	Revision 2: Centerline temperature			Revision 1: Peak temperature		
	n	*B*	*C*	*n*	*B*	*C*
Best-estimate number of failures						
Kr-85m Kr-87 Kr-88	0.325	−8,572	−1.41	0.325	−8,710	−1.47
Xe-135 Xe-137 Xe-138	0.302	−7,793	−2.73	0.302	7,899	−2.80

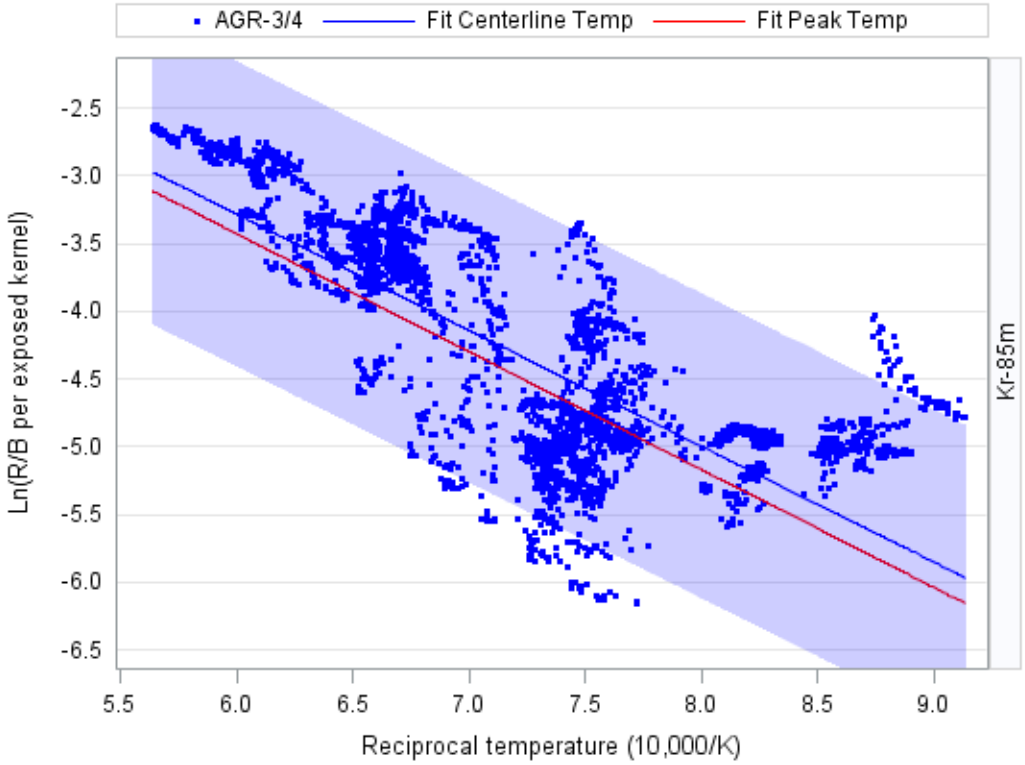

Figure 23. Kr-85m R/B per exposed kernel and the fitted functions of reciprocal average centerline (blue) and peak (red line) fuel temperature.

3.3.3 Release to Birth Ratio Regression Models for Krypton and Xenon Isotopes

The parameter estimates (*n*, B, and C) of the final regression function of R/B per exposed kernel that was calculated using the best-estimated failure counts and capsule-average centerline temperature in 12 AGR-3/4 capsules are presented in Table 8. These parameter estimates are obtained separately for the krypton and xenon isotopes. Estimates for *n* value and Parameter B were more or less similar for the krypton and xenon isotopes while estimates for Parameter C were much lower for the xenon isotopes, indicating their lower release. Therefore, the fitted lines for selected krypton and xenon isotopes are parallel to each other as shown in Figure 24.

Table 8. Parameter estimates using AGR-3/4 R/B per exposed kernel with best estimated failure counts.

Isotope	*n*	*B*	*C*
Kr-85m Kr-87 Kr-88	0.325	−8,572	−1.41
Xe-135 Xe-137 Xe-138	0.302	−7,793	−2.73

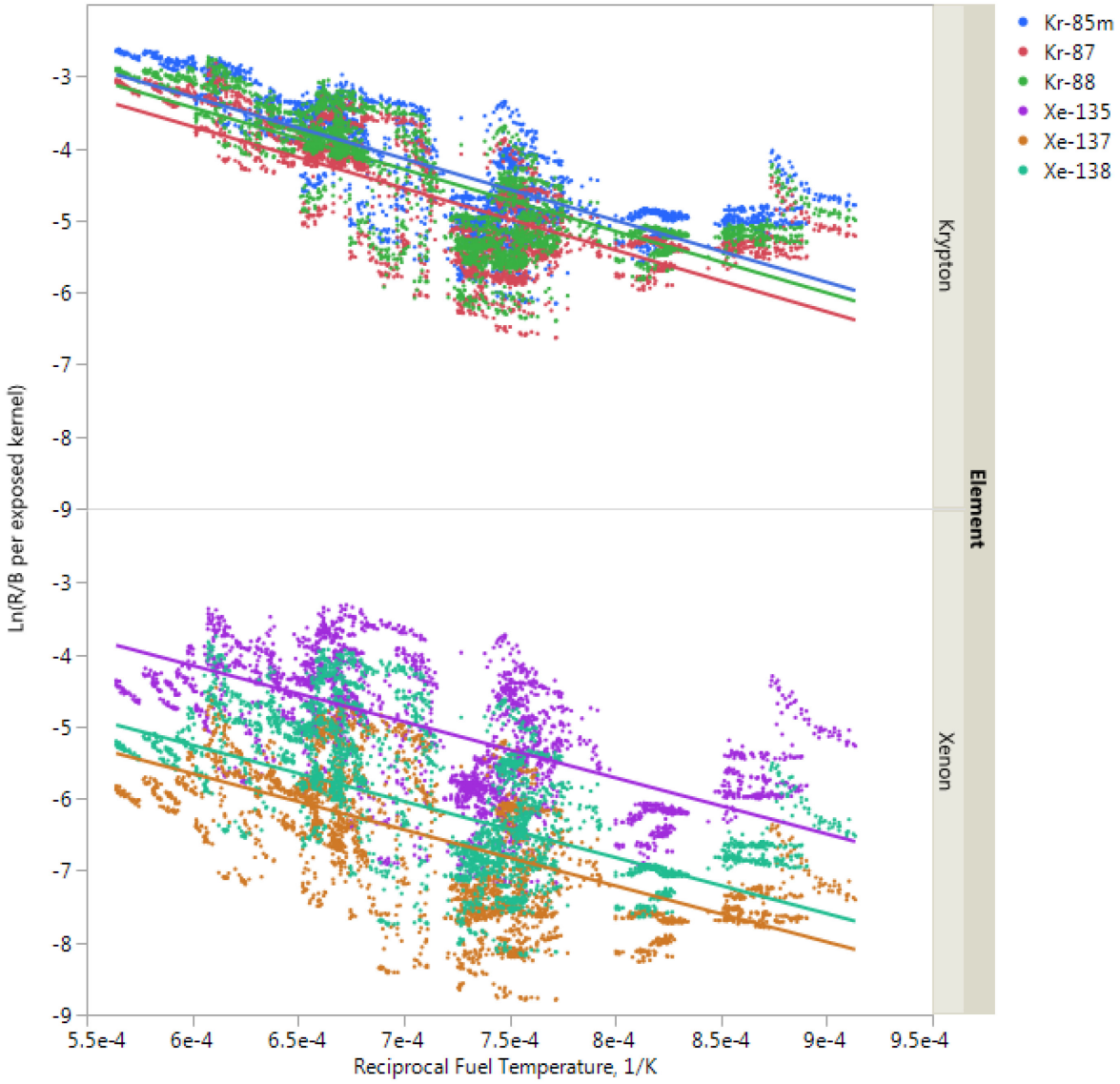

Figure 24. AGR-3/4 release to birth ratio models with data for krypton and xenon isotopes.

For clear visual presentation of data trend, Figure 25 depicts R/B per-exposed-kernel data and the fitted line in natural logarithm scale (top panel) and in linear scale (bottom panel) as a function of reciprocal fuel temperature for Kr-85m only. These plots are similar for the other five isotopes, which are plotted together in Figure 26 for krypton isotopes and Figure 27 for xenon isotopes. Note that the R/B data of the xenon isotopes are more scattered and significantly lower than the R/B data of the krypton isotopes.

The plots of R/B per exposed kernel on a linear scale (bottom plots in Figure 25 through Figure 27) show that R/B per exposed kernel for both krypton and xenon isotopes are less than 1% and are not sensitive to fuel temperature when fuel temperatures are below 1,050°C. However, when fuel temperature is greater than 1,050°C, R/B increases exponentially (top plots) with increasing fuel temperature, which can be described by the model form in *Equation* (7). As a result, the clear downward trend of the fitted lines for R/B per exposed kernel and reciprocal fuel temperature confirm the exponential functional relationship for all isotopes.

For krypton isotopes (Figure 26), the regression fitted functions under predict R/B per exposed kernel at lower fuel temperatures (lower than 800°C or 1/T of 8.5e−4 K-1) and at higher fuel temperatures (higher than 1,450°C or 1/T of 5.8e−4 K-1). However, they can be used to estimate the averaged R/B per exposed kernel for the U.S.-manufactured TRISO fuel particles within the fuel temperature range 800–1,450°C, which is the typical operating temperature range of the designed VHTRs. For xenon isotopes (Figure 27), even though the measured data vary more for a given fuel temperature, the regression-function predictions are right in the middle of the data points, so they can used as a rough estimate of xenon R/B per exposed kernel. In addition, for a given fuel temperature, the R/Bs vary widely for both krypton and xenon isotopes, indicating that other factors that might influence R/B should be included in the regression function, *Equation (*7), in order to achieve better correspondence with the measured data.

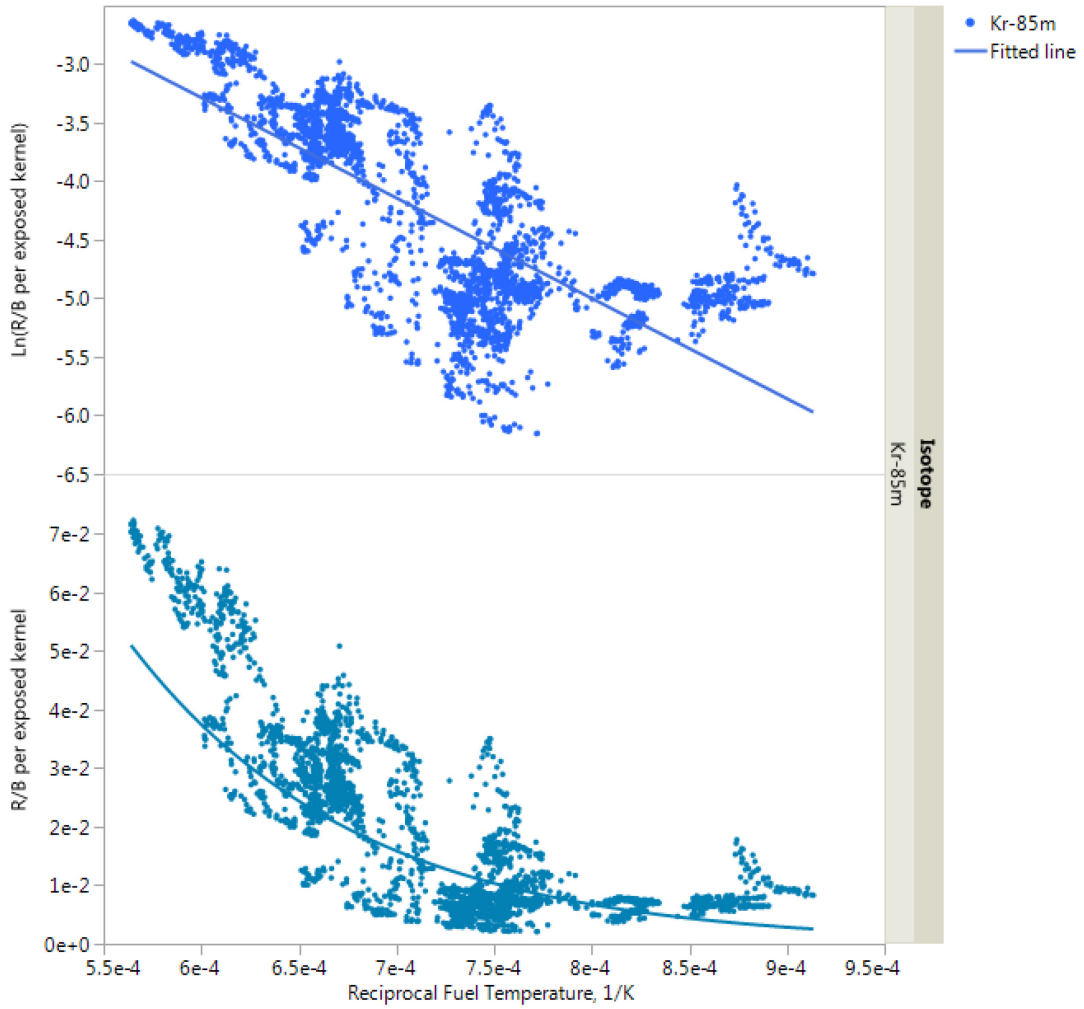

Figure 25. Kr-85m R/B per exposed kernel and the fitted line in natural logarithm scale (top panel) and in linear scale (bottom panel).

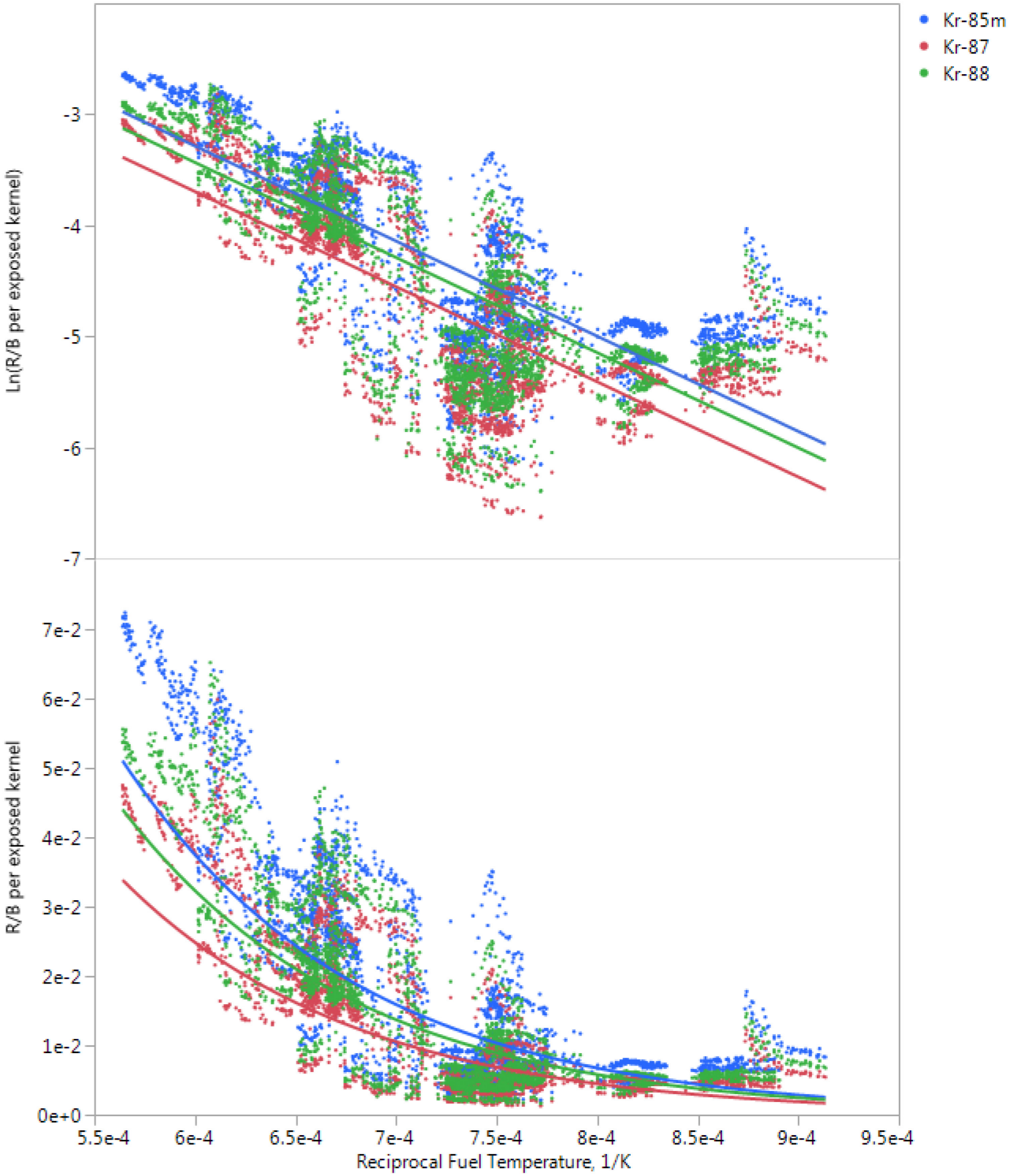

Figure 26. Krypton isotopes: R/B per exposed kernel and the fitted line in natural logarithm scale (top panel) and in linear scale (bottom panel).

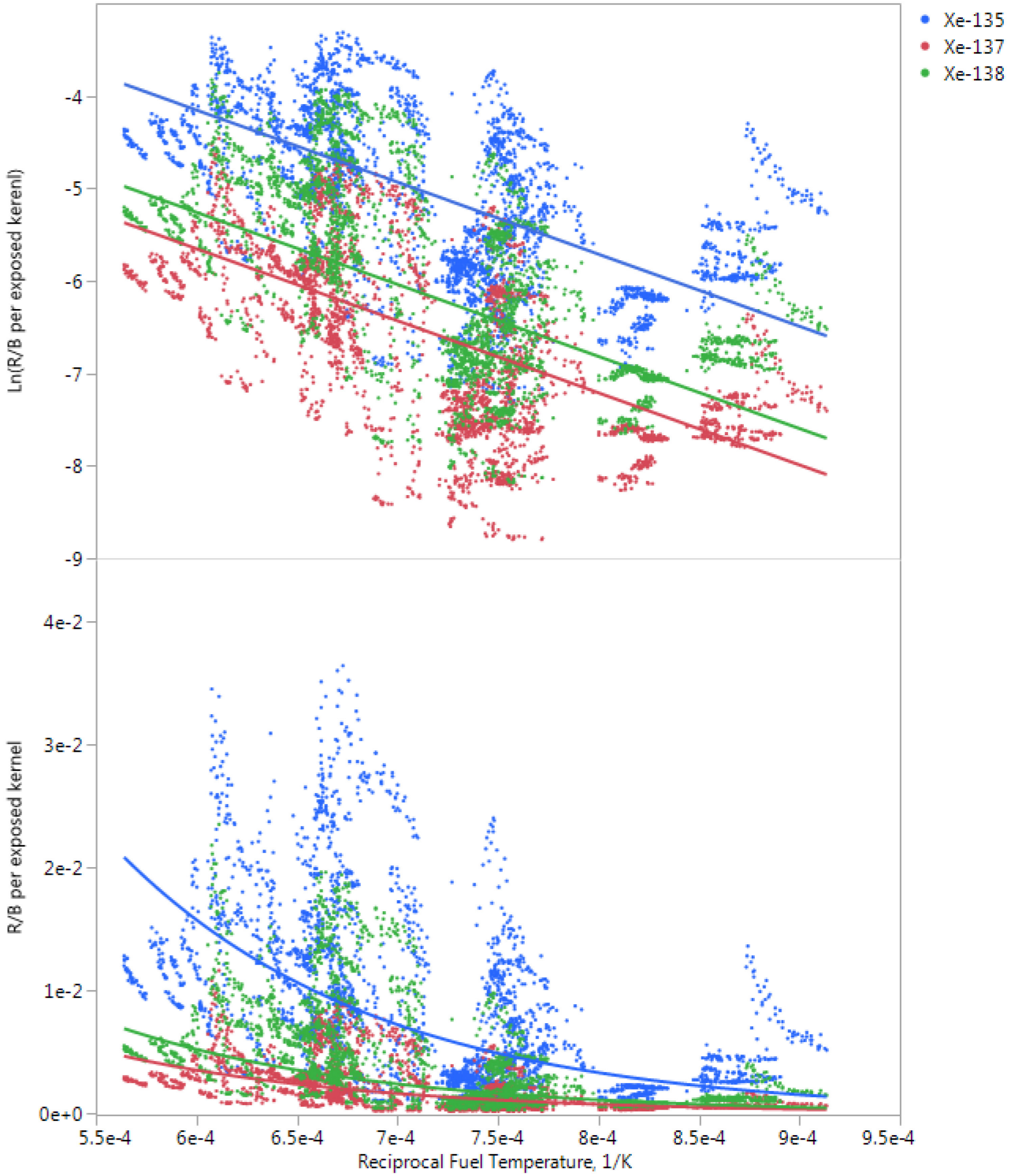

Figure 27. Xenon isotopes: R/B per exposed kernel and the fitted line in natural logarithm scale (top panel) and in linear scale (bottom panel).

3.3.4 Validation of Release to Birth Ratio Regression Model

3.3.4.1 Historical Irradiation Data

A few historical irradiations of low-enriched UCO TRISO fuel had either DTF particles or had in-pile failures that can provide R/B per-exposed-kernel data for validation of the model based on the AGR-3/4 R/B per-exposed-kernel data. In many cases, these experiments were injected with moisture at some point during irradiation to study hydrolysis effects on fission-gas release from UCO kernels. However, the R/B prior to moisture injection provides valuable data for comparison here. Table 9 summarizes the R/B per exposed kernel data for Kr-85m from four key irradiations: (1) HRB-17/18 (General Atomics 1987), (2) COMEDIE-BD1 (Richards 1994), (3) HFR-B1 (ORNL 1994), and (4) HRB-21 (DOE 1995). The corresponding fuel temperatures are the average fuel temperature unless noted otherwise.

Table 9. R/B per exposed kernel for Kr-85m from four key historic irradiations.

Experiment	Fuel Temperature (°C)	R/B per exposed kernel
HRB-17 and18[a]	840	4.0E-4
COMEDIE	1,160	1.0E-2
HFR-B1 Capsule B[b]	1,140 1,015 912	8.0E-3 3.0E-3 2.0E-3
HRB-21[c]	950 (max)/932	9.0E-3 7.0E-3

a. Results were identical for two independent capsules run at the same time in different locations in the reactor (General Atomics 1987).
b. 125°C added to TC temperatures to get fuel temperatures as recommended in report (see Table 6.4.33 in ORNL 1994).
c. The first R/B value represents value for first particle failure (assumed to be at the maximum temperature), and the second value is an average based on the total number of estimated failures (DOE 1995).

Table 10 presents the R/B per exposed kernel for several krypton and xenon isotopes for one irradiation condition extracted from the COMEDIE test results used to compare its n values (or slope between R/B and reciprocal decay constant in natural logarithm scale) to AGR-3/4 results.

Table 10. COMEDIE R/B data for krypton and xenon isotopes.

Isotope	Half-life (s.)	R/B per exposed kernel
Kr-89	180	2.30E-03
Kr-87	4,380	7.10E-03
Kr-88	10,800	8.40E-03
Kr-85m	15,000	1.10E-02
Xe-137	228	8.10E-04
Xe-138	780	1.20E-03
Xe-133m	192,000	2.90E-02
Xe-133	432,000	8.00E-02

In addition, there are two R/B per-exposed-kernel models derived based on these historical irradiations that are used to compare with AGR-3/4 R/B regression model. Specifically, the German model is discussed in IAEA (1997) and the model developed by General Atomics is discussed in Richards (1994).

3.3.4.2 Release-to-Birth Ratio Model and Historical Data

Figure 28 shows Kr-85m R/B per-exposed-kernel data obtained from the AGR-3/4 irradiation, the four historical irradiations presented earlier, and two historical models. The fact that R/B per-exposed-kernel data from all historical irradiations lie fairly well within the 95% bounds (blue shaded area) of the fitted line for the R/B data of the AGR-3/4 irradiation indicates good agreement with previous experimental results and with the German model based on UO_2 fuel. Therefore, the regression function can be used as a best estimate of the R/B per exposed kernel for the U.S. manufactured TRISO fuel even though the prediction uncertainty is quite large.

The German model (brown dashed line) is around the upper end of the AGR data range, and the slope is only slightly steeper, indicating a slightly larger impact of fuel temperature on R/Bs. The Richards model (orange dashed line) that was derived from the HFR B1 capsule data (UCO with DTF particles) (Richards 1994) lies above the AGR fitted line and below the German model and has a notably smaller slope, indicating a decrease in the impact of fuel temperature on R/Bs. In general, the German and Richards models are conservative because they predict higher R/B per exposed kernel than the prediction of the model based on AGR-3/4 data (i.e., the German model for the entire temperature range and the Richards model for lower temperatures). This is because these historical models were intentionally conservative.

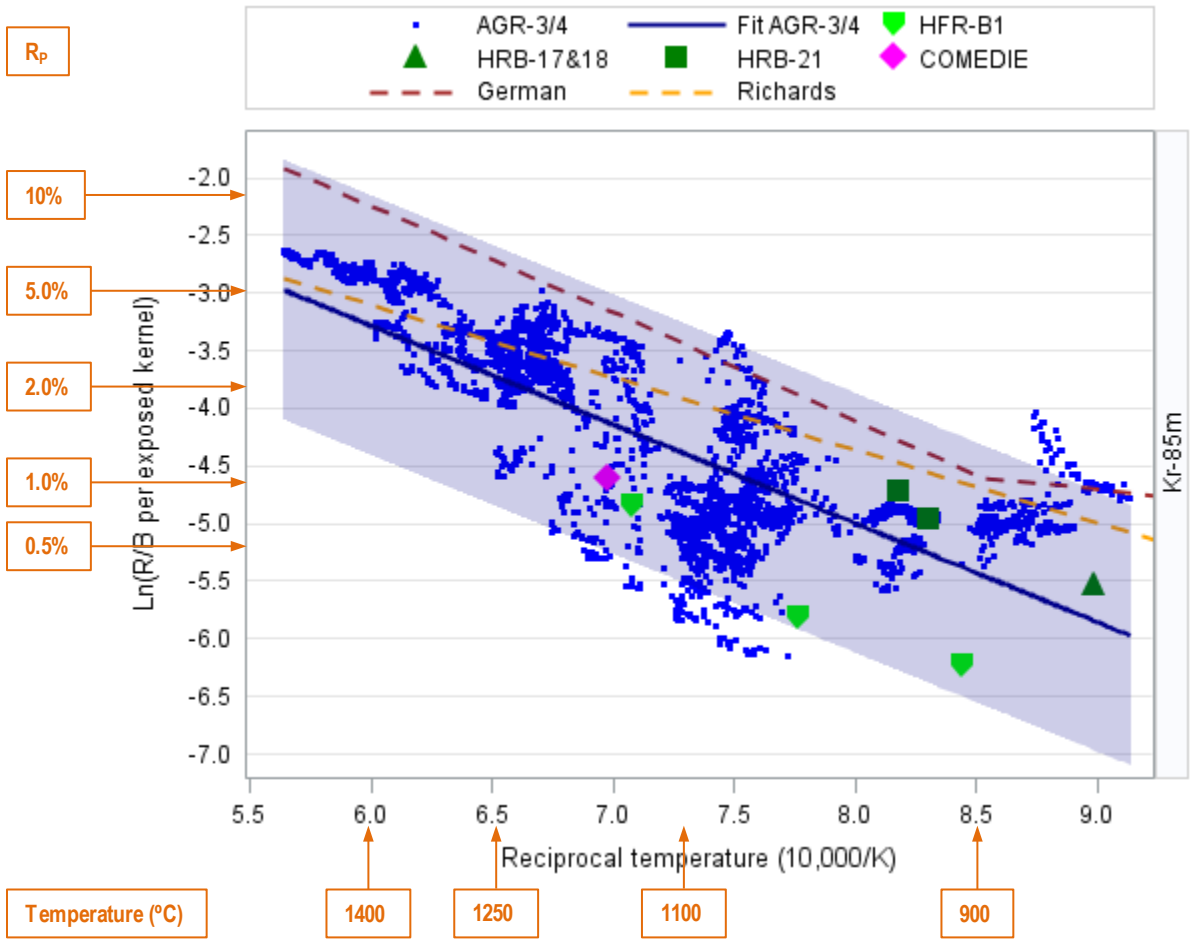

Figure 28. Fitted lines and Kr-85m R/B per exposed kernel data for AGR-3/4 irradiation, historical irradiations, and models (the blue shaded area is 95% bounds of the fitted line).

4. ADVANCED GAS REACTOR-2 IRRADIATION IS NOT SUITABLE FOR RELEASE DATA ANALYSIS

AGR-2 is the second irradiations in a series of planned experiments to test the TRISO-coated low-enriched uranium fuel (Colin, 2015). This section presents evidence that AGR-2 fission product release data cannot be used to study R/B per exposed kernel model and DC release factor calculation due to inconclusive number of particle failures in each capsule. Notably, only data from the four U.S. capsules (2, 3, 5, and 6) are discussed in this report.

4.1 High Uncertainty on Particle Failures

Exposed kernels in a capsule come from either defective coatings generated during fabrication or in-pile failure occurring during irradiation. For AGR-2 capsules, neither the as-fabricated exposed-kernel fraction determined by DLBL analysis nor the initial results from PIE can establish conclusively the number of exposed kernels that were present in each of AGR-2 capsules.

As-fabricated exposed kernel. The exposed-kernel fraction measured during the fabrication DLBL for compact lots used in AGR-2 capsules are presented in Table 11. On a statistical basis, the expected exposed kernels in a capsule are the product of the exposed-kernel fraction and the total number of particles in the capsule. Even though the expected exposed kernels in a capsule are less than 0.5, the existence of one exposed kernel in all AGR-2 capsules cannot be ruled out because, statistically, there is still a reasonable chance that we could have an exposed kernel in one or more capsules. As a result, we cannot assume that no exposed kernel existed in AGR-2 capsules during fabrication.

Exposed kernel determined with PIE. PIE has identified possible exposed-kernel defects in some of the US capsules, primarily by looking for evidence of cesium release to the graphite fuel holders and then performing destructive examination on the compacts to quantity the number of failures. While this approach has revealed between 0–2 particles that may have had exposed kernels in each capsule, it is not conclusive.

Table 11. Expected number of as-fabricated exposed kernels in a capsule.

Capsule #	2, 5, 6 (UCO)	3 (UO_2)
Number of particles per capsule	38,112	18,516
Exposed kernel fraction	9.4E-06	8.1E-06
Expected exposed kernels per capsule	0.36	0.15

4.2 High Release-to-Birth Ratio

This section argues that the measured R/B from AGR-2 capsules also does not support the absence of particle failures; therefore, they cannot be used for DU release analysis.

4.2.1 Gas Flow Issues during Irradiation

Not all of the AGR-2 R/B data are deemed suitable for this R/B data analysis because of issues of the gas-supply systems, as described in Collin (2014). The R/B data during following cycles are not suitable for use:

- The first cycle, 147A, was excluded to allow time for releases to reach their equilibrium state.
- ATR Cycles 149A and 149B were excluded because of relief-valve issues.
- All data from the beginning of Cycle 150B to the end of irradiation were excluded due to a cross-talk failure, which allows gas from one capsule to enter the other capsule somewhere along the capsules'

independent gas lines. This was probably caused by failure of the refractory gas lines in the experiment during handling between ATR cycles.

Both relief-valve issues and cross-talk failures allow the fission-gas atoms from one capsule to get into the FPMS detector for another capsule. In these instances, R/Bs calculated using measurements from one detector are not necessarily representative of the release from the corresponding capsule; therefore, these R/B data are not usable for this analysis. As a result, only R/B data from two remaining cycles at the beginning of irradiation, ATR Cycles 148A and 148B, can be used for this R/B data analysis.

4.2.2 Calculated Fuel Temperatures

A daily as-run thermal analysis was performed for the AGR-2 capsules as reported in ECAR-2476. Figure 29 shows the volume-average calculated fuel temperature in four U.S. capsules as a function of EFPDs for time periods when the R/B data can be used in the analysis. These fuel temperatures are used to predict R/B per exposed kernel (postulated) in AGR-2 capsules based on models established in the previous section.

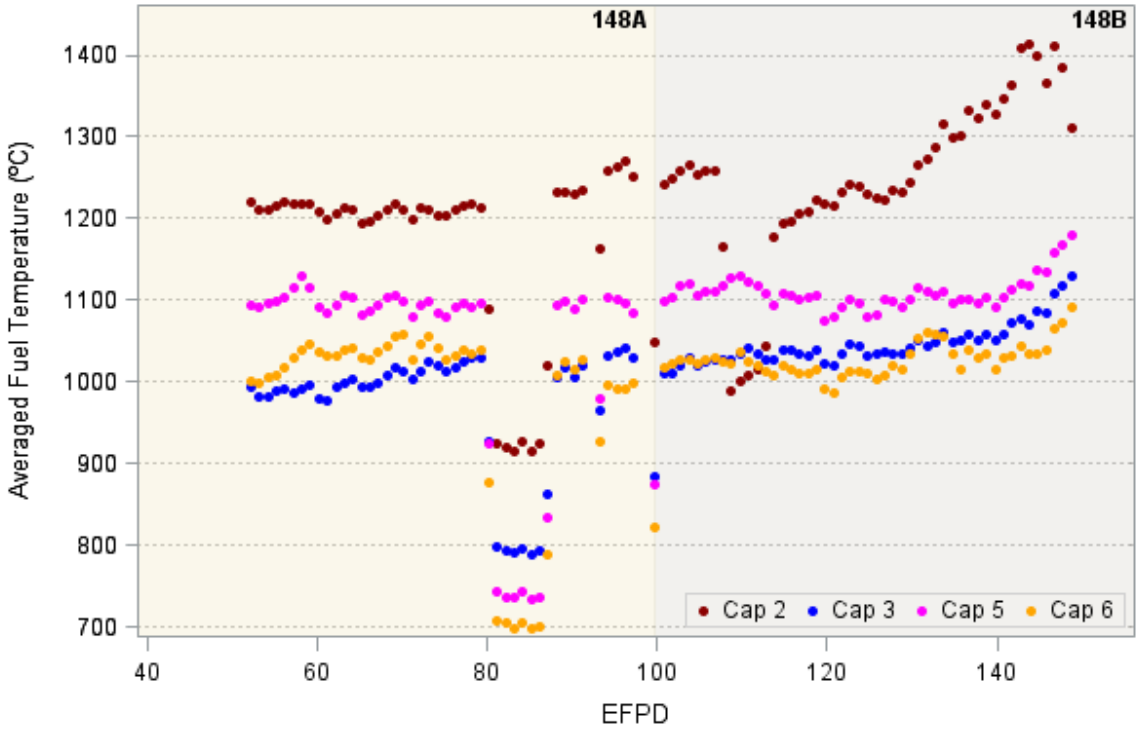

Figure 29. Volume-average fuel temperatures for four AGR-2 U.S. capsules.

4.2.3 Release-to-Birth Ratio

Details of the FPMS measurement and processing methods for the AGR-2 R/B data are documented in ECAR-2420. The R/B in this report represents ratio between measured release rate from a capsule and birthrate from all particles in that capsules. Because of the gas flow issues, only R/B data from two cycles, ATR Cycles 148A and 148B, can be used for this R/B data analysis.

The following approach was used to assess if one or more exposed kernels were present in the AGR-2 capsules. The R/B per exposed kernel was calculated from the measured R/B using *Equation (18)* assuming a single exposed kernel *(n_f=1)*. This value is denoted as the postulated R/B per exposed kernel. The R/B per exposed kernel was also predicted using *Equation* (7) with a set of parameter estimates (*n, B*, and *C*) obtained from AGR-3/4 R/B data and applied to AGR-2 fuel temperature. This value is denoted as

the predicted R/B per exposed kernel. For capsules where the postulated R/B per exposed kernel is greater or equal to the predicted R/B per exposed kernel, it is likely that at least one exposed kernel was present. The summary statistics of daily postulated R/B per exposed kernel during the AGR-2 irradiation used in this analysis are presented in Table 12.

Table 12. Summary of postulated R/B per exposed kernel for selected krypton and xenon isotopes in AGR-2 capsules.

Isotope	λ (1/s)	Number of daily data	Postulated R/B per exposed kernel		
			Average	Minimum	Maximum
Kr-85M	4.30E-05	376	2.246E-02	5.480E-04	7.168E-02
Kr-87	1.52E-04	376	1.612E-02	4.270E-04	5.744E-02
Kr-88	6.78E-05	376	1.727E-02	4.315E-04	5.661E-02
Xe-135	2.12E-05	376	6.128E-03	2.867E-04	1.912E-02
Xe-137	3.01E-03	376	2.537E-03	1.678E-04	5.624E-03
Xe-138	8.19E-04	376	3.816E-03	2.077E-04	1.056E-02

The historical plots of daily postulated and predicted R/B per exposed kernel are shown in Figure 30 for selected krypton isotopes and in Figure 31 for xenon isotopes for the four U.S. capsules during Cycles 148A and 148B. The postulated R/B values (dots) are similar to or higher than the predicted R/B per exposed kernel (solid lines) in the three UCO capsules (2, 5, and 6) for both krypton and xenon isotopes, which suggests at least one exposed kernel in these capsules. Only the UO_2 Capsule 3 had R/B values significantly lower than the predicted R/B per exposed kernel. Therefore, it is not certain whether fission-product release came solely from DU and, thus, cannot be used for DU release analysis. On the other hand, the number of failed particles in each capsule is not conclusively known, so these R/B data also cannot be used for R/B per-exposed-kernel model.

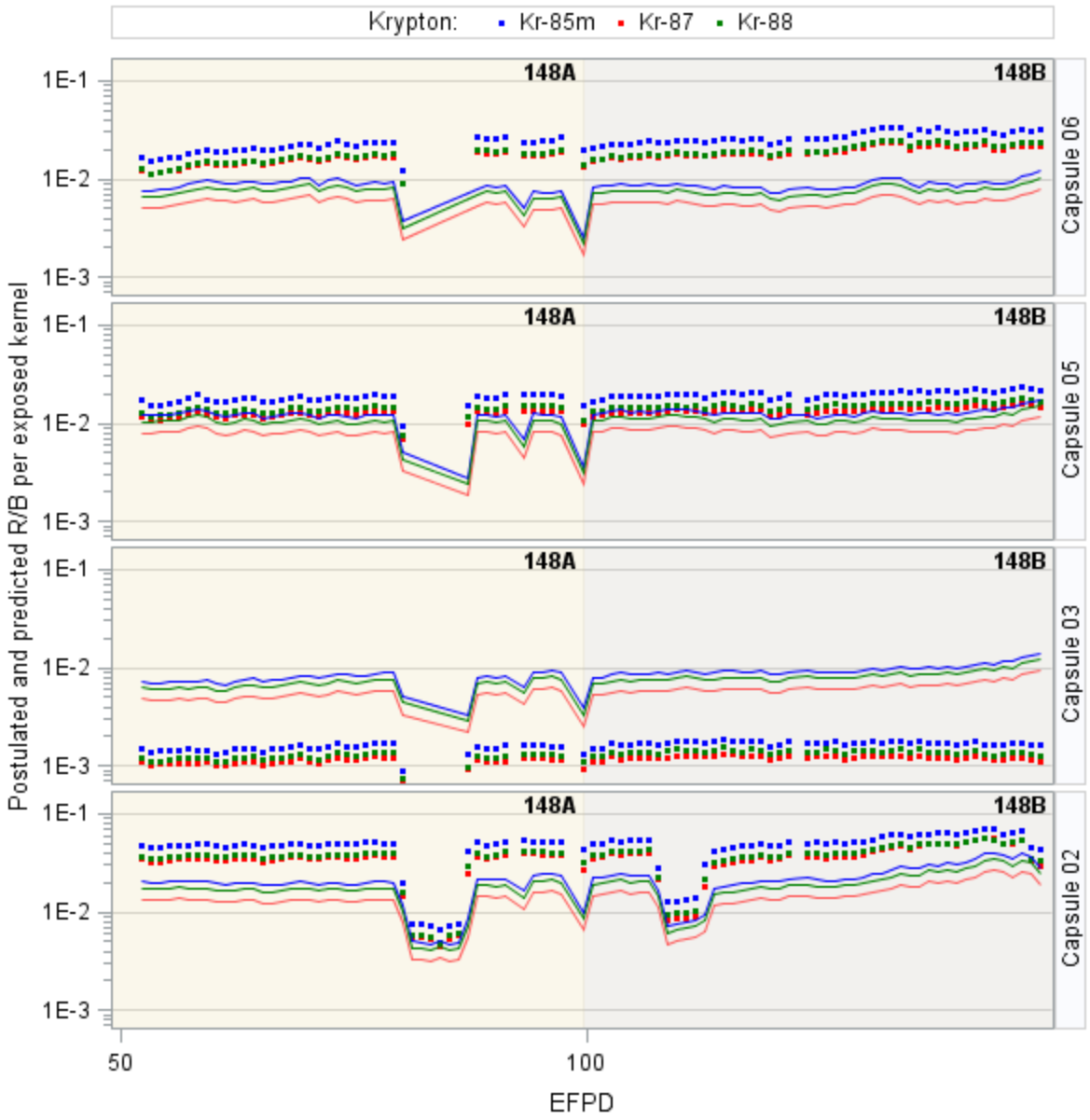

Figure 30. Postulated R/B per exposed kernel (dots) and predicted R/B per exposed kernel (solid lines) in AGR-2 capsules for krypton isotopes.

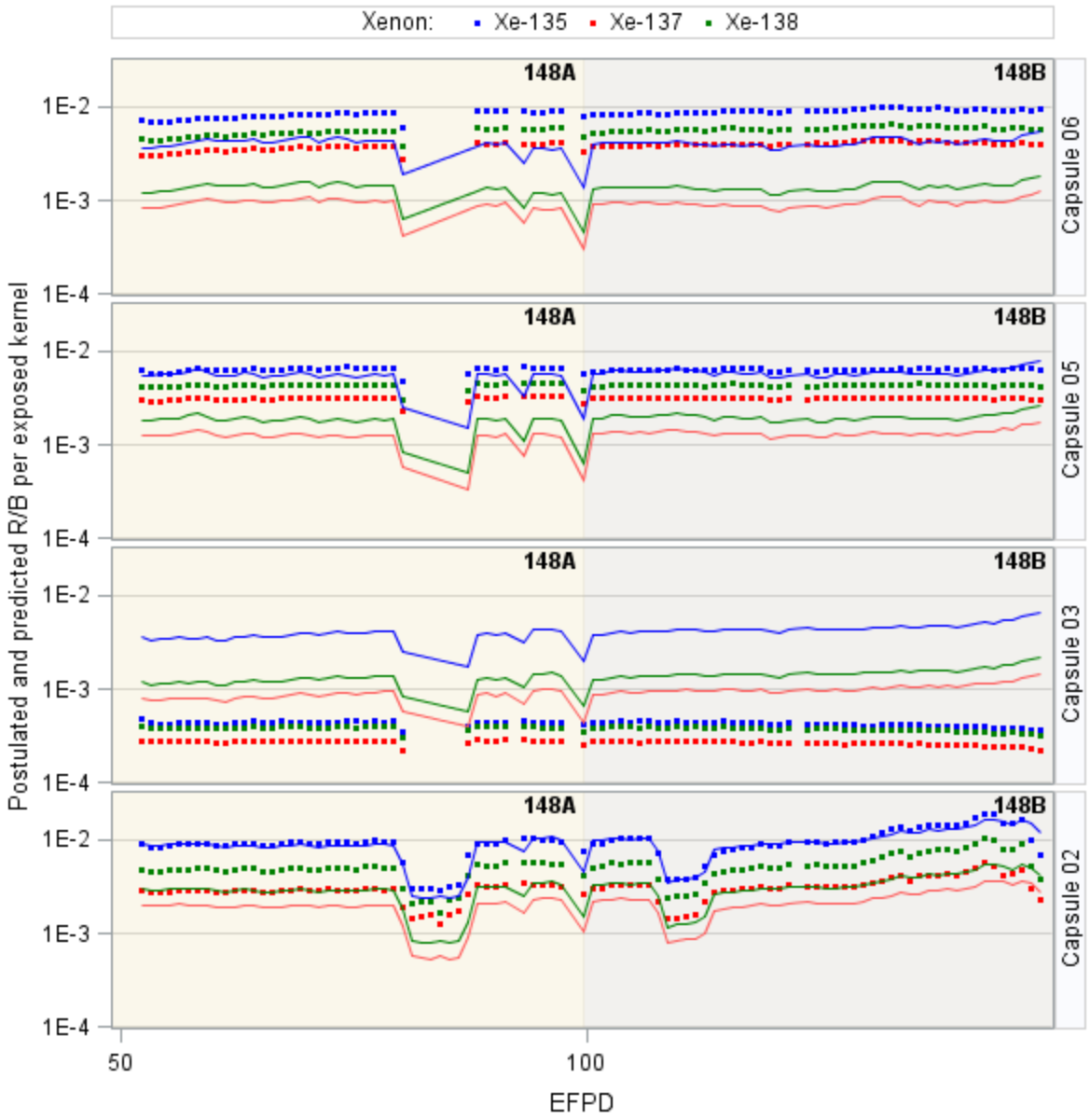

Figure 31. Postulated R/B per exposed kernel (dots) and predicted R/B per exposed kernel (solid lines) in AGR-2 capsules for xenon isotopes.

5. DETERMINING FISSION-GAS RELEASE FROM DISPERSED URANUM BASED ON ADVANCED GAS REACTOR-1 DATA

AGR-1 was the first irradiation in a series of planned experiments to test the TRISO-coated low-enriched UCO fuel (Colin 2014). The test train consisted of six individual capsules stacked on top of each other, and a leadout tube held the experiment in position and protected the gas lines and TC wiring. Because there were no exposed kernels in AGR-1 capsules, the fission-product releases are believed to originate mainly from the DU throughout fuel compacts. As a result, AGR-1 release data can be used for DU release factor analysis.

5.1 Exposed Kernels

Exposed kernels in a capsule come from either defective coatings generated during fabrication or in-pile failure occurring during irradiation. For AGR-1 capsules, the defective fraction measured by DLBL at fabrication, the measured R/B results during the irradiation, and results from the PIE all support the assumption that there were no exposed kernels in any of the AGR-1 capsules.

As-fabricated exposed kernel defects. No exposed kernels were found during the DLBL analysis performed by ORNL for as-fabricated compact lots used in AGR-1 capsules as presented in Table 1 (Section 2.3). However, the number of particles examined does not allow sufficient confidence that there would have been zero exposed kernels in a single AGR-1 capsule.[a] It is likely that larger sample sizes would have reduced the estimated population defect fractions sufficiently to preclude the probability of exposed kernels in each capsule.

Exposed kernels from R/B measurements. The AGR-1 R/B measurements were sufficiently low (Kr-85m values in most capsules $<10^{-7}$ at the end of irradiation) that no exposed kernels were indicated. This will be explained in detail in Subsection 5.3.2.

Exposed kernels determined from PIE. The AGR-1 PIE provided no evidence for in-pile TRISO failures. This is based primarily on the approach of first looking for cesium in the graphite fuel holders (known to be the result of non-retentive SiC or fully exposed kernels), identifying the suspect fuel compacts, and performing destructive examination to identify any particles with failed coatings. A small number of particles were identified that had released cesium during irradiation (a total of four particles in the entire test train), and all of these had SiC layer failures with at least one pyrocarbon layer intact (i.e., they were not exposed kernels) [Hunn et al. 2016].

5.2 Dispersed Uranium Fraction

The DLBL analysis conducted at ORNL effectively measures the total inventory of uranium located in the compact outside of the SiC layer (i.e., it includes the contributions from both the OPyC and matrix) as well as the inventory in any exposed kernels. If no exposed kernels or SiC defects are present in the sample, the results provide a measure of the uranium contamination that is dispersed in the matrix or OPyC layer of the particles. This DUF is expressed as the ratio between measured uranium and total uranium in these compact samples (g leached U/g U in compact). The average DUF with one standard deviation is presented in Table 13 for compact lots used in AGR-1 capsules (Hunn 2017 and Hunn et al. 2017). Generally, the uncertainty in DUF is quite high because only few samples of three compacts each were included in the calculation of DU.

---

[a] Particle sample sizes for each AGR-1 fuel type were between ~75,000 and 100,000, with zero exposed kernels detected in any of the analyses. These lead to population defect fractions of less than $7.0 – 9.6\times10^{-6}$ at 50% confidence, and less than $3 – 4\times10^{-5}$ at 95% confidence using binomial statistics. Using the 50% confidence values results in an expected number of exposed kernels in each capsule (~50,000 particles each) of less than ~ 0.3 to 0.5.

Table 13. Dispersed uranium contamination fraction for AGR-1 compact lots

Compact lot	LEU01-46T	LEU01-47T	LEU01-48T	LEU01-49T
N# of samples	2	4	3	4
DUF	3.849E-07	3.214E-07	2.639E-07	1.619E-07
Standard deviation	2.68E-08	3.906E-08	8.642E-08	1.208E-08

5.3 Irradiation Data

5.3.1 Calculated Fuel Temperatures

A daily as-run thermal analysis was performed to calculate the AGR-1 fuel temperatures as reported in ECAR-968. The capsule volume-average fuel temperature is used for this analysis because the heavy-metal contamination is spread throughout the compacts. Figure 32 displays the calculated fuel temperature in six capsules as a function of EFPDs for time periods when the R/B data were used in the analysis. The first cycle was excluded to let the test materials stabilize as had been done for AGR-3/4 irradiations. The capsule-average fuel temperatures varied in a wide range between 800 and 1350˚C, which allows the impact of fuel temperature on DU release factor to be explored.

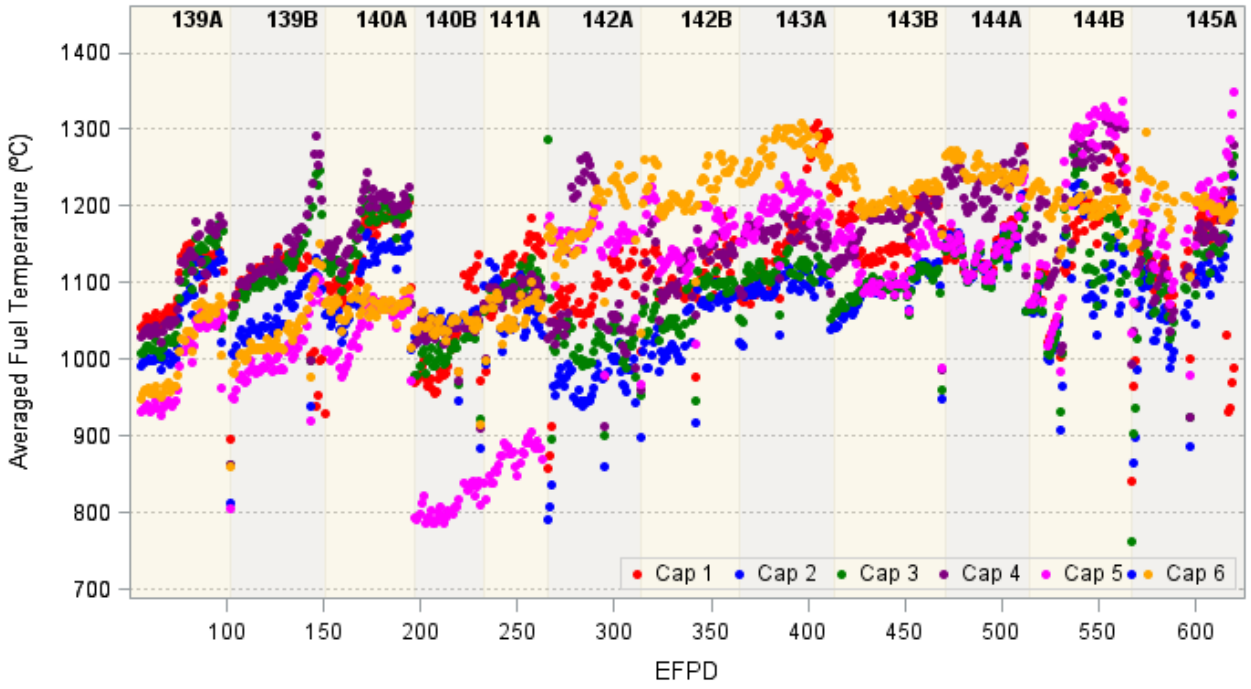

Figure 32. Volume-average fuel temperatures for six AGR-1 capsules.

5.3.2 Release-to-Birth Ratio

Details of the FPMS measurement and processing methods for the AGR-1 R/B data are documented in INL report ECAR-907. As for AGR-2, the postulated R/B per exposed kernel was calculated using *Equation* (18) for one assumed exposed kernel (n_f=1) in each AGR-1 capsules. Data during the first cycle were excluded from this analysis, allowing time for irradiation-induced changes in capsules to stabilize as had been done for AGR-3/4. The statistical summary of capsule daily postulated R/B per exposed kernel over the irradiation used in this analysis are presented in Table 14. Only R/B data with measurement

uncertainty less than 50% were included in this analysis, and so numbers of daily R/B values are slightly different across different isotopes.

Table 14. Summary of AGR-1 R/B data used in analysis for selected krypton and xenon isotopes.

Isotope	λ (1/s)	Number of Daily Values	Postulated R/B per exposed kernel		
			Average	Minimum	Maximum
Kr-85M	4.30E-05	3108	1.19E-03	7.70E-05	1.08E-02
Kr-87	1.52E-04	3110	7.64E-04	6.31E-05	6.64E-03
Kr-88	6.78E-05	3103	8.70E-04	6.81E-05	7.58E-03
Xe-135	2.12E-05	3104	1.82E-04	4.67E-05	1.38E-03
Xe-137	3.01E-03	2974	9.00E-05	4.54E-05	5.96E-04
Xe-138	8.19E-04	3090	1.17E-04	4.57E-05	8.13E-04

The temporal profiles of daily postulated R/B per exposed kernel are shown in Figure 33 for selected krypton isotopes and in Figure 34 for xenon isotopes (dots) for the AGR-1 six capsules. The R/B per exposed kernel is also predicted using *Equation* (7), with parameters, n, B, and C, which were estimated based on AGR-3/4 R/B data (Section 3.3) and applied to AGR-1 fuel temperature. The daily volume-average fuel temperatures in of AGR-1 capsules are used for calculation of the predicted R/B per exposed kernel for each isotope and each time step. The predicted R/B per-exposed-kernel data are plotted as solid lines. The postulated R/B per exposed kernel in all capsules is significantly (more than an order of magnitude) lower than the predicted R/B per exposed kernel, which confirms no particle failure in AGR-1 capsules. Subsequently, the measured release rate comes exclusively from DU in fuel compacts. As a result, AGR-1 fission-gas release data are used for estimation of the DU release factor.

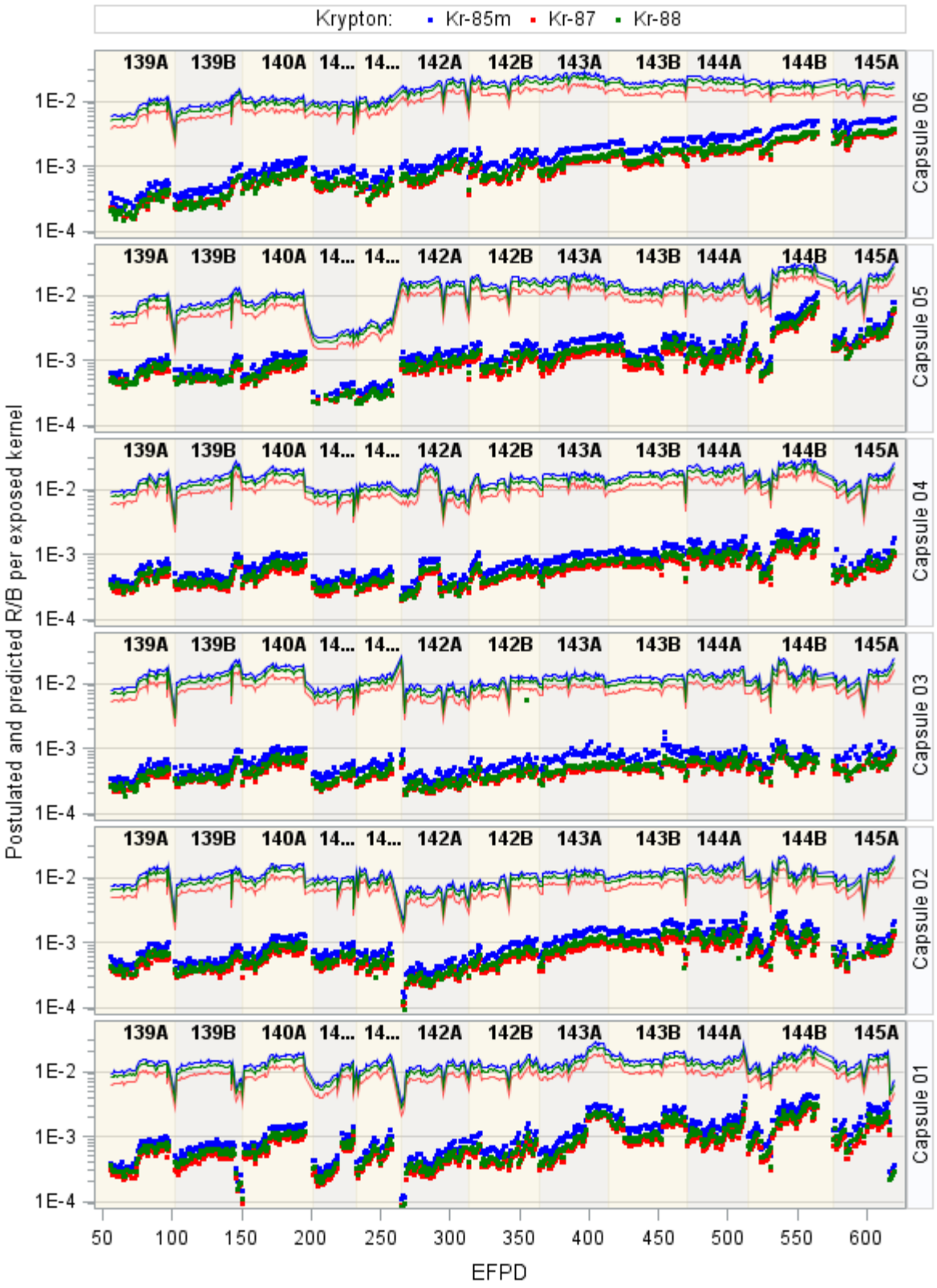

Figure 33. Postulated R/B per exposed kernel (dots) and predicted R/B per exposed kernel (solid lines) in AGR-1 capsules for krypton isotopes.

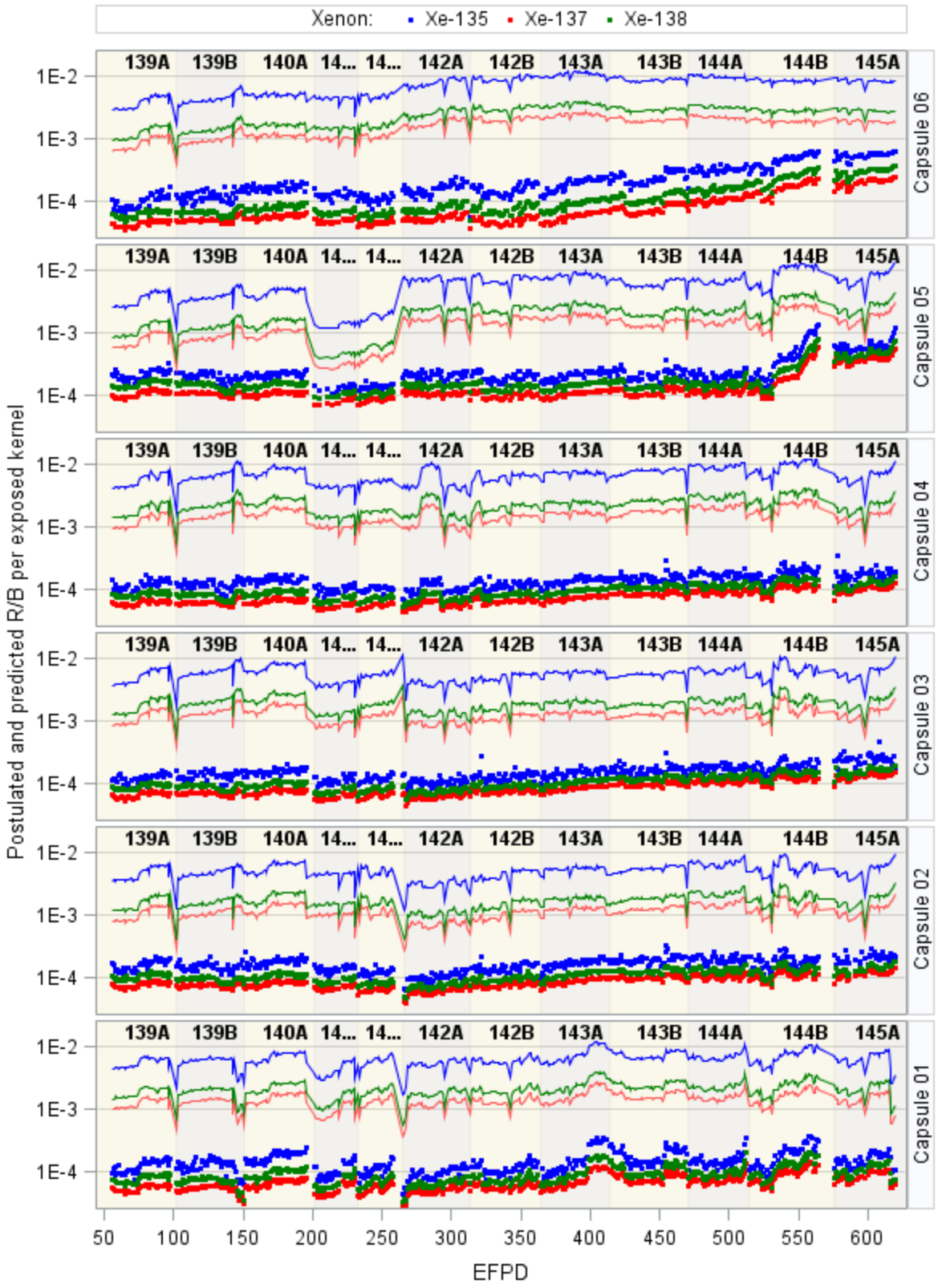

Figure 34. Postulated R/B per exposed kernel (dots) and predicted R/B per exposed kernel (solid lines) in AGR-1 capsules for xenon isotopes.

5.4 Dispersed Uranium Release Factor

5.4.1 Dispersed Uranium Release Factor Calculation

The previous section demonstrated that there were no exposed kernels in any AGR-1 capsules; therefore, a DU release factor can be estimated from the capsule measured R/B. For each isotope, each capsule, and each day the DU release factor is calculated by the following steps:

1. Calculate R/B per exposed kernel (R_p) for the actual daily AGR-1 average fuel temperature using *Equation* (7) with parameter estimates (n, B, and C) established based on the AGR-3/4 R/B data presented in Table 8.
2. Calculate DU release factor from the provided R/B in a capsule using *Equation (14*) as described Section 2.2.

The DUF used for DU release factor calculation are presented in Table 15 for all fabricated compact lots used in AGR-1 capsules. This table includes the number of equivalent DU kernels per capsule calculated as the product of DUF and number of particles. Numbers of equivalent DU kernels in each capsule are significantly smaller than one kernel, which resulted in low fission-product release measured in AGR-1 capsules.

Table 15. Number of equivalent DU kernels per capsule for four coating variants of AGR-1 compacts.

Compact	LEU01-46T	LEU01-47T	LEU01-48T	LEU01-49T
Capsule	3, 6	5	2	1, 4
Particles per capsule	49,740	49,800	49,560	49,512
DUF	3.849E-07	3.214E-07	2.639E-07	1.619E-07
Equivalent DU kernels	0.0191	0.0160	0.0131	0.0080

The DU release-factor statistical summary (i.e., average, standard deviation, minimum, maximum, and number of data points) is calculated from the daily values in all capsules and over the entire irradiation. Results are presented in Table 16 for each isotope separately, and averaged for each element and for all isotopes. According to the t-test, all means are statically different with confidence level of 99% for all isotopes, except for Kr-85m and Kr-87. The high minimum-maximum range and high relative standard deviations (last column in Table 16) are demonstrated graphically in the wide distributions shown by the histograms in Figure 35 and Figure 36. This reflects the wide variation of R/B measured in AGR-1 capsules at a given fuel temperature. Also, the variation of DU release factor is wider for krypton isotopes than xenon isotopes (Figure 36). The majority of DU release factors are in the 1–10 range, with a long tail to the right. The overall average DU release factor is 5.1 for all isotopes, which is lower than the factor of 10 assumed in the Revision 1 report.

The DU release factors are similar for most isotopes, except for Xe-135, the averaged DU release factors of which are less than half of other isotopes (Table 16 and Figure 35). Xe-135 has a half-life two orders of magnitude longer (lower decay constant) than Xe-137 and Xe-138, which led to considerably higher predicted Xe-135 R/B per exposed kernel (solid lines in Figure 34), while the measured R/Bs for Xe-135, Xe-137, and Xe-138 isotopes are close to each other (dotted lines in Figure 34). Consequently, this higher predicted R/B per exposed kernel led to lower DU release factors for Xe-135. Also, DU release-factor distributions for the three krypton (Kr-85m, Kr-87, and Kr-88) and two xenon (Xe-137 and Xe-138) isotopes are quite similar while the Xe-135 distribution is clearly shifted to the left (Figure 35).

Table 16. DU release factors for different isotopes.

Isotope	Half-life (s)	Number of data	DU release factor		
			Average and standard deviation	Minimum	Maximum
Kr-85m	16,127	3,078	6.4±3.7	0.2	29.5
Kr-87	4,560	3,080	6.3±3.5	1.3	28.5
Kr-88	10,223	3,080	5.5±3.1	1.2	26.5
Krypton	--	9,238	6.1±3.5	0.2	29.5
Xe-135	32,767	3,074	2.3±1.0	0.6	12.1
Xe-137	230	2,962	5.2±2.5	1.0	29.0
Xe-138	846	3,075	4.6±2.2	1.0	24.6
Xenon	--	9,111	4.0±2.4	0.6	29.0
All isotopes	--	18,349	5.1±3.1	0.2	29.5

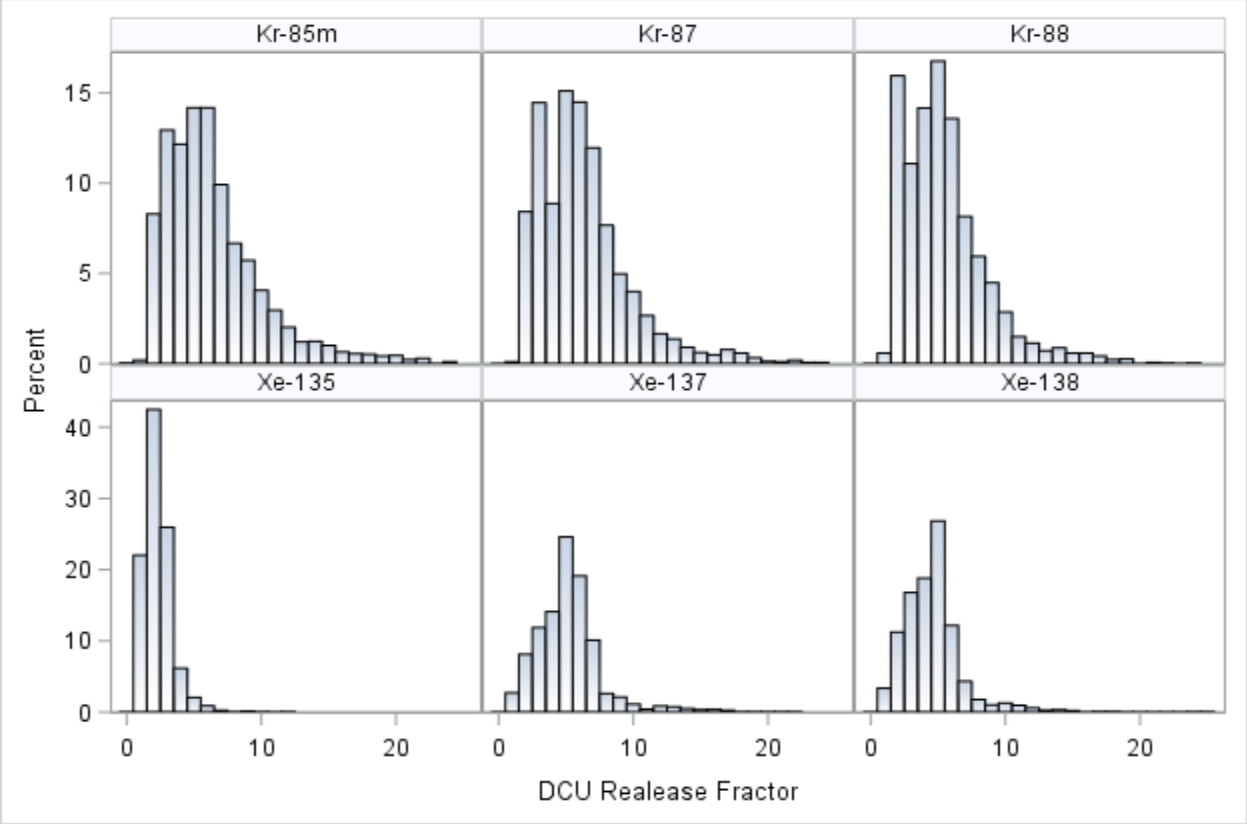

Figure 35. Histograms of DU release factors for each isotope.

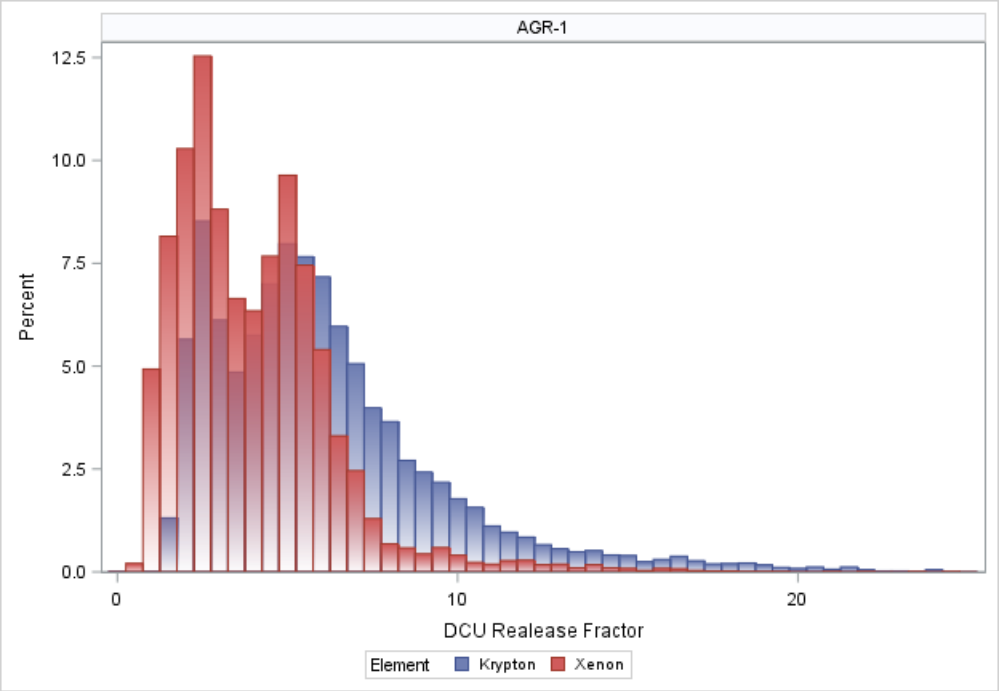

Figure 36. Histograms of DU release factors for krypton and xenon.

5.4.2 DU release factor analysis

5.4.2.1 Impact of Decay Constant

The fitted line of DU release factors versus the natural logarithm of the decay constant in Figure 37 indicates a very weak relationship as the average DU factor stays almost constant with increase in decay constant (or decrease in half-life). The tight 95% confidence limits of the mean value (light blue shaded area overlaid around the fitted line in this figure) indicate sufficient data used for fitting the line.

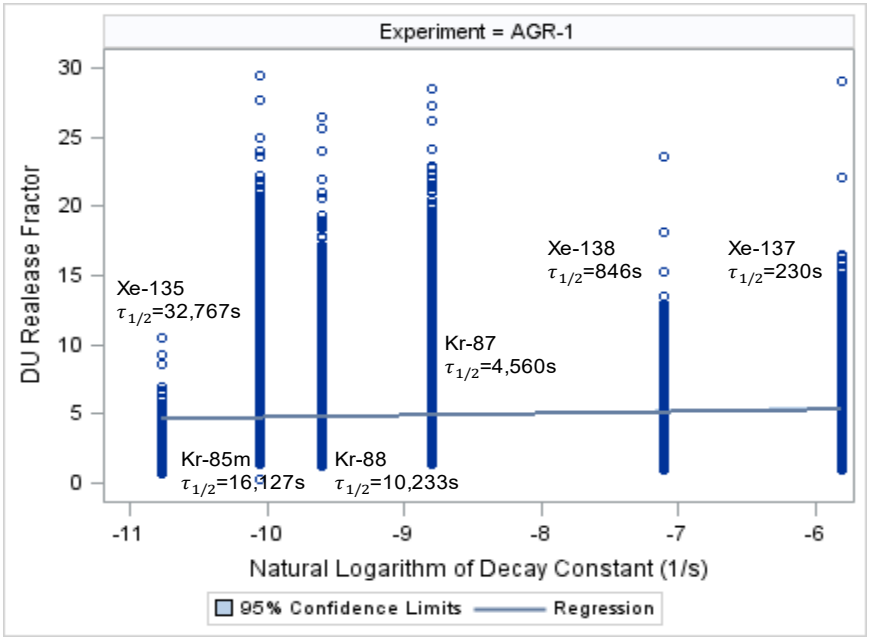

Figure 37. AGR-1 DU release factor versus logarithm of decay constant.

5.4.2.2 Impact of Fuel Temperature

Figure 38 shows AGR-1 DU release factor as a function of reciprocal temperature for krypton and xenon isotopes. The contradicting trends of fuel temperature for krypton and xenon isotopes are clearly revealed: a strong downward trend with increase in reciprocal temperature for krypton isotopes and a weak upward trend for xenon isotopes. This means higher fuel temperatures lead to higher krypton DU release factors and lower xenon DU release factors. Here the 95% confidence limits of the mean are also overlaid around the fitted line and indicate a very small uncertainty due to the large amount of data used for fitting.

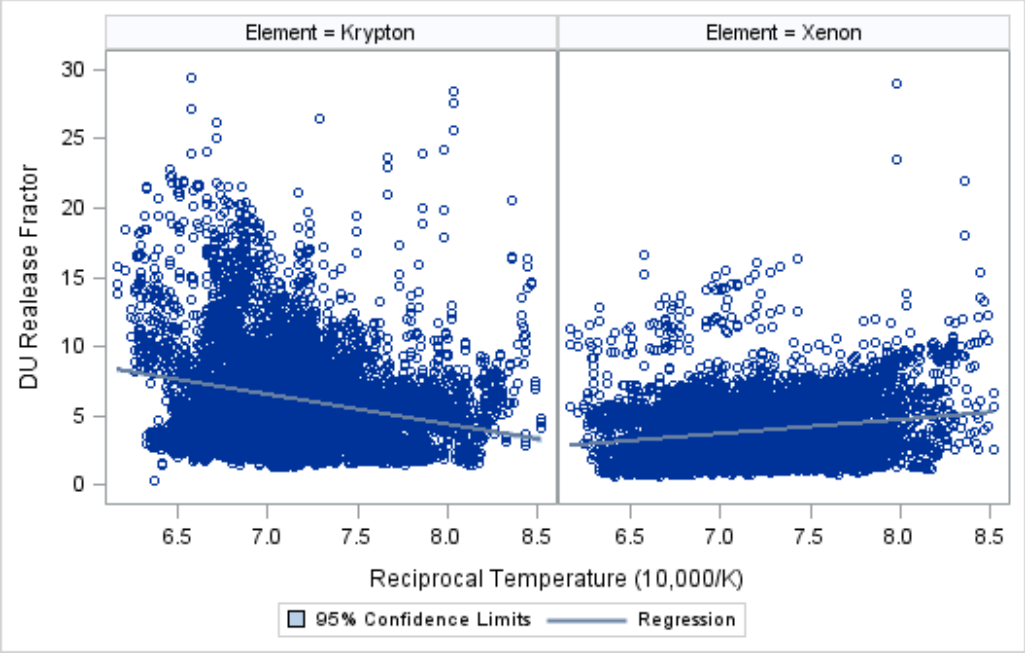

Figure 38. AGR-1 DU release factor versus reciprocal temperature

5.4.2.3 Impact of Fast Fluence and Burnup

The upward trends of DU release factors with fast fluence and burnup are apparent for both krypton and xenon isotopes with a stronger trend for krypton (Figure 39). This trend reflects the upward trend of measured R/B data in AGR-1 capsules (Figure 33 and Figure 34). These relationships are similar for fast fluence and burnup because they are highly correlated in a capsule.

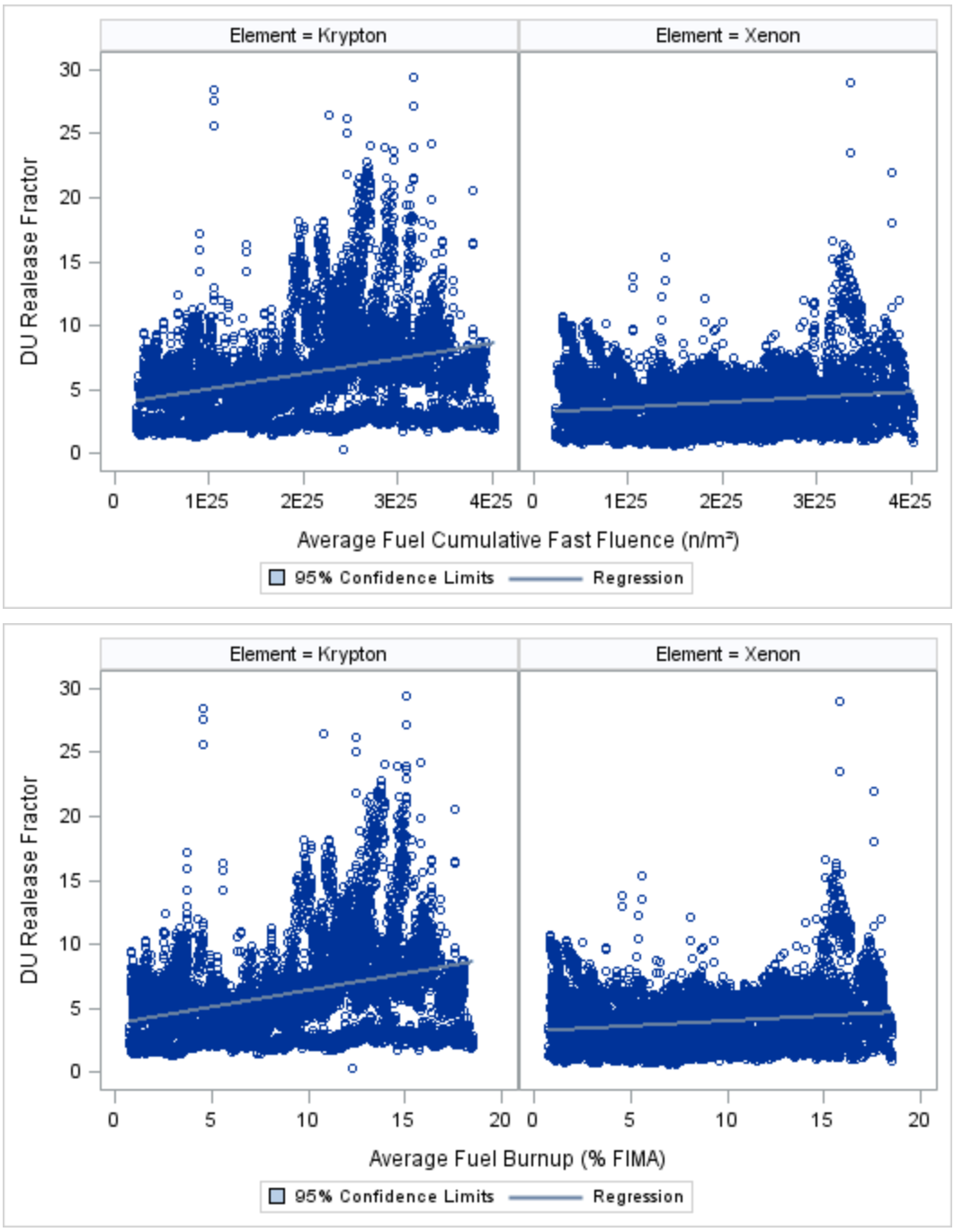

Figure 39. AGR-1 DU release factor versus fast fluence (top) and burnup (bottom).

6. CONCLUSION

To reduce measurement uncertainty of the release rate, the krypton and xenon isotopes selected for regression analysis have a half-life that is short enough to reach equilibrium in the capsule, but long enough to provide a measureable signal in the FPMS detector. These isotopes are Kr-85m, Kr-87, Kr-88, Xe-135, Xe-137, and Xe-138. Additionally, R/B data with measurement uncertainty less than 50% and standard 8-hour sampling durations are included in this analysis.

With embedded DTF fuel particles, AGR-3/4 irradiation provides invaluable R/B data for studying the fission-product behavior of TRISO-coated UCO fuel. AGR-3/4 fuel particles were irradiated for 369.1 EFPDs and reached a peak burnup of 15.3%, a maximum fast neutron fluence of 5.3×10^{21} n/cm^2, and a capsule-average centerline temperature ranging between 820 and 1,500°C. A total of 18,468 daily values of AGR-3/4 R/B per exposed kernel for six selected krypton and xenon isotopes were used for this regression analysis. The krypton R/B per-exposed-kernel data vary widely in the range of 0.13 to 7.3%, and the xenon R/B per-exposed-kernel data are somewhat lower and in the range of 0.015 to 3.6%. The lower capsule-average centerline temperatures relative to the peak fuel temperature used in Revision 1 report led to slightly lower magnitude slope against the reciprocal temperature and a lower constant term in the regression model for R/B per exposed kernel. This resulted in a slightly higher prediction of R/B per exposed kernel at given temperature.

The R/B correlation with isotopic decay constant is characterized by n values, which represent a slope between natural logarithms of R/B per exposed kernel and reciprocal half-life ($\ln R_p$ and $\ln \frac{1}{\lambda}$) for isotopes of each fission gas (e.g., krypton or xenon) calculated for each day. There is no effect of temperature on these *n* values, as indicated by the similar values seen across all capsules, which have a wide range of fuel temperatures. The daily *n* values for AGR-3/4 irradiation are 0.325±0.074 for krypton and 0.302±0.048 for xenon and are stable as a function of irradiation time, indicating no apparent effect of fuel burnup on fission-gas releases.

The R/Bs per failed particle for isotopes of both krypton and xenon are less than 1% and not sensitive to fuel temperature when fuel temperatures are below 1,050°C. However, when fuel temperature is greater than 1,050°C, the R/B per exposed kernel values increase exponentially with increasing fuel temperature. The clear downward trend of the fitted lines for AGR-3/4 R/B data confirms this exponential functional relationship between R/B per exposed kernel and reciprocal fuel temperature for all isotopes. The 95% confidence bands on the distribution are within a factor of 2.1 of the fitted value, indicating the consistency of R/B per exposed kernel data given high uncertainties in both fission-gas release measurement and particle-failure estimation. These R/B correlations can be used by reactor designers to estimate fission-gas release from failed fuel in HTGR cores, which is the key safety factor for fuel performance assessment. Note that no attempt has been made in this study to determine potential differences in fission-gas release from a DTF particle and a failed TRISO-coated particle.

This analysis found that R/B per exposed kernel for AGR-3/4 test fuel is comparable to R/B obtained in historic tests. The German and Richards models predict higher R/B per exposed kernel than does the model based on AGR-3/4 data (i.e., the German model for the entire temperature range and the General Atomics model for lower temperatures). This is expected because these historical models were intentionally conservative.

Due to uncertainty in the number of exposed kernels in the AGR-2 capsules, R/B data were not used in these analyses of R/B per-exposed-kernel model or DU release factors.

Without any particle failures, the AGR-1irradiation provides sufficient R/B data to determine a DU release factor as a ratio between releases from an equivalent DU kernel and an exposed kernel. The large amount of R/B data from AGR-1 irradiation reveals the following trends: (1) the effect of isotopic decay constant on DU release factor is insignificant, (2) fuel temperature has contradicting trends; the factor increases with temperature for krypton isotopes but decreases for xenon isotopes, and (3) higher fast fluence and burnup lead to a higher DU release factor. In general, the DU release factor is 5.1 ±3.1 for all isotopes: 6.1 ±3.5 for krypton and 4.0 ±2.4 for xenon. The AGR-1 DU release factors are significantly lower than values of 10–30, which have historically been assumed based on estimation using data from the past irradiations. One possible reason is that our DTF particles release at a much higher rate than exposed kernels in a TRISO particle, and the other reason could be bias in DU contamination fraction. Even though uncertainty in the DU release factor values was quite high, the DU release factor can still be

used to provide rough estimate of releases from heavy-metal contamination. This can help differentiating releases from failed particles, which could be useful in assessing fuel performance.

7. REFERENCES

ANS, 2011, "American National Standard Method for Calculating the Fractional Release of Volatile Fission Products from Oxide Fuel," American National Standards Institute, Inc., ANSI/ANS 5.4 2011, May 2011.

ASME NQA 1 2008, "Quality Assurance Requirements for Nuclear Facility Applications," 1a 2009 addenda.

Collin, B., 2015, *AGR-1 Irradiation Test Final As-Run Report*, INL/EXT-10-18097, Rev. 3, January 2015.

Collin, B., 2014, *AGR-2 Irradiation Test Final As-Run Report*, INL/EXT-14-32277, Rev. 2, August 2014.

Collin, B., 2016, *AGR-3/4 Irradiation Test Final As-Run Report*, INL/EXT-15-35550, Rev. 1, May 2016.

Collin, B., 2017, Attachment to an email communication on Subject "R/B discussion" sent on September 20, 2017.

Collin, B., P.A. Demkowicz, D.A. Petti, G.L. Hawkes, J. Palmer, B.T. Pham, D.M. Scates, J.W. Sterbentz, 2018, "The AGR-3/4 Fission Product Transport Irradiation Experiment*," Nucl. Eng. Des.* 327 (2018), pp 212–227.

Demkowicz, P. A., et al., 2015, *AGR-1 Post Irradiation Examination Final Report*, INL/EXT-15-36407, Rev. 0, August 2015.

DOE, 1995, *Fuel Capsule HRB 21 Post Irradiation Examination Data Report*, DOE HTGR 100229/ORNL 6836, April 1995.

ECAR 907, 2012, "Release to Birth Ratios for AGR-1 Operating Cycles 138B through 145A," Rev. 1, July 2, 2012.

ECAR 2420, 2014, "Release to Birth Ratios for AGR-2 Operating Cycles 147A through 154B," Rev. 0, March 4, 2014.

ECAR 2457, 2014, "Release to Birth Ratios for AGR-3/4 Operating Cycles 151A 155A," Rev. 1, June 5, 2015.

ECAR 2066, 2014, "JMOCUP As Run Daily Depletion Calculation for the AGR-2 Experiment in ATR B 12 Position," Rev. 2, April 25, 2014.

ECAR 968, 2014, "AGR-1 Daily As-run Thermal Analyses," Rev. 4, September 8, 2014.

ECAR 2476, 2014, "AGR-2 Daily As-run Thermal Analyses," Rev. 1, August 13, 2014.

ECAR 2807, 2015, "AGR-3/4 Daily As Run Thermal Analyses," Rev. 0, June 25, 2015.

ECAR 2807, 2016, "AGR-3/4 Daily As Run Thermal Analyses," Rev. 1, April 21, 2016.

General Atomics, 1987, "Capsule HRB-17/18 Data File," GA 1485, Rev. 4.

General Atomics, 2009, *Technical Basis for NGNP Fuel Performance and Quality Requirements*, GA Project 30302, Rev. 0.

Hawkes, G., J. Sterbentz, and B. Pham, 2014, "Thermal Predictions of the AGR 2 Experiment with Variable Gas Gaps," ANS2014, Reno, Nevada.

Hunn, J., 2017, Attached Excel file "AGR2 Uranium Leached_8_no links.xlsx" to an email communication on Subject "R/B discussion" sent on November 6, 2017.

Hunn, J.D., G.W. Helmreich, T.W. Savage, and C.M. Silva. 2017, *AGR-2 Fuel Compact Pre-Irradiation Characterization Summary Report*, ORNL/TM-2017-043, Oak Ridge, Tennessee: Oak Ridge National Laboratory.

Hunn, J.D., C.A. Baldwin, T.J. Gerczak, F.C. Montgomery, R.N. Morris, C.M. Silva, P.A. Demkowicz, J.M. Harp, S.A. Ploger, I.V. Rooyen, and K.E. Wright, 2016, "Detection and analysis of particles with breached SiC in AGR-1 fuel compacts," *Nucl. Eng. Des.* 306 (2016) 36-46.

IAEA, 1997, *Fuel performance and fission product behaviour in gas cooled reactors*, IAEA TECDOC 978, November 1997, http://www pub.iaea.org/MTCD/Publications/PDF/te_978_prn.pdf.

INL, 2010, *NGNP Fuel Qualification White Paper, Idaho National Laboratory*, INL/EXT-10-17686, July 2010.

Martin, R. G., 1993, *Compilation of Fuel Performance and Fission Product Transport Models and Database for MHTGR Design*, ORNL/NPR 91/6, October 1993.

McIsaac, C. V., et al., 1992, "Concentrations of Fission Product Noble Gases Released During the NP MHTGR Fuel Compact Experiment 1A," *ST PHY* 92 032, April 1992.

ORNL, 1994, *The Operation of Experiment HFR B1 in the Petten High Flux Reactor*, ORNL/TM-12740, September 1994.

ORNL, 2013, *AGR-1 Irradiated Compact 4-4-2 PIE Report: Evaluation of As-Irradiated Fuel Performance with Leach Burn Leach, IMGA, Materialography, and X-Ray Tomography Prepared by Oak Ridge National Laboratory*, ORNL/TM-2013/236, September 2013.

Petti, D. A., J. Buongiorno, J. T. Maki, R. R. Hobbins, and G. K. Miller, 2003, "Key differences in the fabrication, irradiation and high temperature accident testing of U.S. and German TRISO coated particle fuel, and their implications on fuel performance," *Nucl. Eng. Des.*, Vol. 222, pp. 281–297.

Petti, D. A., P. A. Demkowicz, J. T. Maki, and R. R. Hobbins, 2012, "TRISO-Coated Particle Fuel Performance," in Konings R.J.M., (ed.) *Comprehensive Nuclear Materials*, Vol. 3, pp. 151-213 Amsterdam: Elsevier.

Pham, B. T., and J. J. Einerson, 2014, *AGR-2 Final Data Qualification Report for U.S. Capsules ATR Cycles 147A through 154B*, INL/EXT-14-32376, July 2014.

PLN-3636, 2018, "Technical Program Plan for INL Advanced Reactor Technologies Advanced Gas Reactor Fuel Development and Qualification Program," Rev. 7, June 29, 2018.

Rice, F. J., J. D. Stempien, and P. A. Demkowicz, 2016, *Ceramography of Irradiated TRISO Fuel from the AGR 2 Experiment*, INL/EXT-16-39462, July 2016.

Richards, M. B., 1994, *Fission Gas Release from UCO Microspheres: A Theoretical Model for Fractional Release for Non hydrolyzed Fuel with Model Parameters Derived for Capsule HFR B1*, General Atomics, January 1994.

Scates, D. M., 2010, "Fission Product Monitoring and Release Data for the Advanced Gas Reactor 1 Experiment," *Proceedings HTR 2010, Prague, Czech Republic, October 18–20, 2010*, Paper 52.

SPC-1064, 2010, "AGR-2 Irradiation Test Specification," Rev. 1, June 1, 2010.

SPC-1345, 2011, "AGR-3/4 Irradiation Test Specification," Rev. 0, February 2, 2011.